

**DTIC FILE COPY**

2

**RADC-TR-90-157**  
**Interim Report**  
**July 1990**

**AD-A226 296**



# **EFFECTIVE DIELECTRIC CONSTANTS OF FOLIAGE MEDIA**

**ARCON Corporation**

**Douglas Tomasanis**

**DTIC**  
**ELECTE**  
**SEP 04 1990**  
**S** **D**  
**GE**

**APPROVED FOR PUBLIC RELEASE; DISTRIBUTION UNLIMITED.**

**Rome Air Development Center**  
**Air Force Systems Command**  
**Griffiss Air Force Base, NY 13441-5700**

**90 08 31 053**

RADC-TR-90-157 has been reviewed and is approved for publication.

APPROVED:



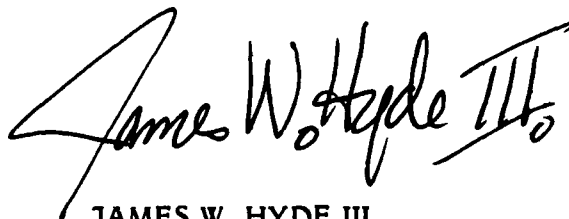
ZACHARY O. WHITE  
Project Engineer

APPROVED:



JOHN K. SCHINDLER  
Director of Electromagnetics

FOR THE COMMANDER:



JAMES W. HYDE III  
Directorate of Plans & Programs

**DESTRUCTION NOTICE** - For classified documents, follow the procedures in DOD 5200.22-M, Industrial Security Manual, or DOD 5200.1-R, Information Security Program Regulation. For unclassified, limited documents, destroy by any method that will prevent disclosure of contents or reconstruction of the document.

If your address has changed or if you wish to be removed from the RADC mailing list, or if the addressee is no longer employed by your organization, please notify RADC (EEAA), Hanscom AFB MA 01731-5000. This will assist us in maintaining a current mailing list.

Do not return copies of this report unless contractual obligations or notices on a specific document requires that it be returned.

# REPORT DOCUMENTATION PAGE

Form Approved  
OPM No. 0704-0188

Public reporting burden for this collection of information is estimated to average 1 hour per response, including the time for reviewing instructions, searching existing data sources, gathering and maintaining the data needed, and reviewing the collection of information. Send comments regarding this burden estimate or any other aspect of this collection of information, including suggestions for reducing this burden, to Washington Headquarters Services, Directorate for Information Operations and Reports, 1215 Jefferson Davis Highway, Suite 1204, Arlington, VA 22202-4302, and to the Office of Information and Regulatory Affairs, Office of Management and Budget, Washington, DC 20503.

1. AGENCY USE ONLY (Leave Blank)		2. REPORT DATE July 1990	3. REPORT TYPE AND DATES COVERED Interim Feb 89 - Jan 90	
4. TITLE AND SUBTITLE EFFECTIVE DIELECTRIC CONSTANTS OF FOLIAGE MEDIA			5. FUNDING NUMBERS C - F19628-89-C-0186 PE - 62702F PR - 4600 TA - 14 WU - 2G	
6. AUTHOR(S) Douglas Tomasanis				
7. PERFORMING ORGANIZATION NAME(S) AND ADDRESS(ES) ARCON Corporation 260 Bear Hill Road Waltham MA 02154			8. PERFORMING ORGANIZATION REPORT NUMBER N/A	
9. SPONSORING/MONITORING AGENCY NAME(S) AND ADDRESS(ES) Rome Air Development Center (EEAA) Hanscom AFB MA 01731-5000			10. SPONSORING/MONITORING AGENCY REPORT NUMBER RADC-TR-90-157	
11. SUPPLEMENTARY NOTES RADC Project Engineer: Zachary O. White/EEAA/(617) 377-2055				
12a. DISTRIBUTION/AVAILABILITY STATEMENT Approved for public release; distribution unlimited.			12b. DISTRIBUTION CODE	
13. ABSTRACT (Maximum 200 words) <p>The output from a model that calculates the effects of multiple scattering processes that influence the scattering and absorption of electromagnetic radiation by dense foliage is presented. Results are presented as effective dielectric constants which can be used to represent the forest environment as a homogeneous dielectric slab in electromagnetic scattering models. An objective of this report is to present a formalism that allows the reader to incorporate the results into a simulation program.</p> <p>Several models of multiple scattering processes in the foliage media are considered for determining the effective parameters. A brief discussion of the Average T-Matrix Approximation (ATA) and the Coherent Potential Approximation (CPA) are presented.</p>				
14. SUBJECT TERMS Foliage Scattering EM Wave Propagation Effective Dielectric Radar Clutter Dielectric Constant			15. NUMBER OF PAGES 122	
			16. PRICE CODE	
17. SECURITY CLASSIFICATION OF REPORT UNCLASSIFIED	18. SECURITY CLASSIFICATION OF THIS PAGE UNCLASSIFIED	19. SECURITY CLASSIFICATION OF ABSTRACT UNCLASSIFIED	20. LIMITATION OF ABSTRACT SAR	

# Contents



Accession For	
NTIS	<input checked="" type="checkbox"/>
DTIC TAB	<input type="checkbox"/>
Unannounced	<input type="checkbox"/>
Justification	
By	
Distribution/	
Availability Codes	
Dist	Special
A-1	

1.0 INTRODUCTION	1
2.0 EFFECTIVE PARAMETERS FOR A HETEROGENEOUS MEDIUM	3
2.1 Basic Theory of the Transition Matrix	3
2.2 The Transition Operator Nomenclature	5
2.2.1 The Average T-Matrix Approximation	8
2.2.2 The Coherent Potential Approximation	9
2.2.3 The Effective Medium Approximation	13
2.2.4 The Self-Consistent Approximation	14
2.3 Heterogeneous Media With M Classes of Embedded Scatterers	15
2.4 Applications of Effective Parameters	16
2.5 Model Limitations	17
3.0 DIELECTRIC CONSTANTS OF FOREST COMPONENTS	18
3.1 Dielectric Properties of Trees	19
3.1.1 Physical Properties of Wood	19
3.1.2 Permittivity of Wood	22
3.1.3 Loss Factor of Wood	27
3.2 Permittivity and Loss Factors of Leaves	34
3.3 Density of Forest Components	40

## Contents

4.0	EXAMPLE CALCULATIONS	41
4.1	Effective Dielectric Constants of Hard Wood Vegetation	54
4.1.1	Hard Wood With Perpendicular E-Field at 25°C	54
4.1.2	Hard Wood With Perpendicular E-Field at 4°C	60
4.1.3	Hard Wood With Randomly Oriented E-Field at 25°C	65
4.1.4	Hard Wood With Randomly Oriented E-Field at 4°C	71
4.2	Effective Dielectric Constants of Soft Wood Vegetation	76
4.2.1	Soft Wood With Perpendicular E-Field at 25°C	76
4.2.2	Soft Wood With Perpendicular E-Field at 4°C	80
4.2.3	Soft Wood With Randomly Oriented E-Field at 25°C	87
4.2.4	Soft Wood With Randomly Oriented E-Field at 4°C	93
5.0	CONCLUSION	98
	REFERENCES	102

## List of Figures

1. Normal distributions of typical dry weight moisture content for 38 hardwood and 26 softwood species. 21
2. Range of the permittivity ( $\epsilon_r'$ ) for common species of live trees at 25°C with the electric field polarization parallel to the wood grain. 24
3. Range of the permittivity ( $\epsilon_r'$ ) for common species of live trees at 25°C with the electric field polarization perpendicular to the wood grain. 25
4. The loss factor of softwood in summer and winter with random and perpendicular orientation of the wood grain to the electric field. 29
5. Revised loss factor of softwood in summer and winter with perpendicular and *random orientation of the electric field polarization relative to the wood grain.* 31
6. Revised loss factor of hardwood in summer and winter with perpendicular and random orientation of the electric field polarization relative to the wood grain. 32
7. Effective complex dielectric constants ( $\epsilon^*$ ) of a hardwood vegetation environment versus the volume fraction of the wood component for an incident radiation frequency of 50MHz. 42
8. Effective complex dielectric constants ( $\epsilon^*$ ) of a hardwood vegetation environment versus the volume fraction of the wood component for an incident radiation frequency of 100MHz. 43
9. Effective complex dielectric constants ( $\epsilon^*$ ) of a hardwood vegetation environment versus the volume fraction of the wood component for an incident radiation frequency of 200MHz. 44

## LIST OF FIGURES

10. Effective complex dielectric constants ( $\epsilon^*$ ) of a hardwood vegetation environment versus the volume fraction of the wood component for an incident radiation frequency of 400MHz. 45
11. Effective complex dielectric constants ( $\epsilon^*$ ) of a hardwood vegetation environment versus the volume fraction of the wood component for an incident radiation frequency of 600MHz. 46
12. Effective complex dielectric constants ( $\epsilon^*$ ) of a hardwood vegetation environment versus the volume fraction of the wood component for an incident radiation frequency of 800MHz. 47
13. Effective complex dielectric constants ( $\epsilon^*$ ) of a hardwood vegetation environment versus the volume fraction of the wood component for an incident radiation frequency of 1.3GHz. 48
14. Effective complex dielectric constants ( $\epsilon^*$ ) of a hardwood vegetation environment versus the volume fraction of the wood component for an incident radiation frequency of 2.4GHz. 49
15. Effective complex dielectric constants ( $\epsilon^*$ ) of a hardwood vegetation environment versus the volume fraction of the wood component for an incident radiation frequency of 3.2GHz. 50
16. Effective permittivity of a sparse hardwood vegetation environment versus the incident radiation frequency in the summer season with the wood grain perpendicular to the electric field polarization. 55

## LIST OF FIGURES

17. Effective loss factor of a sparse hardwood vegetation environment versus the incident radiation frequency in the summer season with the wood grain perpendicular to the electric field polarization. 56
18. Effective permittivity of a dense hardwood vegetation environment versus the incident radiation frequency in the summer season with the wood grain perpendicular to the electric field polarization. 58
19. Effective loss factor of a dense hardwood vegetation environment versus the incident radiation frequency in the summer season with the wood grain perpendicular to the electric field polarization. 59
20. Effective permittivity of a sparse hardwood vegetation environment versus the incident radiation frequency in the winter season with the wood grain perpendicular to the electric field polarization. 61
21. Effective loss factor of a sparse hardwood vegetation environment versus the incident radiation frequency in the winter season with the wood grain perpendicular to the electric field polarization. 62
22. Effective permittivity of a dense hardwood vegetation environment versus the incident radiation frequency in the winter season with the wood grain perpendicular to the electric field polarization. 63
23. Effective loss factor of a dense hardwood vegetation environment versus the incident radiation frequency in the winter season with the wood grain perpendicular to the electric field polarization. 64



## LIST OF FIGURES

24. Effective permittivity of a sparse hardwood vegetation environment versus the incident radiation frequency in the summer season with the wood grain randomly oriented with respect to the electric field polarization. 66
25. Effective loss factor of a sparse hardwood vegetation environment versus the incident radiation frequency in the summer season with the wood grain randomly oriented with respect to the electric field polarization. 67
26. Effective permittivity of a dense hardwood vegetation environment versus the incident radiation frequency in the summer season with the wood grain randomly oriented with respect to the electric field polarization. 69
27. Effective loss factor of a dense hardwood vegetation environment versus the incident radiation frequency in the summer season with the wood grain randomly oriented with respect to the electric field polarization. 70
28. Effective permittivity of a sparse hardwood vegetation environment versus the incident radiation frequency in the winter season with the wood grain randomly oriented with respect to the electric field polarization. 72
29. Effective loss factor of a sparse hardwood vegetation environment versus the incident radiation frequency in the winter season with the wood grain randomly oriented with respect to the electric field polarization. 73
30. Effective permittivity of a dense hardwood vegetation environment versus the incident radiation frequency in the winter season with the wood grain randomly oriented with respect to the electric field polarization. 74

## LIST OF FIGURES

31. Effective loss factor of a dense hardwood vegetation environment versus the incident radiation frequency in the winter season with the wood grain randomly oriented with respect to the electric field polarization. 75
32. Effective permittivity of a sparse softwood vegetation environment versus the incident radiation frequency in the summer season with the wood grain perpendicular to the electric field polarization. 77
33. Effective loss factor of a sparse softwood vegetation environment versus the incident radiation frequency in the summer season with the wood grain perpendicular to the electric field polarization. 78
34. Effective permittivity of a dense softwood vegetation environment versus the incident radiation frequency in the summer season with the wood grain perpendicular to the electric field polarization. 81
35. Effective loss factor of a dense softwood vegetation environment versus the incident radiation frequency in the summer season with the wood grain perpendicular to the electric field polarization. 82
36. Effective permittivity of a sparse softwood vegetation environment versus the incident radiation frequency in the winter season with the wood grain perpendicular to the electric field polarization. 83
37. Effective loss factor of a sparse softwood vegetation environment versus the incident radiation frequency in the winter season with the wood grain perpendicular to the electric field polarization. 84

## LIST OF FIGURES

38. Effective permittivity of a dense softwood vegetation environment versus the incident radiation frequency in the winter season with the wood grain perpendicular to the electric field polarization. 85
39. Effective loss factor of a dense softwood vegetation environment versus the incident radiation frequency in the winter season with the wood grain perpendicular to the electric field polarization. 86
40. Effective permittivity of a sparse softwood vegetation environment versus the incident radiation frequency in the summer season with the wood grain randomly oriented with respect to the electric field polarization. 88
41. Effective loss factor of a sparse softwood vegetation environment versus the incident radiation frequency in the summer season with the wood grain randomly oriented with respect to the electric field polarization. 89
42. Effective permittivity of a dense softwood vegetation environment versus the incident radiation frequency in the summer season with the wood grain randomly oriented with respect to the electric field polarization. 91
43. Effective loss factor of a dense softwood vegetation environment versus the incident radiation frequency in the summer season with the wood grain randomly oriented with respect to the electric field polarization. 92
44. Effective permittivity of a sparse softwood vegetation environment versus the incident radiation frequency in the winter season with the wood grain randomly oriented with respect to the electric field polarization. 94

## LIST OF FIGURES

45. Effective loss factor of a sparse softwood vegetation environment versus the incident radiation frequency in the winter season with the wood grain randomly oriented with respect to the electric field polarization. 95
46. Effective permittivity of a dense softwood vegetation environment versus the incident radiation frequency in the winter season with the wood grain randomly oriented with respect to the electric field polarization. 96
47. Effective loss factor of a dense softwood vegetation environment versus the incident radiation frequency in the winter season with the wood grain randomly oriented with respect to the electric field polarization. 97

## Tables

1. Permittivities of living hard and softwood trees in summer and winter including a slight downward bias as frequency increases. Values reported here are for when the incident radiation electric field polarization is parallel to the wood grain. 26
2. Permittivities of living hard and softwood trees in summer and winter including a slight downward bias as frequency increases. Values reported here are for when the incident radiation electric field polarization is perpendicular to the wood grain. 26
3. Loss factors of wood  $\epsilon_r''$  with the E-field perpendicular to the wood grain orientation, for variable frequencies, and wood types, in the summer season. 33
4. Loss factors of wood  $\epsilon_r''$  with the E-field perpendicular to the wood grain orientation, for variable frequencies, and wood types, in the winter season. 33
5. Loss factors of wood  $\epsilon_r''$  with the E-field arbitrary to the wood grain orientation, for variable frequencies, and wood types, in the summer season. 33
6. Loss factors of wood  $\epsilon_r''$  with the E-field arbitrary to the wood grain orientation, for variable frequencies, and wood types, in the winter season. 34
7. Permittivity of broad leaves and needles for leaves with moisture content of 65% and salinity of 6%. 39
8. Loss factors of broad leaves and needles for leaves with moisture content of 65% and salinity of 6%. 39

## 1.0 INTRODUCTION

The development of simulation programs as a means of testing electromagnetic devices is on the increase in an effort to defray the cost of developing and testing prototype equipment or conducting physical experimentation with existing apparatus. These programs must simulate complex electromagnetic scattering and propagation phenomenon occurring within the natural environment that the majority of these systems must operate in or near. At present, little experimental or theoretical data is available describing the electromagnetic scattering characteristics of natural environments or foliage. Various analytical methods have been derived for the theoretical representation of multiple scattering and absorption events expected to occur within a foliage medium. In many instances, however, application of these processes in a computer simulation are impractical due to their complexity. In order to remain within the practical limits of available computer resources and yet retain the computational accuracy of the model, various assumptions are usually introduced during the development of a model involving electromagnetic scattering. One common simplification involves the representation of natural terrain growth or foliage as a perfectly conducting dielectric slab with some arbitrary thickness equivalent to the mean height of the vegetation. The difficulty associated with this methodology stems from the determination of effective parameters (i.e. dielectric constants or permittivity) that are used to represent the dielectric properties of the homogeneous slab representing the randomly distributed heterogeneous medium that a forest environment actually presents.

In this report, the output of a model that calculates the effective dielectric constants that influence the scattering and absorption of electromagnetic radiation by dense foliage is presented. The reported effective dielectric constants can be used to represent forest environments as a homogeneous dielectric slab in electromagnetic scattering models. Four dielectric mixing models that are be used to determine the effective dielectric constants of heterogeneous random media are briefly developed in section 2; the Average T-Matrix Approximation (ATA), Coherent Potential Approximation (CPA), Effective Medium Approximation (EMA) and a version of the Claussius-Mossotti formula. The Average T-Matrix Approximation represents the field at an individual scattering center

in terms of an equivalent field produced by the other scatterers but includes no provision for multiple interaction processes between scatterers. The version of the Claussius-Mossotti formula discussed is similar to the ATA and also contains no provision for multiple inter-particle interactions. The Coherent Potential Approximation, which neglects the difference between the external excitation field and the average field does account for the interaction processes between particles, as does the Effective Medium Approximation. A format of the Coherent Potential Approximation is described that uses a recursive technique creating a version of the formula known as the Self-Consistent Approximation. Application of the effective dielectric constants of the foliage environments to determine the affect on the magnitude and phase of an electric field caused by propagation through vegetation is also presented. General limitations concerning the use of the effective parameters based on the wavelength and maximum allowable scatterer dimension, within the scattering medium, is also discussed.

Section 3 contains a discussion of the various methods used to determine the dielectric constants of the components that comprise a forest environment. The dielectric constants of hard and softwood trees as well as broad leaves and needles were determined for a variety of conditions and are given in the form of tables or graphs. The dielectric constants of the forest components were estimated using models that calculate these values as a function of the physical characteristics of the components (i.e. moisture content, salinity, etc.) and the environmental conditions (i.e. temperature, wood grain orientation, etc.). Reports that present experimental measurements of the dielectric constants of living wood and leaves were found to be scarce. It was the lack of experimental data that was the main reason for choosing to use models to determine the dielectric values rather than using experimental values reported in the literature. When experimental values of the dielectric constants of foliage for similar conditions to those used in this report were available, they were used as a comparison to the models output to ensure reasonable agreement. From examination of the dielectric constants of various natural foliage materials it was found that these values are difficult to predict due to the changes that can be expected in climate, weather, and growth patterns. Dielectric constants used in this study reflect values determined for specific conditions with the intent of showing possible trends that can be expected in the foliage medium as certain conditions change and are not professed to be absolute. The intention is to determine

the effective dielectric constants of vegetation environments using extreme values for the vegetation components and to allow the reader to extract values that apply to a particular situation of interest.

Section 4 contains the output of the dielectric mixing model. Calculations were done for incident radiation frequencies from 50MHz to 3.2GHz and for foliage densities having volume fractions ranging from 0.01% to 5.00%. Initial model output is given as a plot of the effective dielectric constant versus the volume fraction of one of the embedded scatterers. Points were then taken from these plots and used to create plots that depict the effective dielectric constant versus the frequency of the incident radiation. A variety of these plots were created to demonstrate the influences of season, wood grain orientation to the electric field polarization, and whether the forest is comprised of hard or softwood tree types on the effective complex dielectric constants of the medium. Effects of forest density were demonstrated by creating two sets of plots; one set for sparse vegetation where the volume fraction ranges from 0.01% to 1.00%, and another for dense foliage where the volume fraction falls between 1.00% and 5.00%.

## 2.0 EFFECTIVE PARAMETERS FOR A HETEROGENEOUS MEDIUM

Various analytical techniques have been developed in an attempt to determine effective parameter values to describe heterogeneous media composed of a host medium and various embedded scatterers [Van Beek 1967], [Tinga 1973], [Brown 1982], [Blankenship 1989]. Use of effective parameter values would allow a heterogeneous medium to be treated as a homogeneous medium when applied in a modeling program. The calculations presented in this report represent an extension of the work of [Blankenship 1989] and ([Brown 80] and [Fung 78]) which derive effective parameter approximation equations and dielectric properties of forest components, respectively.

### 2.1 Basic Theory of the Transition Matrix

In this section the transition matrix (T-matrix) formalism is used to describe multiple



scattering events that occur in a medium comprised of two or more different types of dielectric scatterers arranged in a random geometric configuration in a surrounding "host" medium. Modeling of scattering from a medium containing two or more types of randomly oriented scatterers in a host medium is most easily accomplished by defining approximations for the effective dielectric constant. This approach will result in a variety of approximations for effective scattering representation for the heterogeneous medium of interest.

We are given a region, or scattering medium,  $\mathcal{O}$  comprised of a homogeneous medium (free-space) with dielectric constant  $\epsilon_0$  that contains  $m$  different embedded scatterers with dielectric constants  $\epsilon_1, \dots, \epsilon_m$ . Defining  $V_{ij}$ ,  $i = 1, \dots, m$ ,  $j = 1, 2, \dots, N_j$ , as the subset of  $\mathcal{O}$  occupied by embedded scatterers  $j$  of class  $i$ , the dielectric properties of the composite medium occupying  $\mathcal{O}$  are defined by [Blankenship 1988],

$$\epsilon(x) = \epsilon_0 + \sum_{i=1}^m (\epsilon_i - \epsilon_0) \sum_{j=1}^{N_j} \chi_{ij}(x) \quad , \quad (1)$$

where,

$$\chi_{ij}(x) = \begin{cases} 1 & \text{for } x \in V_{ij} \\ 0 & \text{for } x \notin V_{ij} \end{cases} \quad . \quad (2)$$

Assume that  $\delta_i$  is defined to be a dimensionless parameter describing a particular aspect of the elementary scatterers in class  $i$ , such as the radius of spherical scatterers; and  $\rho_i$  is the total volume fraction of  $\mathcal{O}$  occupied by scatterers of class  $i = 1, \dots, m$ . Given a field incident on the region  $\mathcal{O}$ , the objective is to characterize the scattering properties of the composite medium for the limit  $N_i \rightarrow \infty$ ,  $\delta_i \rightarrow 0$ , where  $\rho_i$ ,  $i = 1, \dots, m$  is a constant. Although various methods are available for determination of these approximations [Brown 1982], [Brown 1980], [Pounds 1963] to name a few, the more recent work of [Blankenship 1988], [Lang 1981] and [Kohler and Papanicolaou 1981], that extend the earlier work of [M. Lax 1951, 1952], are used as the basis for this report.

## 2.2 The Transition Operator Nomenclature

The transition operator convention is used as a basis to derive various approximations to solve for effective dielectric constant of a composite medium. Maxwell's equations may be applied to describe the conditions of interest and may be expressed as,

$$\nabla \cdot (\epsilon_0 E) + \sum_{i=1}^m (\epsilon_i - \epsilon_0) \sum_{j=1}^{N_i} \nabla \cdot (\chi_{ij} E) = 0 \quad , \quad (3)$$

and,

$$\nabla \times E = 0 \quad ,$$

with the boundary condition,

$$\langle E \rangle \rightarrow \vec{E} \quad \text{as} \quad N_i \rightarrow \infty \quad , \quad (4)$$

where  $\langle \cdot \rangle$  is the expectation value and  $\vec{E}$  is the constant external field. The relationship,

$$D(x) = \epsilon(x)E(x) \quad , \quad (5)$$

and the condition,

$$\langle D(\cdot) \rangle = \epsilon^* \vec{E} \quad , \quad (6)$$

define the effective dielectric constant for a composite material.

Equation 3 may be expressed in abstract form,

$$(L_0 + M)E = 0 \quad , \quad \nabla \times E = 0 \quad , \quad (7)$$

where,

$$L_0 = \nabla \cdot (\epsilon_0 \cdot) \quad , \quad (8a)$$

$$M = M_1 + \dots + M_m \quad , \quad M_i = \sum_{j=1}^{N_i} V_{ij} \quad (8b)$$

and,

$$V_{ij} = (\epsilon_i - \epsilon_0) \cdot \nabla(\chi_{ij}(\cdot)) \quad , \quad (8c)$$

The integral form of Eq. (3) can be written,

$$E + L_0^{-1}ME = F \quad , \quad (9)$$

where F is chosen so that,

$$L_0 F = 0 \quad , \quad \langle E \rangle = \vec{E} \quad . \quad (10)$$

The transition operator is defined as,

$$\begin{aligned} L_0^{-1}M &= (L_0 + M - M)^{-1}M \\ &= ((L_0 + M)(I - (L_0 + M)^{-1}M))^{-1}M \\ &= T(I - T)^{-1} \quad , \end{aligned} \quad (11)$$

where  $T = (L_0 + M)^{-1}M$ . Therefore, Eq. (9) can be expressed,

$$(I + T(I - T)^{-1})E = F \quad , \quad (12)$$

or,

$$E = (I - T)F \quad . \quad (13)$$

For the conditions assumed in Eq. (10),

$$F = (I - \langle T \rangle)^{-1}\vec{E} \quad , \quad (14)$$

and,

$$E = (I - T)(I - \langle T \rangle)^{-1}\vec{E} \quad . \quad (15)$$

From the definition of the effective dielectric constant, Eqs. (5 and 6), and Eq. (15), it is possible to write,

$$\epsilon \cdot \vec{E} = (\langle \epsilon \rangle - \langle \epsilon T \rangle)(I - \langle T \rangle)^{-1}\vec{E} \quad , \quad (16)$$

defining the effective dielectric constant in terms of the transition operator.

Knowledge of  $T$  is used to characterize the scattering properties of the composite medium. The operator  $T$  is related to the scattering magnitude of the individual scatterers and to their interactions. For single dipole scatterers,  $T$  can be determined from the polarizability of the element; therefore,  $T$  is defined in terms of physical properties. A more in depth analysis of the determination of Eqs. (15 and 16), an extension of the original work presented by [Kohler and Papanicolaou 1981], is presented in [Blankenship 1988].

To examine the conditions where there are multiple scatterers constituting a medium, the initial work would begin with Eq. (9) expressed as follows,

$$E + L_0^{-1}(M_1 + \dots + M_m)E = F \quad , \quad (17)$$

which may be expanded as follows,

$$E = F - T_1 E_1 - T_2 E_2 - \dots - T_m E_m \quad , \quad (18)$$

where,

$$L_0^{-1} M_i = T_i (I - T)^{-1} \quad , \quad (19a)$$

$$T_i = (L_0 + M_i)^{-1} M_i \quad , \quad (19b)$$

$$E_i = (I - T_i)^{-1} E \quad . \quad (19c)$$

Knowing that  $E_i - T_i E_i = E$ , it is possible to write,

$$E_i + \sum_{k \neq i}^m T_k E_k = F \quad . \quad (20)$$

The expressions in Eqs. (18-20) describe the field in terms of the transition matrix and electric fields associated with  $i$  classes of scatterers comprising a composite medium.

The general expression for the effective dielectric constant of a composite medium with  $m \geq 2$  types of embedded scatterers is expressed [Blankenship 1988] as,

$$\epsilon^* \sim \left( \langle \epsilon \rangle - \sum_{i=1}^m \sum_{j \neq i}^m \langle \epsilon (I + T_{ij})^{-1} T_i \rangle \right) \left( 1 - \sum_{i=1}^m \sum_{j \neq i}^m \langle (I + T_{ij})^{-1} T_i \rangle \right)^{-1}, \quad (21)$$

where,

$$\langle \epsilon \rangle \triangleq (1 - \rho_1) \epsilon_0 + \rho_1 \epsilon_1 \quad . \quad (22)$$

### 2.2.1 The Average T-Matrix Approximation

Consider the application of Eq. (21) to the case where a composite medium has one class of embedded scatterers, (i.e.  $m = 1$ ). Assuming the embedded scatterers are uniformly distributed in the host medium and that they are considered infinitely small particles ( $M_1 \rightarrow \infty$ ,  $\delta_1 \rightarrow 0$ , and  $\rho_1$  is constant), the effective dielectric constant  $\epsilon^*$  can be determined by application of Eq. (21),

$$\epsilon^* \simeq \left( \langle \epsilon \rangle - \sum_{i=1}^1 \langle \epsilon T_i \rangle \right) \left( I - \sum_{i=1}^1 \langle T_i \rangle \right)^2 \quad . \quad (23)$$

This expression is known as the Average T-matrix Approximation (ATA) as derived by [Lax 1951, 1973], [Kohler and Papanicolaou 1981]. For typical conditions  $\langle T_i \rangle$ , and  $\langle \epsilon T_i \rangle$  can diverge [Batchelor 1974] so the ATA must be used with caution.

Equation (23) can be evaluated for the limit as the size of the particulate scatterers approach zero. Assuming a spherical shape for the embedded scatterers, the volume fraction of each could be expressed,

$$\rho_i = \frac{4}{3} \pi \delta_i^3 c_i \quad , \quad (24)$$

where  $\delta_i$  is the radius of the scatterers and  $c_i$  is the average number of scattering centers per unit volume. This leads to the approximation,

$$\epsilon^*(\epsilon_0; \epsilon_1, \rho_1) \simeq \frac{\langle \epsilon \rangle + \rho_1 \epsilon_1 \left( \frac{\epsilon_0 - \epsilon_1}{2\epsilon_0 + \epsilon_1} \right)}{1 + \rho_1 \left( \frac{\epsilon_0 - \epsilon_1}{2\epsilon_0 + \epsilon_1} \right)} \quad . \quad (25)$$

Using the Claussius-Mossotti Formula,

$$\epsilon^*(\epsilon_0; \epsilon_1, \rho_1) = \epsilon_0 z \quad , \quad (26)$$

where,

$$\frac{z-1}{z+2} = \frac{\rho_1(k-1)}{k+2} \quad , \quad (27)$$

and  $k = \epsilon_1/\epsilon_0$ . For very low volume fractions  $\epsilon^*(\epsilon_0; \epsilon_1, \rho_1)$  is well approximated by,

$$\epsilon^*(\epsilon_0; \epsilon_1, \rho_1) \simeq \epsilon_0 \left( 1 + 3\rho_1 \left( \frac{\epsilon_1 - \epsilon_0}{2\epsilon_0 + \epsilon_1} \right) + 3\rho_1^2 \left( \frac{\epsilon_1 - \epsilon_0}{2\epsilon_0 + \epsilon_1} \right)^2 \right) \quad , \quad (28)$$

The average T-Matrix approximation is considered a good approximation of the effective dielectric constant for volume fractions  $< 0.01$ , and can not be used with any confidence for conditions much above this threshold. The approximation also fail to account for the interparticle scattering interactions. A more refined technique for determining the effective dielectric constant has been developed [Lax 1951, 1952, 1973], [Elliot et al 1974] that will be examined in the following section.

### 2.2.2 The Coherent Potential Approximation

Another approximation method devised to estimate the effective dielectric constant of a heterogeneous random medium is the coherent potential approximation (CPA). The basis of this technique involves neglecting the difference between the field exciting the medium and the average field. With  $\epsilon_r$  selected as a reference dielectric constant, it is possible to write Maxwell's equations as,

$$\nabla \cdot (\epsilon_r E) + \sum_{i=1}^m \sum_{j=1}^{N_i} \nabla \cdot [(\epsilon_i - \epsilon_0) \chi_{ij} E] + \sum_{i=1}^m \sum_{j=1}^{N_i} \left( \frac{\epsilon_i - \epsilon_r}{m N_i} \right) \nabla \cdot E = 0 \quad , \quad (29)$$

and,

$$\nabla \times E = 0 \quad .$$

Equation (29) can be expressed abstractly as,

$$(L_r + M^r)E = 0 \quad , \quad (30)$$

where notation similar to that used in Eqs. (19a-c) is applied, and may be written,

$$L_r = \nabla \cdot (\epsilon_r \cdot) \quad , \quad (31a)$$

$$M^r = \sum_{i=1}^m \sum_{j=1}^{N_i} V_{ij}^r \quad , \quad (31b)$$

and,

$$V_{ij}^r = \nabla \cdot ((\epsilon_i - \epsilon_0) \chi_{ij} \cdot) + \left( \frac{\epsilon_0 - \epsilon_r}{m N_i} \right) \nabla \cdot \quad . \quad (31c)$$

Using the same methodology as that used in the derivation of Eq. (21) the effective dielectric constant may be expressed,

$$\epsilon^* \simeq \left( \langle \epsilon \rangle - \sum_{i=1}^m \sum_{j=1}^{N_i} \langle \epsilon T_{ij}^r \rangle \right) \left( 1 - \sum_{i=1}^m \sum_{j=1}^{N_i} \langle T_{ij}^r \rangle \right)^{-1} \quad . \quad (32)$$

where,

$$T_{ij}^r = \left( L_r + V_{ij}^r \right)^{-1} V_{ij}^r \quad . \quad (33)$$

The coherent potential approximation is based on choosing  $\epsilon_r$  to optimize the approximation shown in Eq. (32). As derived by [Kohler and Papanicolaou 1981] the optimization of Eq. (32) is obtained by evaluating  $T_{ij}^r$  in the form of,

$$w^{ij}(x) = (T_{ij}^r g)(x) \quad , \quad (34)$$

where  $g(x)$  is a continuous function, so that Eq. (29) may be expressed as,

$$\begin{aligned} \nabla \cdot [\epsilon_r w^{ij}] + \nabla \cdot [(\epsilon_i - \epsilon_0) \chi_{ij} w^{ij} + \left( \frac{\epsilon_0 - \epsilon_r}{m N_i} \right) w^{ij}] \quad , \\ = \nabla \cdot [(\epsilon_i - \epsilon_0) \chi_{ij} g + \left( \frac{\epsilon_0 - \epsilon_r}{m N_i} \right) g] \quad , \end{aligned} \quad (35)$$

where,

$$\nabla \times w^{ij} = 0.$$

By further establishing,

$$\epsilon_i^{r,N} = [\epsilon_r + \frac{1}{mN_i}(\epsilon_r - \epsilon_0)] \simeq \epsilon_r \quad \text{for large } N_i, \quad (36)$$

and  $w^{ij} = w_1^{ij} + w_2^{ij}$  where,

$$\nabla \cdot (\epsilon_i^{r,N} w_1^{ij}) + \nabla \cdot [(\epsilon_i - \epsilon_0) \chi_{ij} w_1^{ij}] = \nabla \cdot [(\epsilon_i - \epsilon_0) \chi_{ij} g] \quad , \quad (37)$$

and,

$$\nabla \cdot (\epsilon_i^{r,N} w_2^{ij}) + \nabla \cdot [(\epsilon_i - \epsilon_0) \chi_{ij} w_2^{ij}] = \left( \frac{\epsilon_0 - \epsilon_r}{mN_i} \right) \nabla \cdot g \quad , \quad (38)$$

with,

$$\nabla \times w_1^{ij} = \nabla \times w_2^{ij} = 0 \quad .$$

Assuming  $\{y_{ij}^N\}$  is the location of the center of the individual scattering elements and knowing that  $\delta_i$  is small, it is possible to substitute  $g(y_{ij}^N) = g_{ij}$  in Eqs. (37 and 38). The solution for  $w_1^{ij}$  and  $w_2^{ij}$  as given by [Kohler 81] can then be written as,

$$w_1^{ij}(x) \simeq - \frac{\epsilon_0 - \epsilon_i}{3\epsilon_r + \epsilon_i - \epsilon_0} \delta_i^3 \nabla_x \left( \frac{g_{ij} \cdot (x - y_{ij}^N)}{|x - y_{ij}^N|^3} \right) \quad , \quad \text{for } |x - y_{ij}^N| > \delta_i \quad , \quad (39)$$

$$w_1^{ij}(x) \simeq - \frac{\epsilon_0 - \epsilon_i}{3\epsilon_r + \epsilon_i - \epsilon_0} g_{ij} \quad , \quad \text{for } |x - y_{ij}^N| < \delta_i \quad , \quad (40)$$

and,

$$w_2^{ij}(x) = \frac{(\epsilon_0 - \epsilon_r)}{4\pi\epsilon_r mN_i} \nabla_x \int \frac{(x - y) \cdot g(y)}{|x - y|^3} dy + w_3^{ij}(x) \quad , \quad (41)$$

where,

$$w_3^{ij}(x) \simeq \frac{\epsilon_0 - \epsilon_i}{3\epsilon_r + \epsilon_i - \epsilon_0} \frac{(\epsilon_0 - \epsilon_r)}{\epsilon_r mN_i} \delta_i^3 \nabla_x \left( \frac{g_{ij} \cdot (x - y_{ij}^N)}{|x - y_{ij}^N|^3} \right) \quad , \quad \text{for } |x - y_{ij}^N| > \delta_i \quad , \quad (42)$$



$$w_3^{ij}(x) \simeq \frac{\epsilon_0 - \epsilon_i}{3\epsilon_r + \epsilon_i - \epsilon_0} \frac{(\epsilon_0 - \epsilon_r)}{\epsilon_r m N_i} g_{ij} \quad , \quad \text{for } |x - y_{ij}^N| < \delta_i \quad , \quad (43)$$

where,  $\epsilon_i^{r,N} \simeq \epsilon_r$  when  $N_i$  is large.

Combining terms it is possible to write,

$$\begin{aligned} \sum_{j=1}^{N_i} (T_{ij}^r g)(x) &\simeq \frac{(\epsilon_0 - \epsilon_r)}{4\pi\epsilon_r m N_i} \nabla_x \int \frac{(x - y) \cdot g(y)}{|x - y|^3} dy \\ &- \frac{\epsilon_0 - \epsilon_i}{3\epsilon_r + \epsilon_i - \epsilon_0} \delta_i^3 \sum_{j=1}^{N_i} (1 - \chi_{ij}) \nabla_x \left( \frac{g_{ij} \cdot (x - y_{ij}^N)}{|x - y_{ij}^N|^3} \right) \\ &- \frac{\epsilon_0 - \epsilon_i}{3\epsilon_r + \epsilon_i - \epsilon_0} \sum_{j=1}^{N_i} \chi_{ij} g_{ij} + \sum_{j=1}^{N_i} w_3^{ij}(x) \quad . \end{aligned} \quad (44)$$

The  $w_3^{ij}(x)$  term in Eq. (44) is given by Eqs. (42 and 43) where its solution is seen to be  $O(N^{-1})$  on average when  $N \rightarrow \infty$  [Kohler 81]. Taking the expectation and choosing  $\epsilon_r$  such that,

$$\left\langle \sum_{i=1}^m \sum_{j=1}^{N_i} T_{ij}^r \right\rangle = 0 \quad . \quad (45)$$

will provide an optimal approximation to  $\epsilon^*$ .

This is the Coherent potential approximation, and demands that,

$$\frac{\epsilon_0 - \epsilon_r}{3\epsilon_r} = \sum_{i=1}^m \rho_i \frac{\epsilon_0 - \epsilon_i}{3\epsilon_r + \epsilon_i - \epsilon_0} \quad , \quad (46)$$

where  $\rho_i$  is the average number of scattering centers, of each class  $i$ , per unit volume, and can be defined for spherical scatterers as,  $\rho_i = 4/3\pi\delta_i^3 c_i$ , where  $c_i$  is defined as the average number of scatterers centers per unit volume.

Choosing  $\epsilon_r$  constrained by the above conditions, the effective dielectric constant can be approximated using the coherent potential approximation by evaluating Eq. (32),

$$\epsilon^* \simeq \epsilon_0 + \left( \sum_{i=1}^m \rho_i \epsilon_i - \rho \epsilon_0 \right) - (1-\rho) \epsilon_0 \left( \frac{\epsilon_0 - \epsilon_r}{3\epsilon_r} \right) + \left( \sum_{i=1}^m \rho_i \epsilon_i \cdot \frac{\epsilon_0 - \epsilon_i}{3\epsilon_r + \epsilon_i - \epsilon_0} \right) - \left( \sum_{i=1}^m \rho_i \epsilon_i \right) \left( \frac{\epsilon_0 - \epsilon_i}{3\epsilon_r + \epsilon_i - \epsilon_0} \right) \quad (47)$$

where,

$$\rho = \sum_{i=1}^m \rho_i \quad (48)$$

When the heterogeneous medium is composed of one class of embedded scatterer ( $m=1$ ) in the host medium, and the embedded scatterers are considered infinitely small particles that are uniformly distributed throughout the host medium, the coherent potential approximation may be obtained for Eq. (47),

$$\epsilon^*(\epsilon_0; \epsilon_1, \rho_1) \simeq \epsilon_0 \left( 1 + 3\rho_1 \left( \frac{\epsilon_1 - \epsilon_0}{2\epsilon_0 + \epsilon_1} \right) + \rho_1^2 \left( \frac{(\epsilon_1 - \epsilon_0)^2 (\epsilon_1^2 + 13\epsilon_0\epsilon_1 - 5\epsilon_0^2)}{\epsilon_0(\epsilon_1 + 2\epsilon_0)^3} \right) \right) \quad (49)$$

### 2.2.3 The Effective Medium Approximation

The results obtained from the Coherent Potential Approximation in Eqs. (47 and 49) can be contrasted with the result obtained from the effective medium theory (EMA) developed by [Elliot et al 1974] which results in the following expression,

$$\frac{\epsilon^* - \epsilon_0}{2\epsilon^* + \epsilon_0} (1-\rho) + \sum_{i=1}^m \rho_i \left( \frac{\epsilon^* - \epsilon_i}{2\epsilon^* + \epsilon_i} \right) = 0 \quad (50)$$

For the same conditions outlined in the solution of Eq. (49),  $\epsilon^*$  must satisfy,

$$\frac{\epsilon^* - \epsilon_0}{2\epsilon^* + \epsilon_0} (1-\rho) + \rho_1 \left( \frac{\epsilon^* - \epsilon_1}{2\epsilon^* + \epsilon_1} \right) = 0 \quad (51)$$

or that  $\epsilon^*(\epsilon_0; \epsilon_1, \rho_1)$  is the positive solution of,

$$2(\epsilon^*)^2 + \left( (\epsilon_1 - 2\epsilon_0) + 3(\epsilon_0 - \epsilon_1)\rho_1 \right) \epsilon^* - \epsilon_0 \epsilon_1 = 0 \quad , \quad (52)$$

which leads to the effective medium approximation for one embedded scatterer ( $m=1$ ) in a host medium,

$$\epsilon^*(\epsilon_0; \epsilon_1, \rho_1) \simeq \epsilon_0 \left( 1 + 3\rho_1 \left( \frac{\epsilon_1 - \epsilon_0}{2\epsilon_0 + \epsilon_1} \right) + 9\rho_1^2 \left( \frac{\epsilon_1 - \epsilon_0}{2\epsilon_0 + \epsilon_1} \right)^2 \left( \frac{\epsilon_1}{\epsilon_1 + 2\epsilon_0} \right) \right) \quad . \quad (53)$$

#### 2.2.4 The Self-Consistent Approximation

The most accurate estimation of the effective dielectric constant of a composite medium is obtained by using a recursive technique, where  $\epsilon^*$  is used as the reference medium in the Coherent Potential Approximation. This technique is known as the Self-Consistent Approximation and may be written for the general case as,

$$\epsilon^* = \frac{\langle \epsilon \rangle + \sum_{i=1}^m \rho_i \epsilon_i \left( \frac{\epsilon_0 - \epsilon_i}{3\epsilon^* + \epsilon_i - \epsilon_0} \right)}{1 + \sum_{i=1}^m \rho_i \left( \frac{\epsilon_0 - \epsilon_i}{3\epsilon^* + \epsilon_i - \epsilon_0} \right)} \quad . \quad (54)$$

For the specific conditions outlined in the derivations of Eqs. (49 and 53) the self-consistent approximation may be expressed as,

$$\epsilon^*(\epsilon_0; \epsilon_1, \rho_1) \simeq \frac{\langle \epsilon \rangle + \rho_1 \epsilon_1 \left( \frac{\epsilon_0 - \epsilon_1}{3\epsilon^*(\epsilon_0; \epsilon_1, \rho_1) + \epsilon_1 - \epsilon_0} \right)}{1 + \rho_1 \left( \frac{\epsilon_0 - \epsilon_1}{3\epsilon^*(\epsilon_0; \epsilon_1, \rho_1) + \epsilon_1 - \epsilon_0} \right)} \quad . \quad (55)$$

Therefore,  $\epsilon^*(\epsilon_0; \epsilon_1, \rho_1)$  for the self-consistent approximation is the positive solution to,

$$3(\epsilon^*)^2 + \left( (\epsilon_1 - 4\epsilon_0) + 4(\epsilon_0 - \epsilon_1)\rho_1 \right) \epsilon^* - \epsilon_0(\epsilon_1 - \epsilon_0)(1 - \rho_1) = 0 \quad . \quad (56)$$

### 2.3 Heterogeneous Media With M Classes of Embedded Scatterers

The derivation of the effective dielectric constants above are valid for a composite medium in which the particles  $\epsilon_1$  are uniformly mixed into the background medium  $\epsilon_0$ . The use of effective parameter approximations will substitute the heterogeneous mixture with  $\epsilon^*(\epsilon_0; \epsilon_1, \rho_1)$  being the effective dielectric constant of the medium.

It is possible to extend the case of  $m=1$  (one embedded scatterer in a host medium) to the case of several embedded scatterers in a host medium ( $m \geq 2$ ) by using an iterative procedure. When a background medium  $\epsilon_0$  contains the classes of embedded scatterers,  $\epsilon_1$  and  $\epsilon_2$ , the effective dielectric constant of the medium can be defined as  $\epsilon^*(\epsilon_0; \epsilon_1, \rho_1 / (1 - \rho_2))$  where the embedded particles are characterized by  $(\epsilon_2, \rho_2)$ . An alternate to this would be to determine the effective dielectric as  $\epsilon^*(\epsilon_0; \epsilon_1, \rho_2 / (1 - \rho_1))$  where the embedded scatterers are characterized by  $(\epsilon_1, \rho_1)$ . This recursive technique constructs models of media containing several classes of scatterers by embedding the "next" class of scatterers into a medium whose effective parameters have been derived for the "previous" classes of scatterers.

For the case of two embedded scatterers where the volume fractions,  $\rho_1$  and  $\rho_2$ , are in the low to moderate range,

$$\epsilon^*(\epsilon_0; \epsilon_1, \rho_1; \epsilon_2, \rho_2) \simeq \epsilon^*(\epsilon^*(\epsilon_0; \epsilon_1, \frac{\rho_1}{1 - \rho_2}); \epsilon_2, \rho_2) \quad , \quad (57)$$

or,

$$\epsilon^*(\epsilon_0; \epsilon_1, \rho_1; \epsilon_2, \rho_2) \simeq \epsilon^*(\epsilon^*(\epsilon_0; \epsilon_2, \frac{\rho_2}{1 - \rho_1}); \epsilon_1, \rho_1) \quad , \quad (58)$$

will yield good approximations of the effective dielectric constant of the composite medium. The terms  $\rho_1 / (1 - \rho_2)$  and  $\rho_2 / (1 - \rho_1)$  in Eqs. (57 and 58) represent the effective volume fractions of the intermediate mixtures of  $(\epsilon_0, \epsilon_1)$  and  $(\epsilon_0, \epsilon_2)$ , respectively. When  $\rho_1 < \rho_2$ , Eq. (57) will be the preferred approximation and if  $\rho_2 < \rho_1$ , Eq. (58) will be the preferred approximation.

To compute the effective dielectric constant of a medium with M classes of embedded scatterers, a technique similar to "iterated homogenization" [Bensoussan, Lions, and

Papanicolaou 1978] is applied. One can determine the approximation of  $\epsilon^*(\epsilon_0; \epsilon_1, \rho_1; \dots; \epsilon_m, \rho_m)$ , where  $\rho_i \leq \rho_{i+1}$ , by recursively adding scatterers to the "new" background medium in order of increasing density. The effective volume fraction of a scatterer of type  $j$  in the medium defined by the background medium and the first  $j$  scatterers  $(\epsilon_0, \epsilon_1, \dots, \epsilon_j)$  may be expressed,

$$\rho_j^M \triangleq \frac{\rho_j}{1 - \sum_{j=1}^M \rho_j} \quad (59)$$

Using this expression, the estimate of  $\epsilon^*$  can be expressed by,

$$\begin{aligned} \epsilon^*(\epsilon_0; \epsilon_1, \rho_1; \dots; \epsilon_M, \rho_M) &\simeq \epsilon^*\left(\epsilon_0; \epsilon_1, \frac{\rho_1}{(1 - \rho_M)}; \dots; \epsilon_{M-1}, \frac{\rho_{M-1}}{(1 - \rho_M)}\right); \epsilon_M, \rho_M \\ &\simeq \epsilon^*\left(\epsilon^*\left(\epsilon_0; \epsilon_1, \frac{\rho_1}{(1 - \rho_M - \rho_{M-1})}; \dots; \epsilon_{M-2}, \frac{\rho_{M-2}}{(1 - \rho_M - \rho_{M-1})}\right); \epsilon_{M-1}, \frac{\rho_{M-1}}{(1 - \rho_M - \rho_{M-1})}\right); \epsilon_M, \rho_M \\ &\simeq \epsilon^*\left(\epsilon^*\left(\dots \epsilon^*\left(\epsilon_0; \epsilon_1, \rho_1^M\right); \epsilon_2, \rho_2^M\right); \dots; \epsilon_{M-1}, \rho_{M-1}^M\right); \epsilon_M, \rho_M \end{aligned} \quad (60)$$

## 2.4 Applications of Effective Parameters

The effective dielectric constants can be used to determine the magnitude of an electric field that has propagated some distance through a heterogeneous random medium. For the values presented in this study, the heterogeneous media is a vegetation environment. The magnitude of the electric field can be determined by using the relationship,

$$\vec{E} = \vec{E}_0 \cdot \exp(jk_0 \sqrt{\epsilon^*} \cdot z) \quad , \quad (61)$$

where  $k_0 = 2\pi/\lambda$ ,  $\vec{E}_0$  is the magnitude of the incident electric field,  $\vec{E}$  is the magnitude of the electric field after propagating through the media,  $\epsilon^*$  is the effective complex

dielectric constant of the media, and  $z$  is the distance the wave travels through the media.

Application of the effective dielectric constants for foliage are numerous, but would be primarily of use in electromagnetic simulation programs where ray tracing techniques are employed. The effective parameters allow the simulation of vegetation covered terrain by treating the vegetation layer as a homogeneous dielectric slab that covers a rough surface (the ground). Simulating foliage as a dielectric slab provides a quick method that can reasonably account for the effects of a foliage layer without consuming a large amount of computer processing time. Inclusion of the effects of a vegetation covering will yield a more accurate representation of ground scattering in the presents of foliage covered terrain.

## 2.5 Model Limitations

The total field inside a vegetation medium can be mathematically divided into the sum of a mean, average, or coherent part and a zero mean fluctuating part [Brown 87],

$$\vec{E} = \langle \vec{E} \rangle + \delta \vec{E}_{fluc} \quad , \quad (62)$$

where  $\langle \cdot \rangle$  denotes average and  $\delta \vec{E}$  is a zero mean field quantity. For the application of effective parameters to describe the absorption and scattering of electromagnetic waves from a vegetation environment, certain conditions must be met. First, the average field  $\langle \vec{E} \rangle$  must be much greater than the zero mean fluctuation field  $\delta \vec{E}_{fluc}$ ,

$$\langle \vec{E} \rangle \gg \delta \vec{E}_{fluc} \quad . \quad (63)$$

Secondly, the difference between the wave numbers of the wave propagating in the vegetation medium and in free space should be less than the reciprocal of the maximum dimension of the embedded scatterers [Varadan 79],

$$(k - k_0) \cdot L < 1.0 \quad . \quad (64)$$

For spherical embedded scatterers  $L$  will be the on the order of the diameter of the spheres. The limitations of the frequency and scatterer dimension on the determination of the effective parameters of foliage media in this study will be bounded by,

$$(\sqrt{\epsilon^*} - 1) \left( \frac{2\pi}{\lambda_0} \right) \cdot L \leq 0.5 \quad , \quad (65)$$

where  $\epsilon^*$  is the effective complex dielectric constant of the foliage medium,  $L$  is the largest dimension of the embedded scatterers, and  $\lambda_0$  is the wavelength of the incident radiation. The condition given by Eq. (65) essentially requires that the scattering properties of a body in free space and in the random medium not be substantially different. Equation (65) was used to define the upper frequency bound that was used in this report. Knowing that the values of the effective complex dielectric constant of the vegetation were on the order of  $(1.1, 10^{-4})$  [Tamir 67], an incident radiation frequency of 3.2GHz would allow the maximum embedded scatterer dimension to be approximately 15 centimeters (the smallest practical dimension of vegetation scatterers) and still satisfy Eq. (65). Therefore the upper bound was established as 3.2GHz in this study. The maximum scatterer dimension is dependent on the frequency and actual value of  $\epsilon^*$  determined by the model and will vary as these parameters change.

### 3.0 DIELECTRIC CONSTANTS OF FOREST COMPONENTS

The model used in this report utilizes the transition matrix formalism, described in section 2, to determine approximations for the effective parameters that can be used to describe the dielectric characteristics of a heterogeneous random media. Input parameters to the model require a priori knowledge of the dielectric properties of the individual scatterers embedded within the host medium, as well as those of the host medium itself (air in this study). In the scope of this report we are concerned with the different dielectric constants of the materials that make up a natural terrain or forest. Discussion in this section will examine the methods used to determine the dielectric constants of tree trunks, branches, broad leaves, and needles that are expected to be found in a common forest.

The dielectric constant effectively relates the polarization and conduction effects to field quantities inside and outside an object. It is usually a complex quantity and can be expressed as,

$$\epsilon = \epsilon' - j\epsilon'' \quad , \quad (66)$$

where  $\epsilon'$  is the permittivity and  $\epsilon''$  is the loss factor resulting from propagation in a lossy media. The loss factor accounts for losses arising from polarization phenomena in the medium. The following sections contain a brief discussion of various methods that are used in this study to determine the dielectric properties of the individual components that make up a forest environment.

### 3.1 Dielectric Properties of Trees

Studies have been done [Broadhurst 70] to determine the dielectric properties of trees [Brown 80 and 82], [Skaar 49], [Yarvorski 51], [James 75]. Despite this, reliable dielectric measurements of living wood are scarce, although some data has been compiled for dry wood or lumber. The major difference between the dielectric properties of lumber and those of living wood are attributable to the moisture content of each. Some differences could be attributable to sap and other nutrients within the wood that may also affect the electrolytic nature of the wood, but these effects are secondary when compared to the moisture content [Brown 80].

#### 3.1.1 Physical Properties of Wood

The wood moisture content  $\mu$ , defined by wood technologists and forestry professionals, is defined in terms of the oven dry weight of the wood [Kollmann 68],

$$\mu = \frac{W_{\mu} - W_0}{W_0} \quad , \quad (67)$$

where  $W_{\mu}$  is the weight of the green moist wood and  $W_0$  is the weight after oven drying.



Taking this definition as a percentage ( $100 \times \mu$ ) it is readily observable that it is possible to have values of greater than 100%. This is not an uncommon occurrence in the moisture content of living wood. To obtain some estimates of the moisture content of living wood, the statistical data of 38 common hardwood, and 26 common softwood trees found in the USDA handbook of wood were analyzed [Brown 80]. Normalized distributions were developed to determine the distribution of water content found in hard and softwood trees, figure 1. From the curves it can be seen that the hardwood exhibits little or no change in the moisture content from the sap wood (outer layer) to the heart wood (core) with the typical moisture content being around 80%. Softwood trees (conifers), however, show great variance in moisture content from the outer sap wood layer to the inner core layer. This may be attributable to the relative dryness of the heart wood of conifers relative to their sap wood.

The density, or specific gravity, of wood can be defined as  $\rho = W_0/V_g$  where  $V_g$  is the volume of green wood. The density or specific gravity values vary greatly for all species of trees throughout the world (from 0.25 to 1.25). The more common species, found in more temperate climates, have a much smaller variation (0.3 to 0.7) [Brown 80]. These density values may be applied to either lumber or living wood because the definition prevents variation in moisture content from affecting values of density once  $V_g$  is established. During the search for the values of the dielectric constants of forest components, it was discovered that there is very little data available that reports these values with a great deal of confidence. Because of this, an exhaustive review of various reports was done to obtain as many possible sources that define these values both theoretically and experimentally. From the data collected, tables of permittivities and loss factors of wood and leaves were created using what appeared to be the most widely accepted experimental results or modeling techniques. As with most other reports examining the dielectric properties of living vegetation, the values of the dielectric constants used in this report will not be absolute and represent reasonable estimates of the dielectric constants of the vegetation for the specific conditions that are stated with each reported value. The results obtained using these values are intended to demonstrate trends that can be expected as various physical properties of foliage or external climate conditions change. The accuracy of these predictions can, ultimately, only be substantiated by corroboration of the results with experimental findings

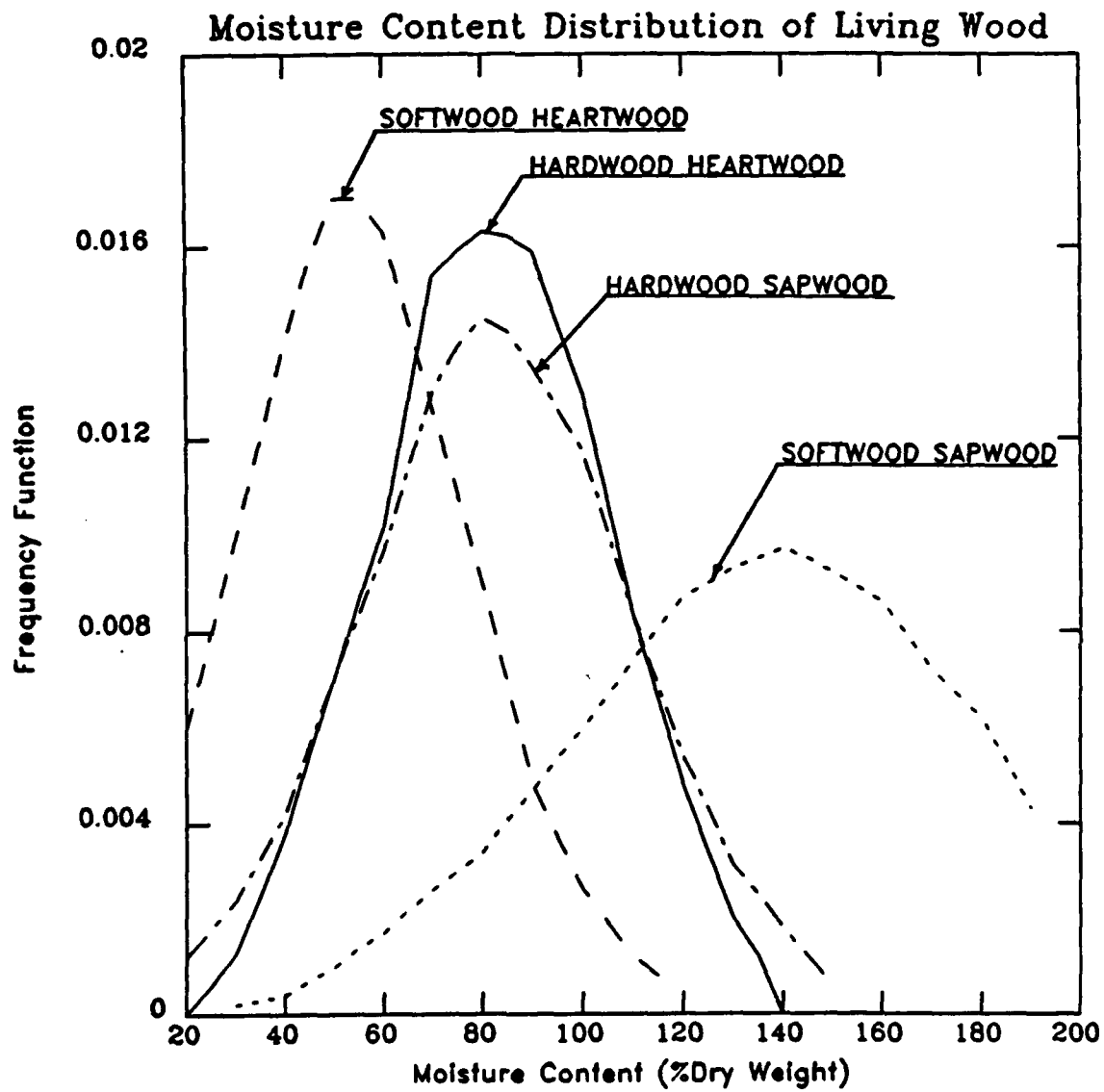


Figure 1. Normal distributions of typical dry weight moisture content for 38 hardwood and 26 softwood species.

### 3.1.2 Permittivity of Wood

A reasonable model to determine the permittivity of wood  $\epsilon'$  has been developed by [James 75] and further enhanced by [Brown 80]. The model includes the effects of polarization phenomenon as a function of frequency. Input parameters of the model are functions of the physical parameters affecting the dielectric properties of wood. The model is expressed as,

$$\epsilon' = a + \frac{b}{(1 + f/f_0)} + \frac{c}{f^l} \quad , \quad (68)$$

where  $a$  represents electronic and atomic polarization effects,  $b$  implies dipolar effects in which  $f_0$  is the center frequency in the range of influence,  $c$  denotes interfacial effects for which  $l$  differs slightly from 1.0. This model fits the data reported by [James 75] quite well. The model does substantiate one feature of  $\epsilon'$  for wood shown in the experimental data. At certain frequencies and beyond,  $\epsilon'$  becomes nearly a constant as the effects of  $c$  diminish. The leveling off seems to occur at frequencies beyond 20MHz. This feature proves to be very useful in predicting the value of  $\epsilon'$  over the range of frequencies of interest in this study, which fall within this plateau region where  $\epsilon'$  will only vary slightly as a function of frequency and will primarily vary as a function of the physical properties of the wood.

Determination of the actual values of  $\epsilon'$  for living wood reported by [Skaar 49] [James 75] and [Broadhurst 70] shows that  $\epsilon'$  increases as a nearly linear function of the moisture content  $\mu$  (with the density held constant) for moisture contents beyond 20-30%. Therefore, assuming the moisture content to be a constant quantity and proportional to the density, the permittivity can be determined with reasonable confidence independent of the frequency for hardwood and softwood species. To determine a range of values for  $\epsilon'$  for all trees, data representative of high and low density species were examined. Following the technique used by James, the trees were divided into two groups and a representative tree was selected from each group. The oak tree was selected as the hardwood representative and is a moderately high density hardwood, while the Douglas fir was selected as the representative softwood and is considered a medium density softwood. Using the data presented by James, which

extends to 50MHz, a range of the relative permittivities ( $\epsilon'_r = \epsilon'/\epsilon_0$ ) for the hardwoods and softwoods was produced and are shown in figures 2 and 3. The variations were produced by expanding the data based on a plus-or-minus one standard deviation from the mean of values produced for the hardwood and softwood species. It is expected that only a few species will fall outside the one standard deviation range, and that those who do will lie within a narrower spread due to the inverse relationship of  $\epsilon'_r$  and wood density [Brown 80].

As can be seen from figures 2 and 3, the relative permittivity of the hard and softwood s do not vary a great deal over the frequency range of interest in this report. The data reported from experimental measurements of the permittivity of living wood also exhibited this leveling off above 20MHz [Yavorsky 51], [Broadhurst 70], and [Skaar 49]. These data do however show a slight but constant downward trend in the magnitude of the permittivity as the frequency increases from the audio to radio to infra-red frequency bands. By close examination of these data it was determined that the permittivity consistently decreased over the frequency range of interest in this study. The permittivities reported in Tables 1 and 2 reflect this slight downward trend as the frequency increases. The magnitude of the changes were based on the results of experimental data reported for wood of similar densities and moisture contents [Broadhurst 70], [Yavorsky 51] and [Skaar 49]. The maximum change was observed in hardwood trees when the electric field polarization was perpendicular to the wood grain. In this case the dielectric constant decreased an average of 35% over the frequency range of interest, from a value of 23 at 50MHz to a value of 15 at 3.2 GHz. The minimum change observed was an 18% decrease in the dielectric constant over the same frequency range for softwood tree types when the electric field polarization was parallel to the wood grain. The slight decrease in the dielectric constant as the frequency increases may be attributable to the fact that at higher frequencies the time required for polarization to occur may be equal to or even exceed the period of alternation of the applied electric field. Therefore, the magnitude of the polarization decreases resulting in a subsequent decrease in the dielectric constant. Tables 1 and 2 contain the permittivities of hard and softwood trees when the electric field polarization is parallel and perpendicular to the wood grain, respectively. Experimental measurements confirm

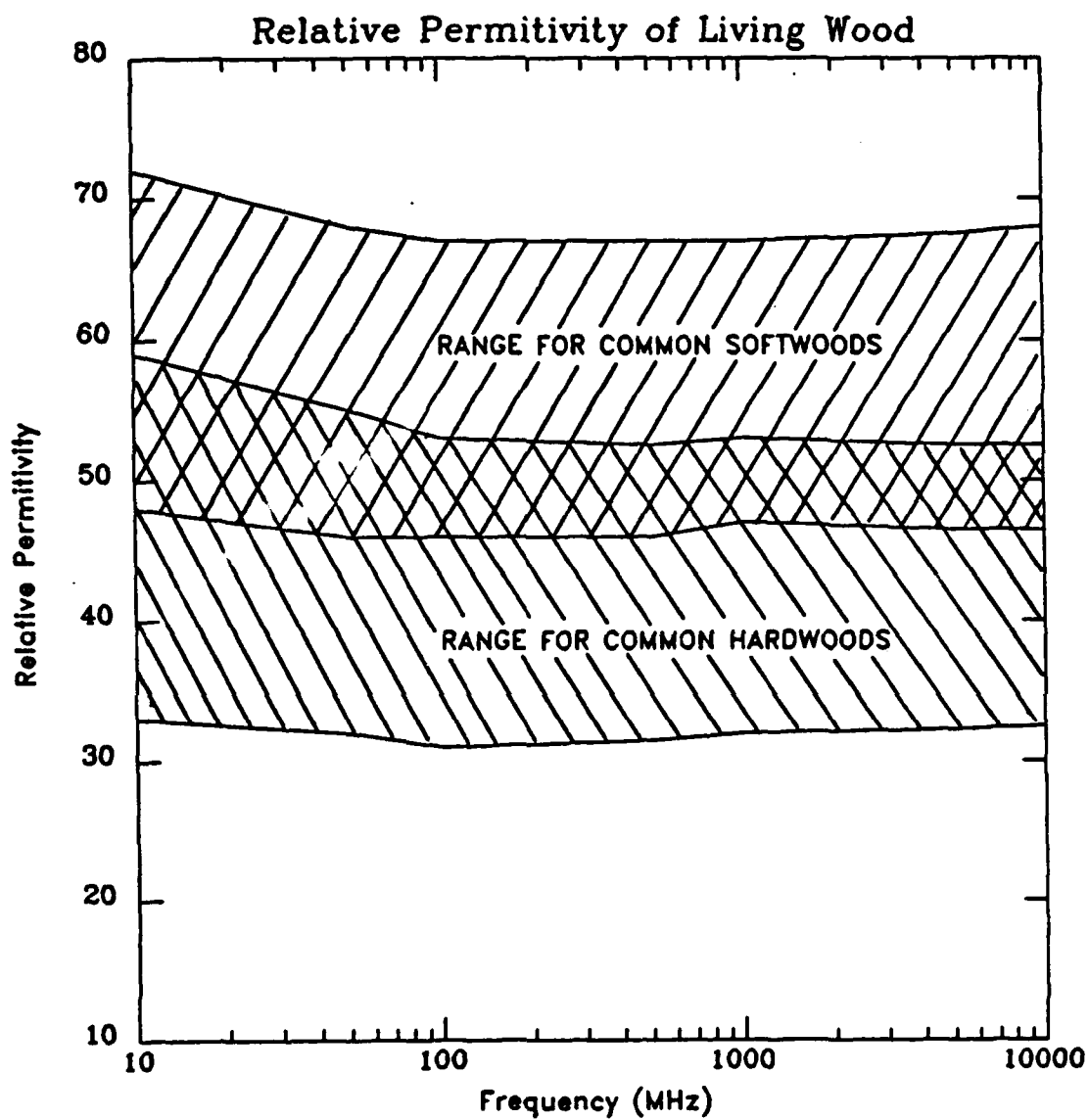


Figure 2. Range of the permittivity ( $\epsilon_r'$ ) for common species of live trees at 25°C. The electric field polarization is parallel to the wood grain.

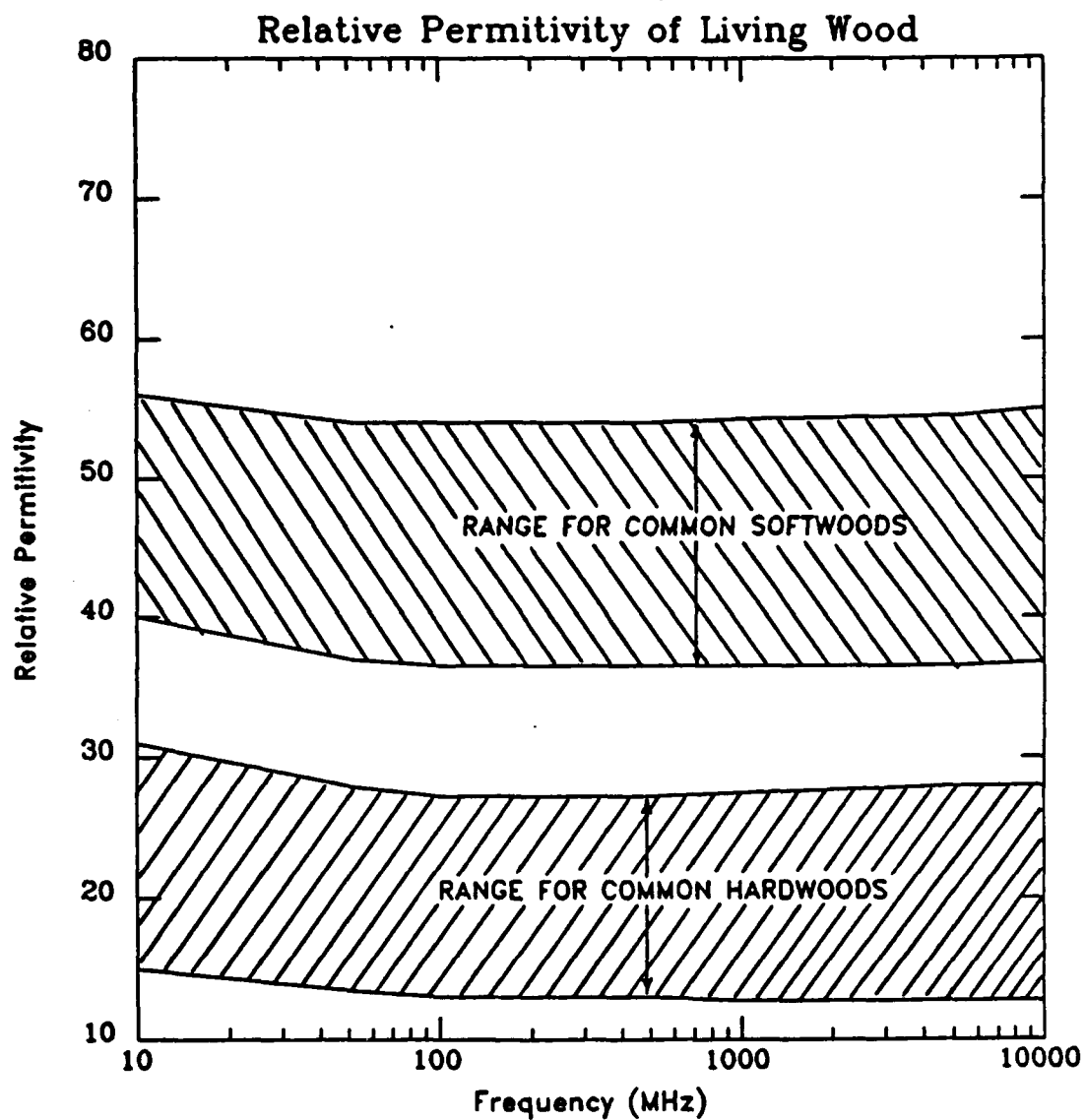


Figure 3. Range of the permittivity ( $\epsilon_r'$ ) for common species of live trees at 25°C. The electric field polarization is perpendicular to the wood grain.

[Skaar 49] that the permittivity of wood when the electric field is parallel to the wood grain orientation will be significantly greater than a corresponding perpendicular to the wood grain value. This effect may be attributable to the fact that cellulose (the primary organic component in wood) is composed of straight chain molecules which form crystallites whose long axes are parallel to the grain of the wood. Hydroxyl groups and chemically bounded water molecules located beside these chain molecules result in permanent dipoles whose rotation and displacement in an electric field have a direct affect on the dielectric constant. Therefore, when an electric field is impressed parallel to the long axes of these chains, a greater rotation is exhibited by these hydroxyl groups and water molecules than when the electric field is perpendicular to the chains [Yavorsky 51].

Complex Dielectric Constants of Wood Parallel E-Field										
WOOD TYPES	SEASON	Frequency (MHz)								
		50	100	200	400	600	800	1300	2400	3200
SOFT	WINTER	65	64	62	60	59	58	55	53	52
	SUMMER	61	60	59	58	57	56	53	52	50
HARD	WINTER	46	45	43	41	40	39	37	36	35
	SUMMER	43	42	41	41	40	39	36	35	33

Table 1. Permittivities of living hard and soft wood trees in summer and winter including a slight downward bias as frequency increases. Values reported here are for when the incident radiation electric field polarization is parallel to the wood grain.

Complex Dielectric Constants of Wood Perpendicular E-Field										
WOOD TYPES	SEASON	Frequency (MHz)								
		50	100	200	400	600	800	1300	2400	3200
SOFT	WINTER	55	53	51	50	48	46	44	42	40
	SUMMER	50	48	47	46	45	44	41	40	38
HARD	WINTER	25	24	23	22	21	20	18	17	16
	SUMMER	23	21	21	20	20	19	17	16	15

Table 2. Permittivities of living hard and soft wood trees in summer and winter including a slight downward bias as frequency increases. Values reported here are for when the incident radiation electric field polarization is perpendicular to the wood grain.

Values given in Tables 1 and 2 are further divided show the dielectric constants of hard and softwood species in both summer and winter seasons. The summer months are represented by an ambient air temperature of 25°C, while the winter months are represented by an ambient air temperature of 4°C. The permittivity of a particular tree type can be expected to increase as the ambient temperature approaches the freezing point [Brown 82]. The variation chosen here was based on the relative change in the permittivity of water for the same temperatures and frequencies as those used for the wood. For example, at 50Mhz the permittivity of water at 4°C is approximately 8% greater than at 25°C. Based on this it is reasonable to assume that the permittivity of wood will exhibit similar changes in magnitude as the dielectric constant of wood is extremely dependent on the water content of the wood. Experimental data reported seems to substantiate the slight increase in permittivity as temperature decreases but this conclusion was not apparent from the data all reports cited [Skaar 49], [Yavorsky 51], [Brown 82] and [Broadhurst 70].

Because of the complex nature of the dielectric properties of living wood and the ever changing conditions of the forest environment, the values presented in Tables 1 and 2 are not professed to be absolute, but are intended to represent reasonable estimates of these parameters for the stated conditions. Changes in any one of the input conditions could result in a significantly different value of permittivity.

### 3.1.3 Loss Factor of Wood

The variation of the loss factor with the physical properties of wood is more difficult to predict than the permittivity. A great disparity is reported to exist between the loss factor of cut wood [James 75] and a sample from a living tree branch [Brown 80] [Yavorsky 51]. The loss factor represents the loss of electromagnetic energy in a medium of propagation. The loss due to dipolar depolarization is sometimes the only type of loss considered in high frequency models for leaves and wood. In wood and leaves, water volume is considered to dominate the variation of  $\epsilon''$ , and so a mixing type of formula is generally based on the estimates of the water volume in a unit volume of material. A model to determine the wood loss factor, accounting for each type of dominant loss phenomenon, has been derived by [Brown 80] and is written,



$$\epsilon_r'' = \frac{A}{f^{1-m}} + \frac{B(f/f_c)}{1 + (f/f_c)^2} \quad , \quad (69)$$

where  $f_c$  is the critical or relaxation frequency of water, and  $f$  is the frequency of the incident electromagnetic radiation. The value of  $A$  is reported to be dependent on the dry weight moisture content of the wood and is given by,

$$A_c = (1.29 + 0.15\mu) \times 10^9 \quad , \quad (70)$$

for a combination of orientations of the grains relative to the electric field, and

$$A_p = (3.49 + 0.15\mu) \times 10^8 \quad , \quad (71)$$

for the electric field perpendicular to the grain. Brown also reported a value of 0.041 for  $m$ , and showed  $B$  as,

$$B = 43.4 + 8.1\mu \quad , \quad (72)$$

regardless of orientation. The critical frequency of water is reported to be 20 GHz for the summer season and 10 GHz for the winter season. Figure 4 depicts the loss factors of wood versus frequency using the model presented in Eq. (69). In figure 4 curves are shown for the winter and summer season and for the wood grain perpendicular to the incident electric field, as well as when the wood grain is randomly oriented relative to the electric field. The output of this model was compared to experimental data [Broadhurst 70] and compared favorably, although widespread application is doubtful.

Because of a paucity of the data above 1GHz with which the data can be compared to the model, the expression shown in Eq. (72) for  $B$  was not received with a great deal of confidence. To alleviate this discrepancy, experimental data was used [Studzman 79] to verify the output of the modeling of the loss factor. By doing this a revised expression for  $B$  was determined by Brown,

$$B = 0.07 + 29.5(\mu\rho) - 4.8(\mu\rho)^2 + 63(\mu\rho)^3 \quad , \quad (73)$$

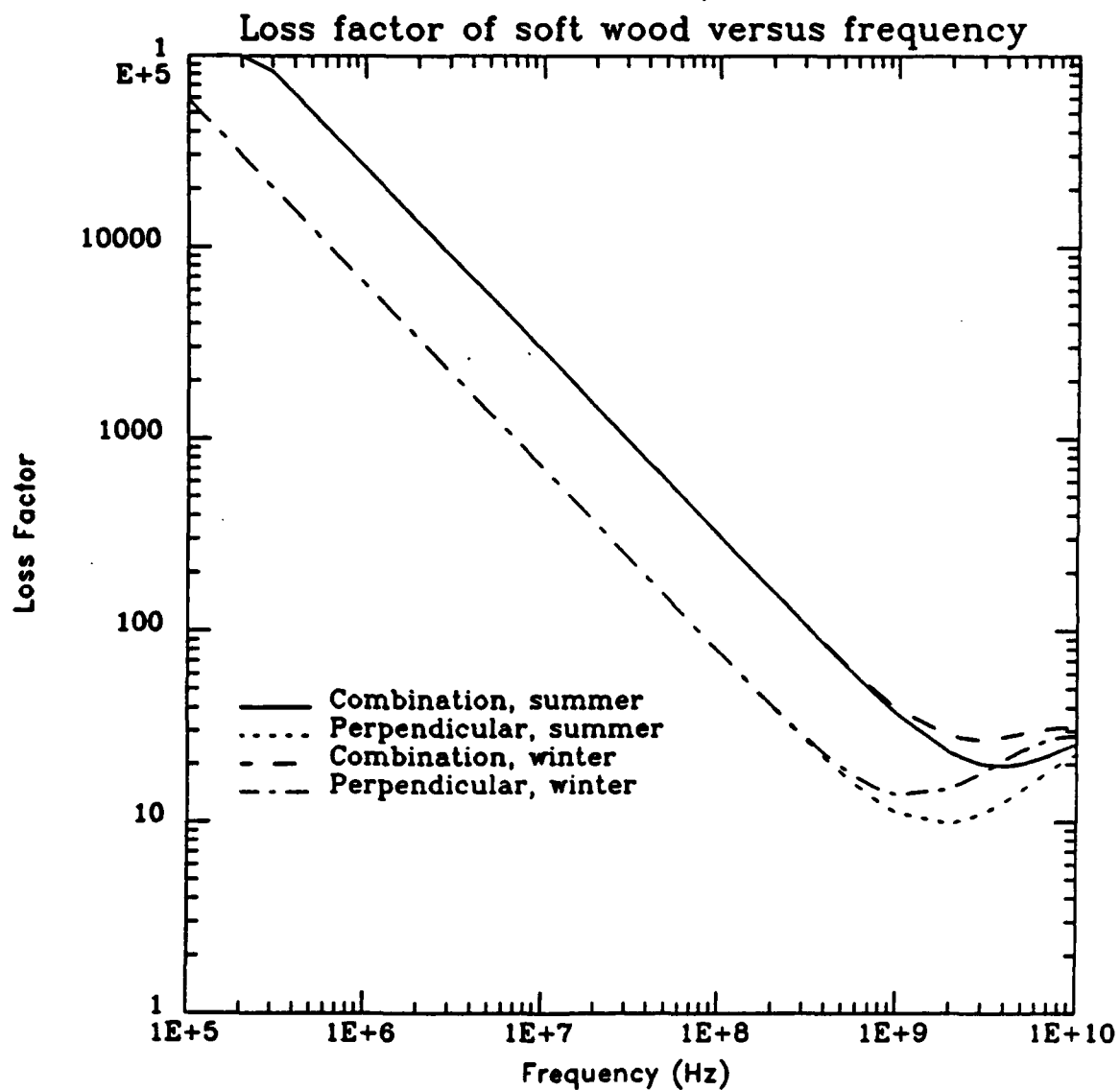


Figure 4. Model determination of the loss factor of softwood in summer and winter with random and perpendicular orientation of the wood grain to the electric field and a mean moisture content of 140%.

which results in a new expression for the loss factor of wood of,

$$\epsilon_r'' = \frac{A}{f^{0.96}} + \frac{[0.07 + 29.5(\mu\rho) - 4.8(\mu\rho)^2 + 63(\mu\rho)^3] \cdot (f/f_c)^{0.9}}{1 + 0.3129(f/f_c)^{0.9} + (f/f_c)^{1.8}}, \quad (74)$$

where  $A = 1.5E9$  when the wood grain has a combination of orientations relative to the incident electric field and  $A = 3.7E8$  when the electric field is perpendicular to the grain of the wood. Figure 5 depicts the output of the revised model given by Eq. (74) versus the frequency of the incident radiation using the same physical parameters that were used in the determination of figure 4. A better fit to the experimental data is obtained for values above the 1GHz range using the revised value for B. Two sets of curves were generated using the revised model, and are shown in figures 5 and 6. Figure 5 depicts the loss factor of softwood trees versus the frequency of the incident radiation, while figure 6 shows the loss factor of hardwood trees versus the frequency of the incident radiation. As can be seen, the frequency dependence of the loss factor relative to the frequency of the incident radiation is quite complex and may be considerable in magnitude. The plots in figures 5 and 6 contain separate curves demonstrating the effects of season and electric field polarization relative to the wood grain. The variation of the loss factor with respect to the temperature has been shown experimentally [Yavorsky 51] to decrease in moist wood as the temperature increases. This reversal is attributable to the fact that at higher temperatures the water dipoles experience less frictional effects. The correlation of the loss factor with the wood grain orientation relative to the electric field has not been established experimentally. It does seem reasonable to assume that the loss factor as measured with an electric field parallel to the wood grain would be greater than that with the electric field perpendicular to the grain as the model output shows in figures 5 and 6. The reason for this behavior may again be attributed to the basic structure of cellulose crystallites [Yavorsky 51].

Values of the loss factors of wood for conditions of interest in this study were determined using Eq(74) and are summarized in Tables (3-6) as a function of wood type, moisture content, frequency, season, and electric field orientation. Calculations of the softwood

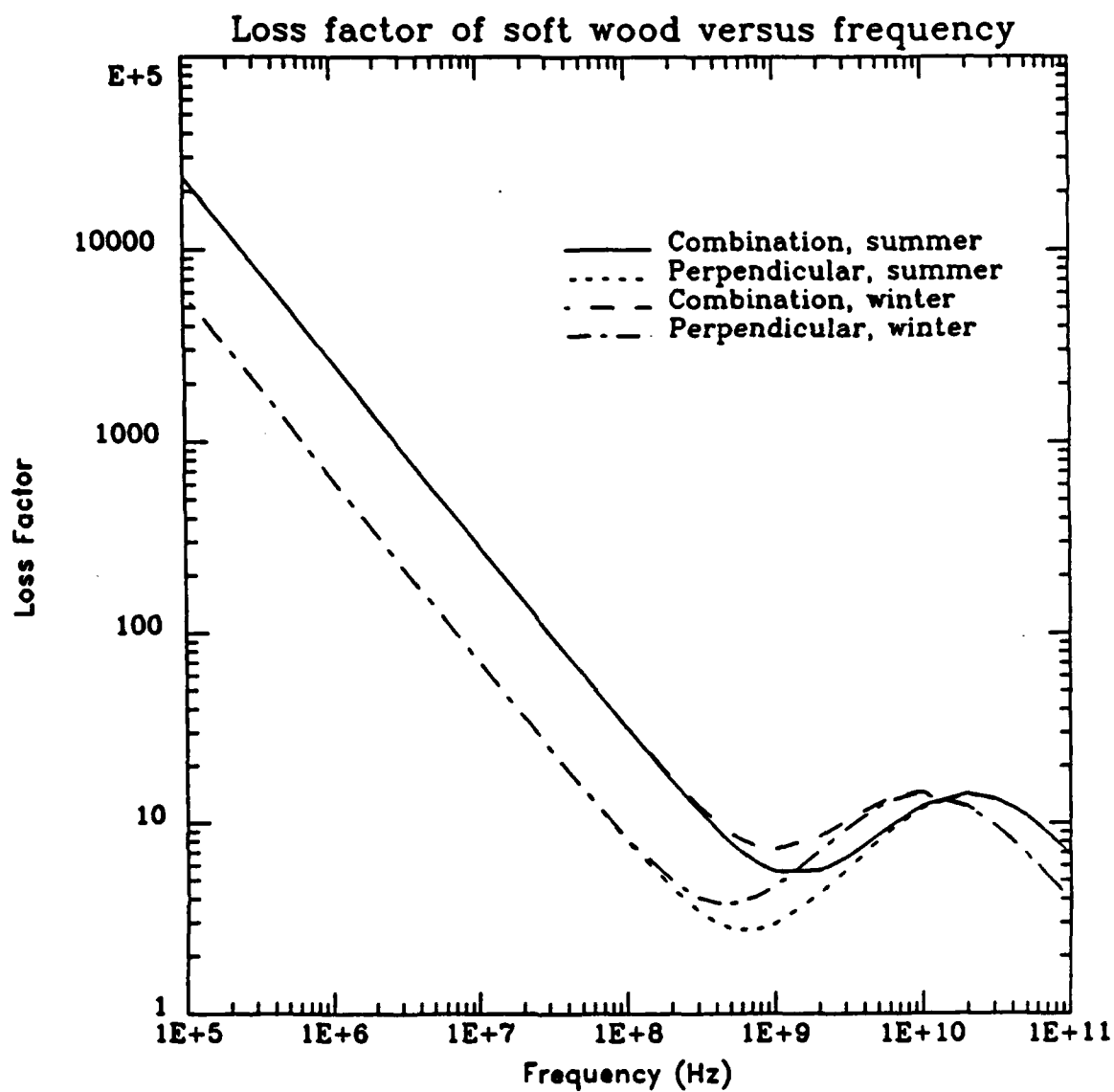


**Figure 5.** Revised model determination of the loss factor of softwood in summer and winter with random and perpendicular orientation of the electric field polarization relative to the wood grain and mean moisture content of 140%.

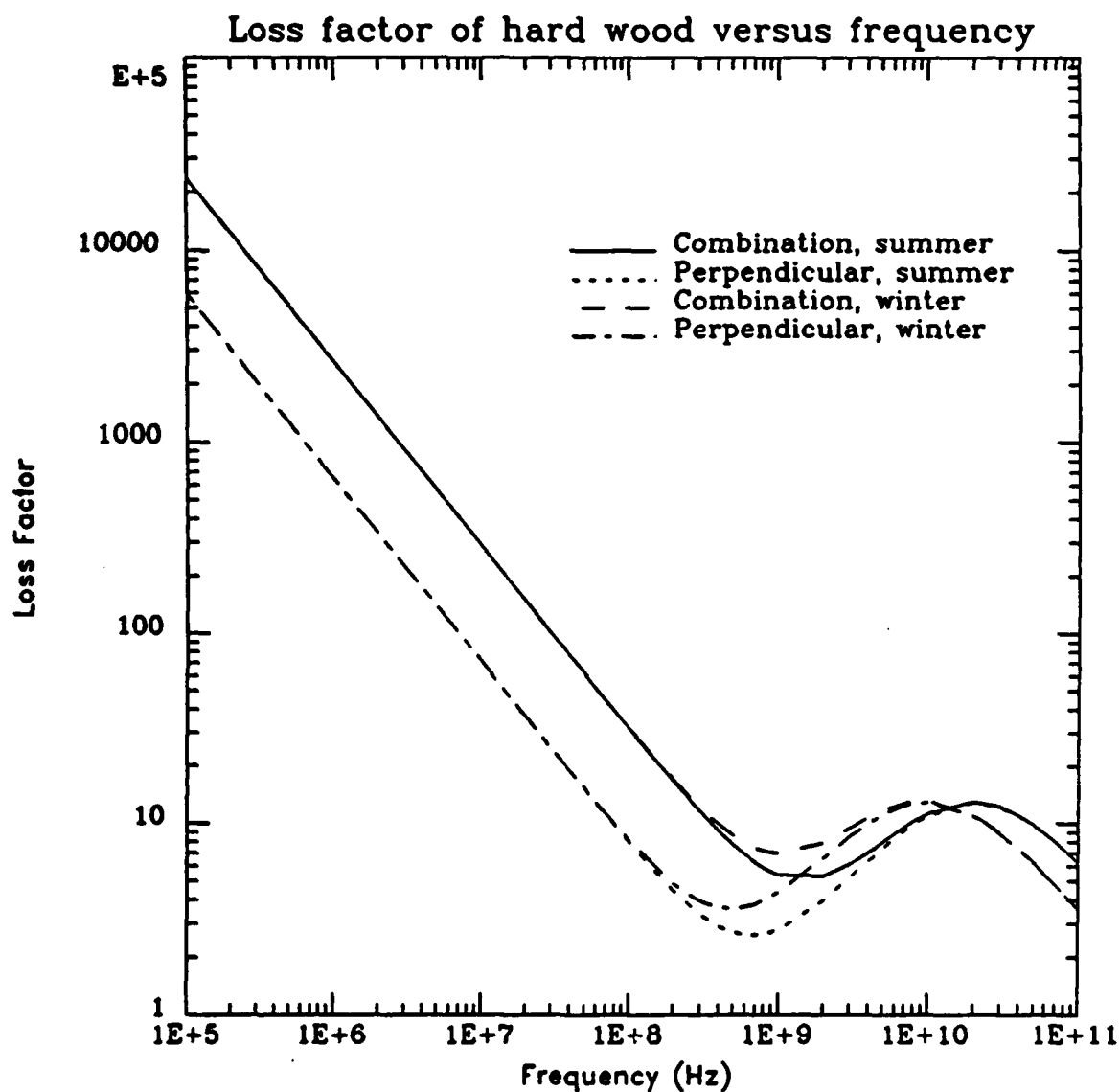


Figure 6. Revised model determination of the loss factor of hardwood in summer and winter with random and perpendicular orientation of the electric field polarization relative to the wood grain and mean moisture content of 80%.

values use a mean moisture content of 140% [Brown 80] and a wood density of 0.45 [Skaar 48], while hardwood values are calculated using a mean moisture content of 80% [Brown 80] and a density of 0.75 [Skaar 48].

Wood Grain Perpendicular to E-Field (Summer)									
Wood Type	Frequency (MHz)								
	50	100	200	400	600	800	1300	2400	3200
Softwood	15.2	8.01	4.50	3.01	2.78	2.85	3.40	5.00	6.10
Hardwood	15.2	7.98	4.41	2.91	2.63	2.65	3.11	4.48	5.47

Table 3. Loss factors of wood  $\epsilon_r''$  with the E-field perpendicular to the wood grain orientation, for variable frequencies, and wood types, in the summer season.

Wood Grain Perpendicular to E-Field (Winter)									
Wood Type	Frequency (MHz)								
	50	100	200	400	600	800	1300	2400	3200
Softwood	15.3	8.25	4.95	3.84	3.94	4.33	5.58	8.27	9.87
Hardwood	15.3	8.20	4.84	3.65	3.67	3.98	5.05	7.42	8.85

Table 4. Loss factors of wood  $\epsilon_r''$  with the E-field perpendicular to the wood grain orientation, for variable frequencies, and wood types, in the winter season.

Wood Grain Randomly Oriented to E-Field (Summer)									
Wood Type	Frequency (MHz)								
	50	100	200	400	600	800	1300	2400	3200
Softwood	61.1	31.6	16.6	9.23	6.98	6.02	5.36	6.00	6.82
Hardwood	61.1	31.6	16.6	9.15	6.86	5.86	5.12	5.60	6.32

Table 5. Loss factors of wood  $\epsilon_r''$  with the E-field arbitrary to the wood grain orientation, for variable frequencies, and wood types, in the summer season.

Wood Grain Randomly Oriented to E-Field (Winter)									
Wood Type	Frequency (MHz)								
	50	100	200	400	600	800	1300	2400	3200
Softwood	61.2	31.9	17.1	10.1	8.12	7.47	7.49	9.22	10.5
Hardwood	61.2	31.8	17.0	9.90	7.90	7.19	7.07	8.54	9.69

*Table 6. Loss factors of wood  $\epsilon_r''$  with the E-field arbitrary to the wood grain orientation, for variable frequencies, and wood types, in the winter season.*

### 3.2 Permittivity and Loss Factors of Leaves

To obtain a valid estimate of the effective parameters of a foliage medium, values describing the dielectric properties of individual leaves must be defined. Although some reports [Brown 82] site that the leaves on leaf-bearing trees can be ignored below frequencies of 3GHz, the scope of this study includes operating frequencies near this boundary which will necessitate the inclusion of the effects of leaves. There are very few sources in the literature that provide measured data for the dielectric constants of leaves. Those that are available [Broadhurst 70] [Ulaby 83], report the dielectric constants of only certain types of leaves and for a limited number of incident radiation frequencies. For the application here, values are needed for a wide frequency spectrum (50MHz to 3.2GHz), variable climate conditions, and variable moisture content of the leaves. To obtain approximations for these constants for the wide variety of conditions necessary, it was decided to use modeling techniques that determine the dielectric constants of the leaves based on the moisture content of the leaves, ambient air temperature, and incident radiation frequency.

Various reports are available that include examination of methods to create a reliable model to determine the dielectric properties of individual leaves [Bush 76], [Fung 78], [Brown 82]. Most reports cited consider a leaf to be a mixture of organic leaf material and liquid water. A leaf can be modeled by considering the leaf to be comprised of a background medium composed of organic material and that ellipsoidal disks of water are randomly distributed throughout this material. DeLoor proposed a dielectric mixing model based on

these assumptions and determined a dielectric mixing formula that is a function of the volume fraction of the water inclusions and the dielectric constants of the host material and water [DeLoor 68],

$$\epsilon_i = \epsilon_b - \frac{V_w}{3} \cdot (\epsilon_b - \epsilon_w) \left( 2 + \frac{\epsilon_i}{\epsilon_w} \right) \quad (75)$$

In Eq. (75),  $\epsilon_i$  is the relative complex dielectric constant of the mixture,  $\epsilon_b$  is the relative complex dielectric constant of the host material,  $\epsilon_w$  is the relative complex dielectric constant of the inclusions, and  $V_w$  is the volume fraction of the inclusions. For the vegetation leaf,

$$\epsilon_i = \epsilon'_i + j\epsilon''_i \quad , \quad (76a)$$

$$\epsilon_b = \epsilon'_b + j\epsilon''_b \quad , \quad (76b)$$

and,

$$\epsilon_w = \epsilon'_w + j\epsilon''_w \quad . \quad (76c)$$

Because  $\epsilon''_w$  can be expected to be several orders of magnitude greater than  $\epsilon''_b$  in the microwave region, the latter will have negligible effect on the dielectric constant of the mixture and can be taken to be zero. The permittivity of the bulk material  $\epsilon'_b$  is reported to range from 2.4 to 5.0 [DeLoor 68]. A value of  $\epsilon'_b = 3.0$  will be adopted here as it has been shown [Ulaby 83] that it will result in good agreement with experimental measurements. Thus, substituting the dielectric constant of the bulk material  $\epsilon_b = 3.0 + j0.0$  into Eq. (75) and rearranging terms leads to the expression,

$$(\epsilon'_i - j\epsilon''_i) \left( 1 - \frac{V_w}{3} \cdot \left( 1 - \frac{\epsilon'_b}{\epsilon'_w - j\epsilon''_w} \right) \right) = \epsilon'_b \left( 1 - \frac{2V_w}{3} \right) + \frac{2V_w}{3} \cdot (\epsilon'_w - j\epsilon''_w) \quad (77)$$

As suggested in [Ulaby 83], the relationship,

$$\epsilon'_w - j\epsilon''_w = \frac{(\epsilon'_w)^2 + (\epsilon''_w)^2}{\epsilon'_w + j\epsilon''_w} \triangleq \frac{|\epsilon_w|^2}{\epsilon'_w + j\epsilon''_w} \quad , \quad (78)$$



can be used to simplify the left side of Eq. (76). By equating the real and imaginary parts of the above equations it is possible to write,

$$\epsilon'_i \left(1 - \frac{V_w}{3}\right) + \frac{V_w}{3} \cdot \frac{\epsilon'_b}{|\epsilon_w|^2} \cdot (\epsilon'_i \epsilon'_w + \epsilon''_i \epsilon''_w) = \epsilon'_b \left(1 - \frac{2V_w}{3}\right) + \frac{2V_w}{3} \cdot \epsilon'_w \quad , \quad (79)$$

and,

$$\epsilon''_i \left(1 - \frac{V_w}{3}\right) + \frac{V_w}{3} \cdot \frac{\epsilon'_b}{|\epsilon_w|^2} \cdot (\epsilon''_i \epsilon'_w - \epsilon'_i \epsilon''_w) = \frac{2V_w}{3} \cdot \epsilon''_w \quad . \quad (80)$$

Equations (79 and 80) can be solved simultaneously to define independent expressions for  $\epsilon'_i$  and  $\epsilon''_i$ . The solutions can be simplified by noting that the ratio of  $\epsilon''_w/\epsilon'_w$  is much smaller than unity except for frequencies near the relaxation frequency of water. From this it can be ascertained that the ratio of  $\epsilon''_i/\epsilon'_i$  is also much smaller than unity since  $\epsilon''_b = 0$ . Therefore, the simplification,

$$\epsilon'_i \epsilon'_w - \epsilon''_i \epsilon''_w = \epsilon'_i \epsilon'_w \left(1 - \frac{\epsilon''_i \epsilon''_w}{\epsilon'_i \epsilon'_w}\right) \simeq \epsilon'_i \epsilon'_w \quad , \quad (81)$$

is valid. Using the approximation shown in Eq. (81) the real and imaginary parts of the leaf dielectric constant can be expressed by,

$$\epsilon'_i = \frac{\epsilon'_b + \frac{2V_w}{3} \cdot (\epsilon'_w - \epsilon'_b)}{1 + \frac{V_w}{3} \cdot \left(\frac{\epsilon'_b \epsilon'_w}{|\epsilon_w|^2} - 1\right)} \quad , \quad (82)$$

and,

$$\epsilon''_i = \frac{\frac{V_w}{3} \epsilon''_w \cdot \left(2 + \frac{\epsilon'_b \epsilon'_i}{|\epsilon_w|^2}\right)}{1 + \frac{V_w}{3} \cdot \left(\frac{\epsilon'_b \epsilon'_w}{|\epsilon_w|^2} - 1\right)} \quad . \quad (83)$$

For a known set of values of  $\epsilon'_b$ ,  $\epsilon_w$ , and  $V_w$  Eq. (82) can be used to determine  $\epsilon'_i$  which can then be used in Eq. (83) to obtain a value for  $\epsilon''_i$ .

The dielectric constant of water is very dependent upon the temperature and salinity of the water. For the work being done here the temperature range of interest is 4°C to 25°C which is large enough to cause a significant change in the dielectric constant of water. Additionally the salinity of water should be considered. According to information on the chemical properties of leaves, the salinity can be as high as 12%. Changes in salinity have little effect on  $\epsilon'_w$  but can have great influence on  $\epsilon''_w$ , and this influence increases in importance with decreasing microwave frequencies [Ulaby 83]. As an example,  $\epsilon''_w$  increases from 4.37 for S=0 to 29.17 for S=9%, where S is the salinity in parts per thousand on a percent weight basis.

The real and imaginary parts of the dielectric constant of saline water are given by [Ulaby 83],

$$\epsilon'_{sw} = \epsilon_{sw\infty} + \frac{\epsilon_{sw0} - \epsilon_{sw\infty}}{1 + (2\pi f\tau_{sw})^2} \quad , \quad (84)$$

and,

$$\epsilon''_{sw} = \frac{2\pi f\tau_{sw}(\epsilon_{sw0} - \epsilon_{sw\infty})}{1 + (2\pi f\tau_{sw})^2} + \frac{\sigma_i}{2\pi\epsilon_0 f} \quad , \quad (85)$$

where  $\epsilon_{sw0}$  is the static dielectric constant of saline water,  $\epsilon_{sw\infty}$  is the high-frequency (or optical) limit of  $\epsilon_{sw}$ , (both of which are dimensionless),  $\tau_{sw}$  is the relaxation time of saline water in seconds,  $f$  is the electromagnetic frequency in Hz,  $\sigma_i$  is the ionic conductivity of the aqueous solution in  $\Omega^{-1}\text{m}^{-1}$ , and  $\epsilon_0$  is the permittivity of free space ( $\epsilon_0 = 8.854\text{E-}12 \text{ Fm}^{-1}$ ). The value of the high-frequency dielectric constant is 4.9 and there appears to be no evidence to indicate a dependence on salinity [Lane 52] [Stogryn 71].

The dependence of  $\epsilon_{sw0}$  on the salinity  $S_{sw}$  (%) and temperature  $T$  (°C) is given by,

$$\epsilon_{sw0}(T, S_{sw}) = \epsilon_{sw0}(T, 0) \cdot a(T, S_{sw}) \quad , \quad (86)$$

where,

$$\epsilon_{sw0}(T, 0) = 87.134 - 1.949\text{E-}1 \cdot T - 1.276\text{E-}2 \cdot T^2 + 2.491\text{E-}4 \cdot T^3 \quad , \quad (87)$$

and

$$a(T, S_w) = 1.0 + 1.613E-5 \cdot TS_w - 3.656E-3 \cdot S_w + 3.210E-5 \cdot S_w^2 - 4.232E-7 \cdot S_w^3, \quad (88)$$

These expressions are polynomial fits to experimental data and are considered valid for salinities of  $4 \leq S_w \leq 35\%$  [Ulaby 83].

The relaxation time of saline water is defined in a similar manner to that used in the determination of  $\epsilon_{w0}$ . The polynomial expression that is used to define the relaxation time of saline water can be expressed,

$$\tau_{sw}(T, S_w) = \tau_{sw}(T, 0) \cdot b(T, S_w), \quad (89)$$

where  $\tau_{sw}(T, 0)$  is the relaxation time of pure water and  $b(T, S_w)$  is a polynomial fit to experimental data [Grant 57] and derived by [Stogryn 71] and [Klein 77] that is given by,

$$b(T, S_w) = 1.0 + 2.282E-5 \cdot TS_w - 7.638E-4 \cdot S_w - 7.760E-6 \cdot S_w^2 + 1.105E-8 \cdot S_w^3, \quad (90)$$

Equation (90) is considered valid when  $0 \leq S_w \leq 157\%$  and  $0 \leq T \leq 40^\circ\text{C}$ .

The final parameter is the ionic conductivity  $\sigma_i$ , which was derived by [Weyl 64] and [Stogryn 71] and is expressed,

$$\sigma_i(T, S_w) = \sigma_i(25, S_w)e^{-\phi}, \quad (91)$$

where  $\sigma_i(25, S_w)$  is the ionic conductivity of sea water at  $25^\circ\text{C}$  which is given by,

$$\sigma_i(25, S_w) = S_w(0.18252 - 1.4619E-3S_w + 2.093E-5S_w^2 - 1.282E-7S_w^3), \quad (92)$$

The function  $\phi$  is dependent on  $S_w$  and  $\Delta = 25 - T$ , and is given by,

$$\phi = \Delta(2.033E-2 + 1.266E-4\Delta + 2.464E-6\Delta^2 - S_{sw}(1.849E-5 - 2.551E-7\Delta + 2.551E-8\Delta^2)) \quad , \quad (93)$$

Equations (92 and 93) are valid for  $0 \leq S_{sw} \leq 40\%$ .

The dielectric constants of leaves under various conditions of interest in this study have been computed, using the models described above, and are shown in Tables 7 and 8. The leaf used in the calculation has a moisture content of 65% and salinity of 6%. These values are by no means expected to be constants but are representative of what could be considered reasonable values for a leaf. To arrive at the dielectric values for the leaves, the dielectric constant of water, at the frequency of interest, is first determined using Eqs. (84 and 85). These values are then substituted into Eqs. (82 and 83) to determine the dielectric constants of the leaves. The values calculated by the model compared favorably with experimental data found in the literature for leaves for similar physical and environmental conditions [Ulaby 82], [Brown 82], [Broadhurst 70], [Lang 83], and [Ulaby 86].

Temp	Frequency (MHz)								
	50	100	200	400	600	800	1300	2400	3200
4°C	48.9	48.9	48.7	48.5	48.3	48.2	47.8	46.3	44.7
25°C	44.6	44.7	44.6	44.5	44.3	44.3	44.0	43.4	43.0

Table 7. Permittivity of broad leaves and needles for leaves with moisture content of 65% and salinity of 6%.

Temp	Frequency (MHz)								
	50	100	200	400	600	800	1300	2400	3200
4°C	126.0	64.0	32.0	18.0	13.0	11.0	11.0	12.0	14.0
25°C	209.0	105.0	53.0	27.0	19.0	15.0	11.0	10.0	11.0

Table 8. Loss factors of broad leaves and needles for leaves with moisture content of 65% and salinity of 6%.

### 3.3 Density of Forest Components

Having defined values for the electrical properties of forest constituents (wood and leaves), quantitative values describing the density of the various foliage components must be established. The most typical parameter used to define the density of foliage is the volume fraction that the foliage components occupy in a typical forest. The volume fraction is defined as the ratio of volume occupied by foliage components to the total volume of the layer containing the forest environment. Quantitative measurements of the volume fractions of forests are sparse, and determination of a valid estimate requires the development of sophisticated modeling programs. Although models are available to determine the volume fractions of forests stands [Brown 82], [Brown 80], [Ulaby 86], and [Ulaby 79], actual values of volume fractions can be expected to vary a greatly depending on the region, season and weather pattern. The data presented in this study is given as a function of the volume fraction, which allows the reader to determine the volume fraction of a forest stand of interest and obtain the effective dielectric constants of the forest associated with that volume fraction. Therefore, the only task is to determine a suitable range of volume fractions over which to do the calculation of the effective dielectric constants that will be representative of typical forest environments.

From the literature reviewed, it was found that in the typical mature forest the wood will occupy approximately 1.0% of the total volume. In some cases, well managed forests can attain wood volume fractions in the vicinity of 5.0%. This is considered an extreme case. It is interesting to note that the jungle forests of Southeast Asia were found to have wood volume fractions somewhat below the average of 1.0%. This result was attributed to the lack of large trees or the underbrush limiting effects of the relatively dense canopy comprised of mostly leaves [Brown 82]. For the purpose of this work, calculations will be done for wood volume fractions over a range of 0.01% to 5.0%. The data is divided into two segments, one for a sparse forest (volume fractions from 0.01% to 1.0%) and the other for dense forest (volume fractions of 1.0% to 5.0%).

The volume fraction of broad leaves or needles, was typically reported to be between 10 to 25 percent of the volume fraction occupied by the wood. Therefore, the volume fractions

of leaves in this report will be consistently reported as 10% percent of the total volume fraction which is considered typical [Brown 83]. It is the intent to used a range volume fractions significantly broad so that most all possible forest stands, with similar vegetation composition, can at least be approximately represented.

#### 4.0 EXAMPLE CALCULATIONS

The model, in its present form, produces plots of the effective permittivity and loss factor versus the volume fraction of the embedded scatterer. If there are multiple embedded scatterer types comprising the heterogeneous medium, the model is capable of varying the volume fraction of only one of the embedded scatterers in any one calculation. Because in most cases wood will represent up to 95% of the total embedded scatterers volume fraction in a forest environment, wood was the scatterer varied in all of the example calculations presented in this report. Plots produced using the model that represent the effective complex dielectric constants of a forest environment composed of hardwood tree types with the wood grain randomly oriented with respect to the electric field polarization at a temperature of 25°C are shown in Figures 7 through 15. Each plot represents the calculation of the effective dielectric constants of the forest environment for a different incident radiation frequency from 50MHz to 3.2GHz. The input dielectric constants were obtained using the models described in section 3.0 of this report. The volume fraction of the leaves in Figures 7 through 15 were taken to be 0.001, and the volume fraction of the wood was varied from 0.0001 to 0.05. All plots contain four curves showing the results of calculations using the ATA, CPA, EMA, and MOD\_ATA (which are all discussed in Section 2.0). It is apparent that the estimations provided by the ATA, EMA, and CPA all show good agreement with one another. The MOD\_ATA, however, appears to produce poor agreement with the other estimations. The discrepancy could perhaps be attributable to the large difference between the complex dielectric constant of the background medium and those of the embedded scatterers as the MOD\_ATA was consistently off scale, higher than all of the other estimations. The magnitude of the effective parameters reported in the literature correspond with the values calculated using the ATA, CPA, and EMA. Effectively, this would mean that the calculation of the effective parameters of a heterogeneous medium using the MOD\_ATA method is limited to media whose embedded

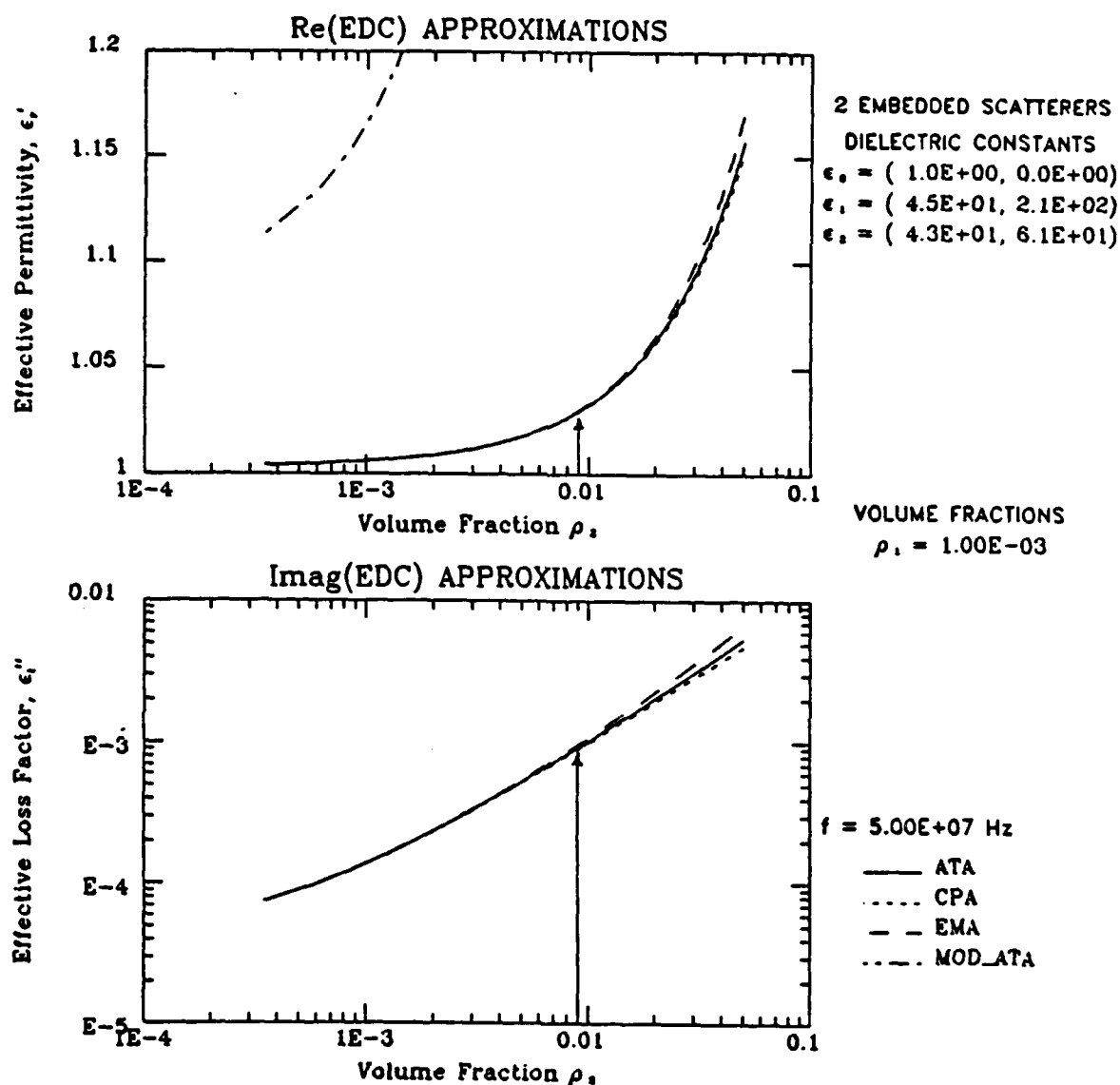


Figure 7. Effective complex dielectric constants ( $\epsilon^*$ ) of a vegetation environment versus the volume fraction of the wood component. The values represent a vegetation environment comprised of hardwood foliage at 25°C with the wood grain randomly oriented with respect to the electric field polarization. Leaf moisture content is 65%, leaf salinity is 6% and the leaf volume fraction is 0.1%. Values are calculated for an incident radiation frequency of 50MHz.

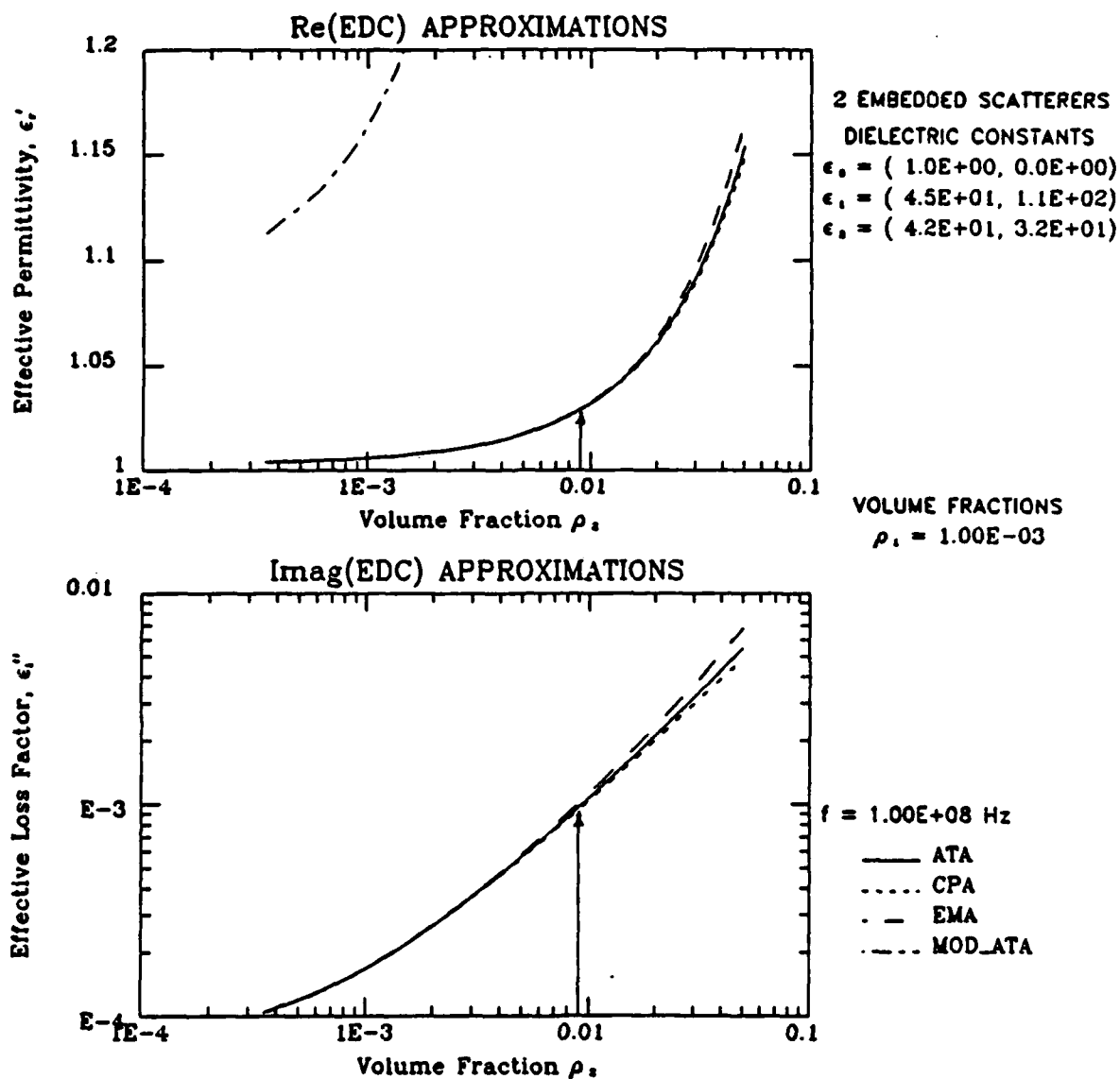


Figure 8. Effective complex dielectric constants ( $\epsilon^*$ ) of a vegetation environment versus the volume fraction of the wood component. The values represent a vegetation environment comprised of hardwood foliage at 25°C with the wood grain randomly oriented with respect to the electric field polarization. Leaf moisture content is 65%, leaf salinity is 6% and the leaf volume fraction is 0.1%. Values are calculated for an incident radiation frequency of 100MHz.



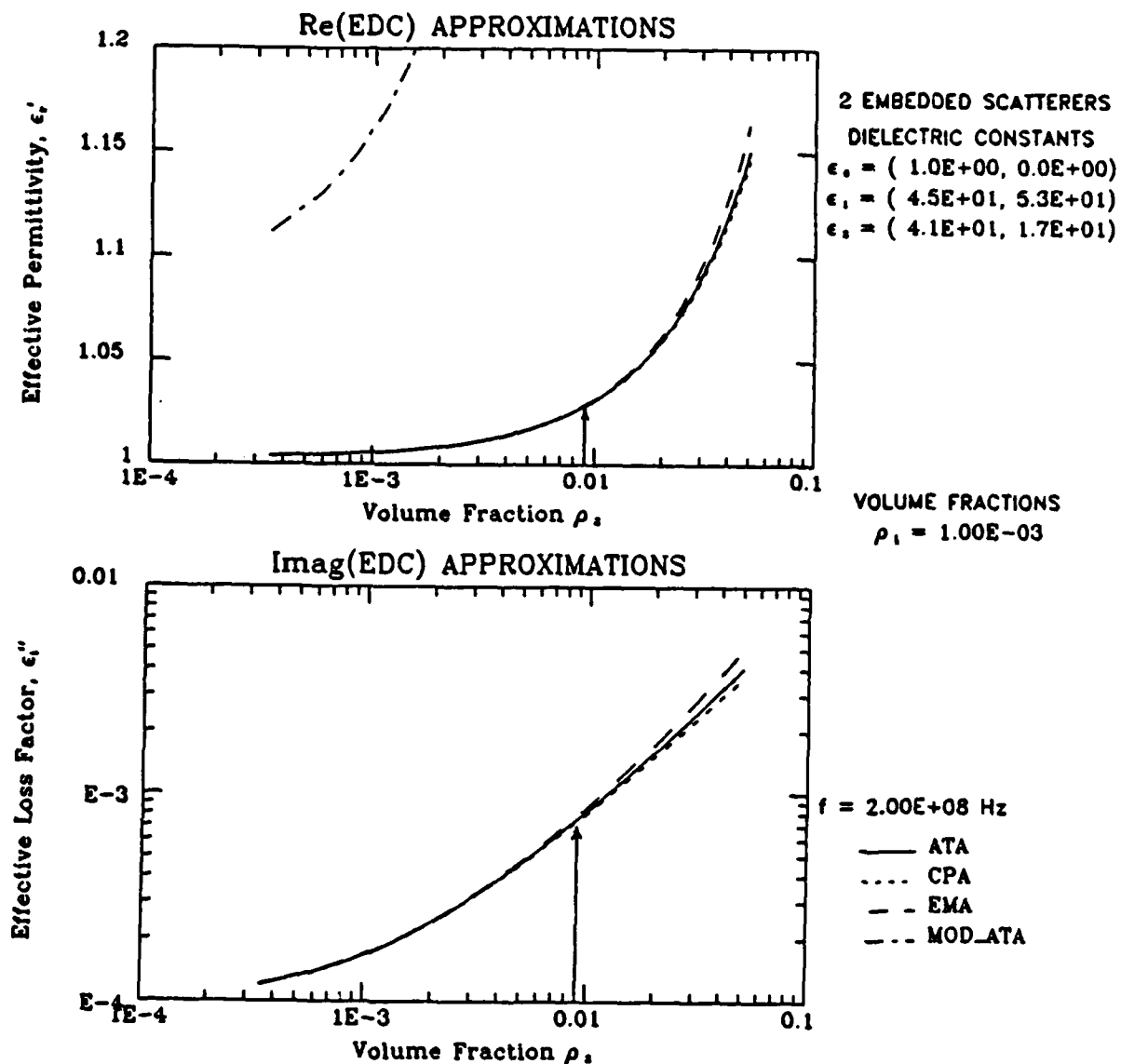


Figure 9. Effective complex dielectric constants ( $\epsilon^*$ ) of a vegetation environment versus the volume fraction of the wood component. The values represent a vegetation environment comprised of hardwood foliage at 25°C with the wood grain randomly oriented with respect to the electric field polarization. Leaf moisture content is 65%, leaf salinity is 6% and the leaf volume fraction is 0.1%. Values are calculated for an incident radiation frequency of 200MHz.

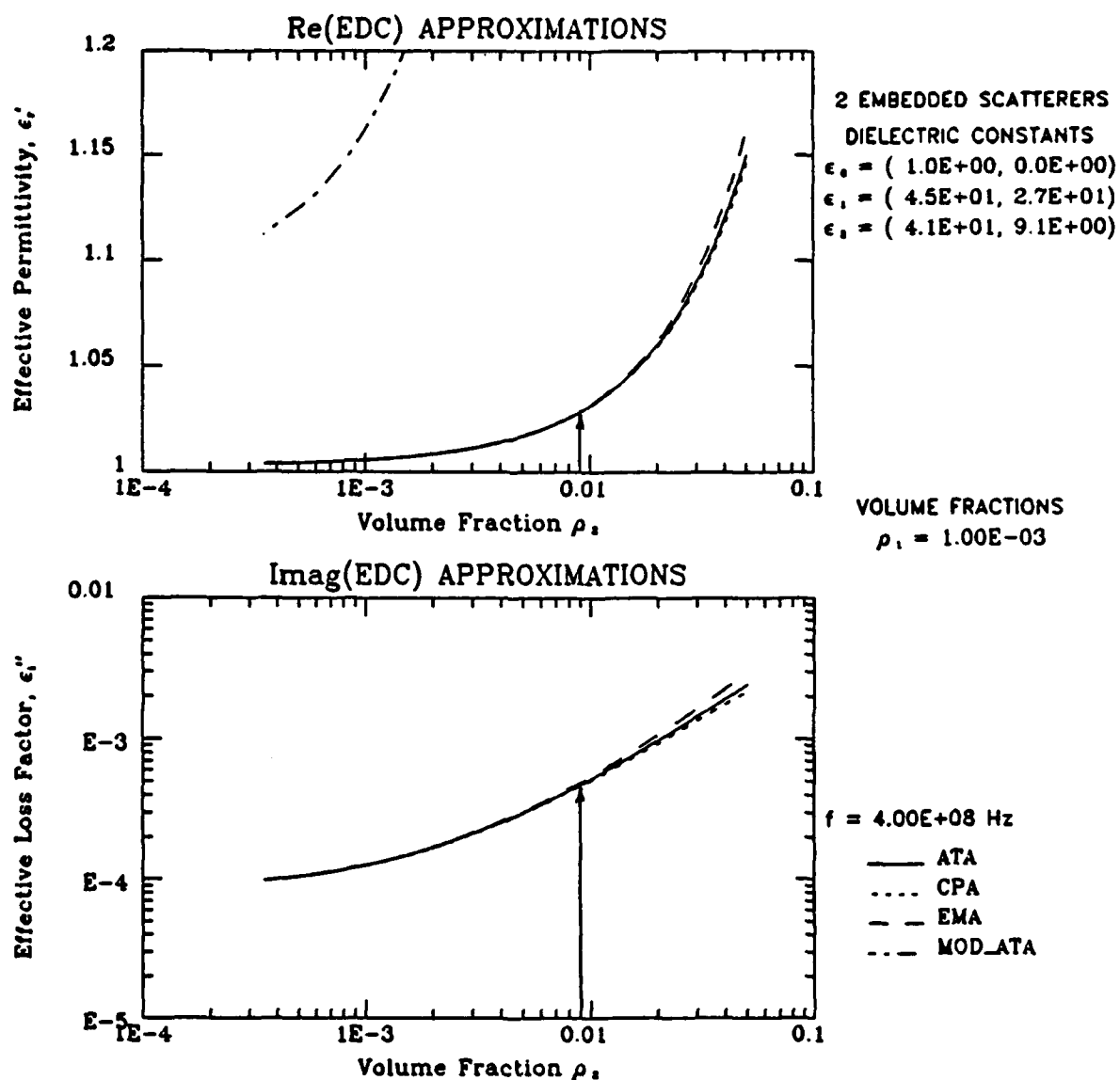


Figure 10. Effective complex dielectric constants ( $\epsilon^*$ ) of a vegetation environment versus the volume fraction of the wood component. The values represent a vegetation environment comprised of hardwood foliage at 25°C with the wood grain randomly oriented with respect to the electric field polarization. Leaf moisture content is 65%, leaf salinity is 6% and the leaf volume fraction is 0.1%. Values are calculated for an incident radiation frequency of 400MHz.

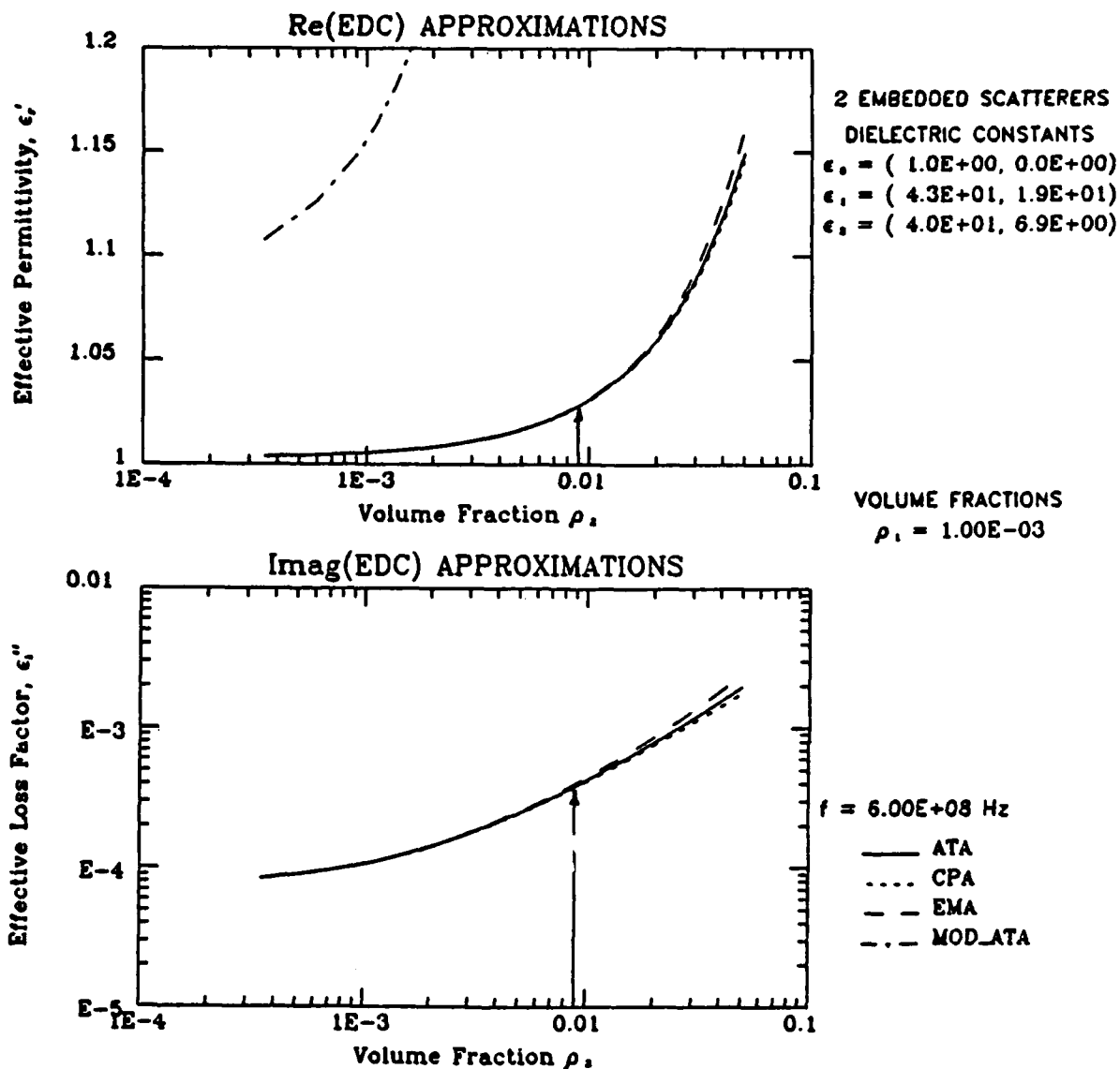


Figure 11. Effective complex dielectric constants ( $\epsilon^*$ ) of a vegetation environment versus the volume fraction of the wood component. The values represent a vegetation environment comprised of hardwood foliage at 25°C with the wood grain randomly oriented with respect to the electric field polarization. Leaf moisture content is 65%, leaf salinity is 6% and the leaf volume fraction is 0.1%. Values are calculated for an incident radiation frequency of 600MHz.

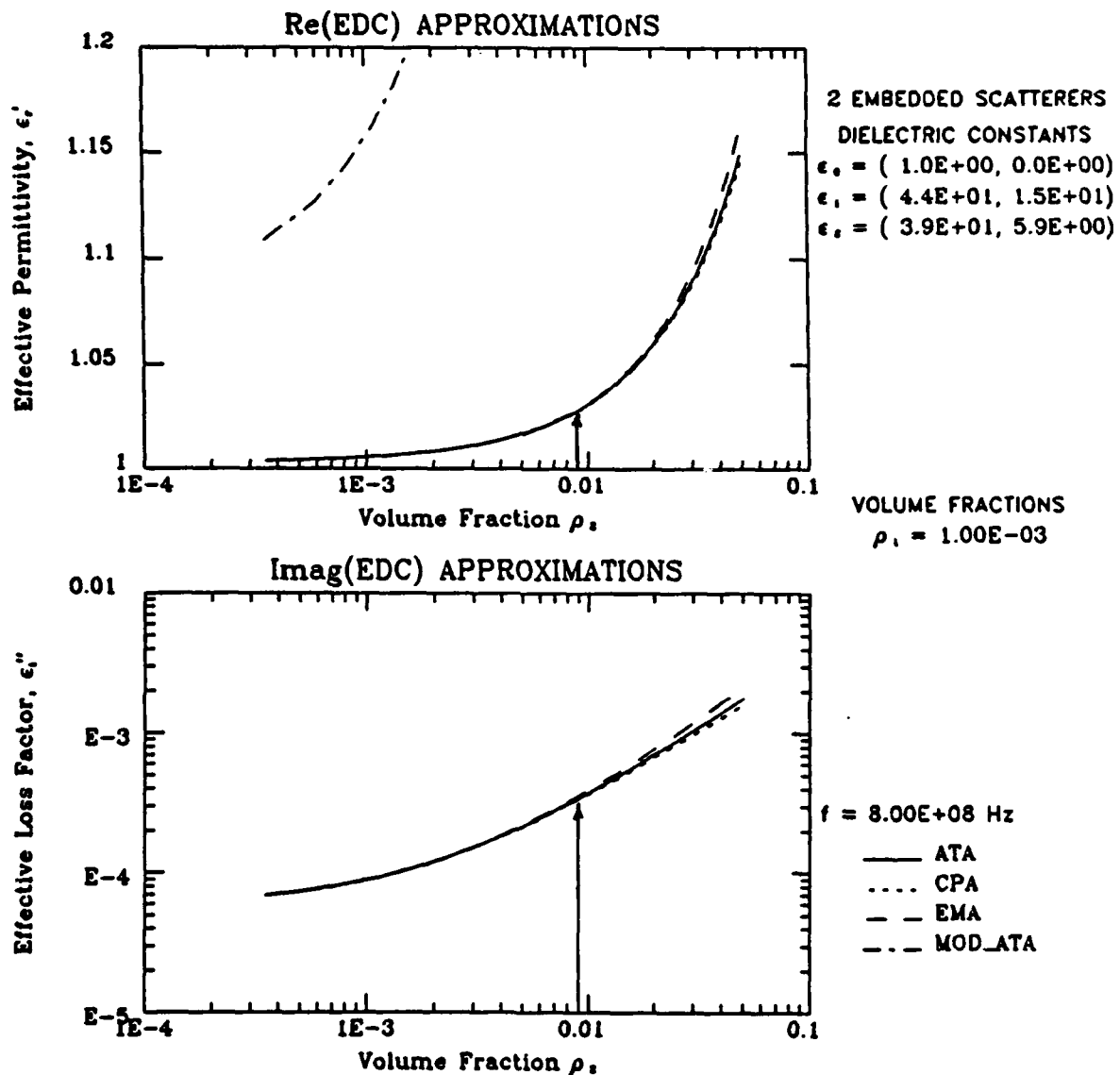


Figure 12. Effective complex dielectric constants ( $\epsilon^*$ ) of a vegetation environment versus the volume fraction of the wood component. The values represent a vegetation environment comprised of hardwood foliage at 25°C with the wood grain randomly oriented with respect to the electric field polarization. Leaf moisture content is 65%, leaf salinity is 6% and the leaf volume fraction is 0.1%. Values are calculated for an incident radiation frequency of 800MHz.

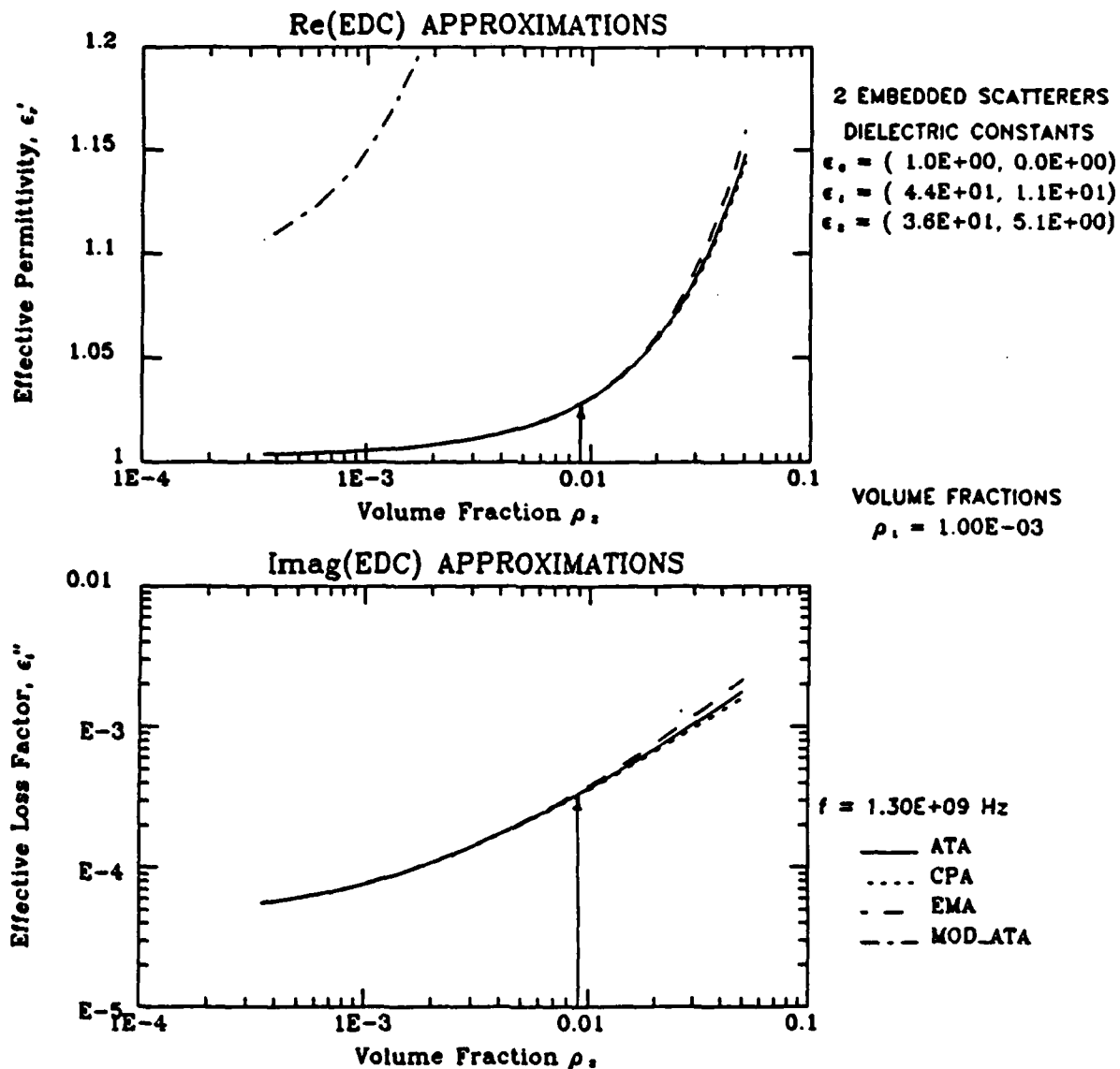


Figure 13. Effective complex dielectric constants ( $\epsilon^*$ ) of a vegetation environment versus the volume fraction of the wood component. The values represent a vegetation environment comprised of hardwood foliage at 25°C with the wood grain randomly oriented with respect to the electric field polarization. Leaf moisture content is 65%, leaf salinity is 6% and the leaf volume fraction is 0.1%. Values are calculated for an incident radiation frequency of 1.3GHz.

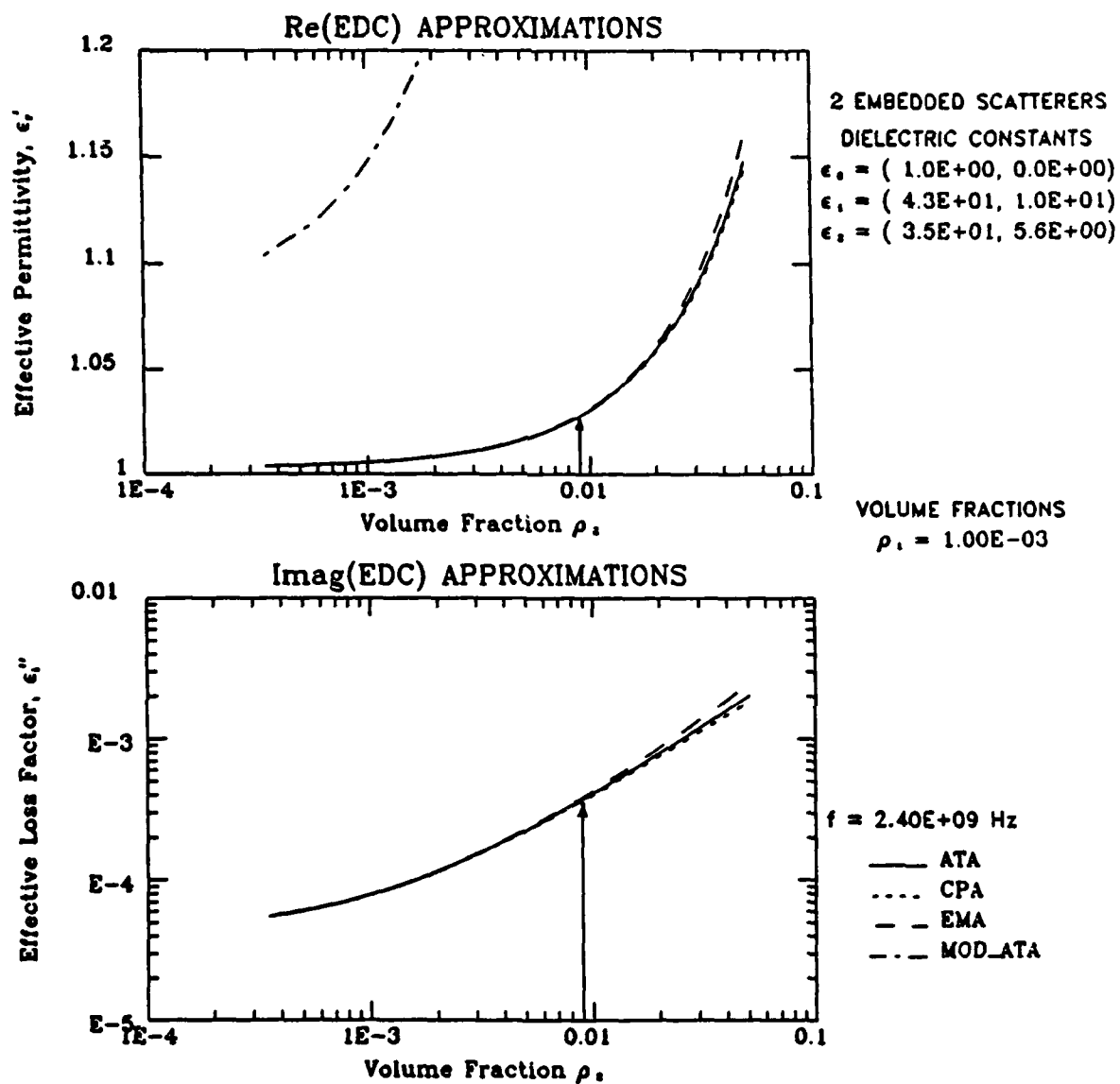


Figure 14. Effective complex dielectric constants ( $\epsilon^*$ ) of a vegetation environment versus the volume fraction of the wood component. The values represent a vegetation environment comprised of hardwood foliage at 25°C with the wood grain randomly oriented with respect to the electric field polarization. Leaf moisture content is 65%, leaf salinity is 6% and the leaf volume fraction is 0.1%. Values are calculated for an incident radiation frequency of 2.4GHz.

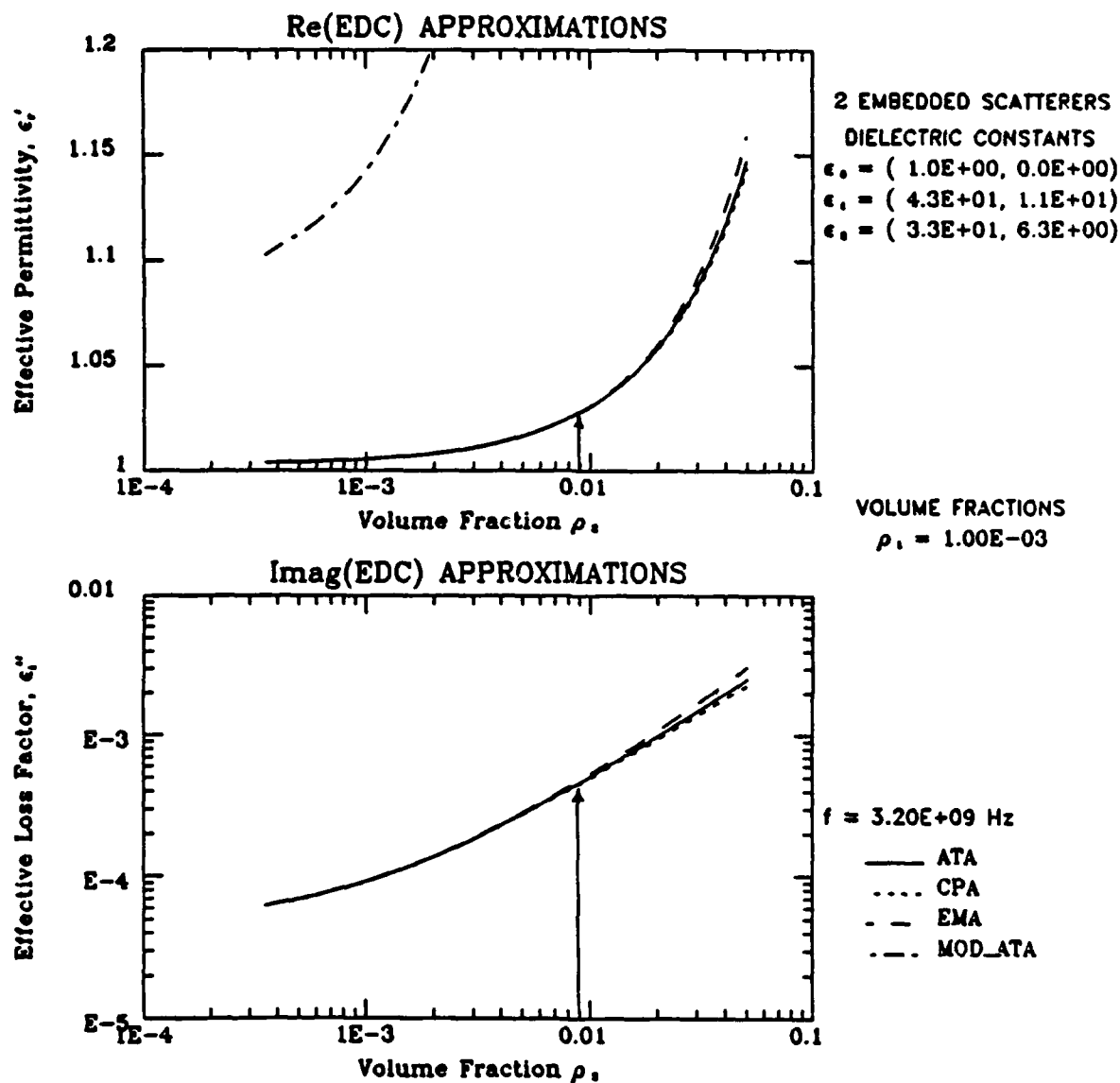


Figure 15. Effective complex dielectric constants ( $\epsilon^*$ ) of a vegetation environment versus the volume fraction of the wood component. The values represent a vegetation environment comprised of hardwood foliage at 25°C with the wood grain randomly oriented with respect to the electric field polarization. Leaf moisture content is 65%, leaf salinity is 6% and the leaf volume fraction is 0.1%. Values are calculated for an incident radiation frequency of 3.2GHz.

scatterer dielectric constants are close in magnitude to the dielectric constant of the host medium. From this assumption, the MOD\_ATA method will not provide a good approximation of the effective parameters of a foliage medium because the dielectric constants of the embedded scatterers are much greater than the host medium of air.

As previously mentioned, the total volume fraction of the vegetation matter in a forest environment rarely exceeds 0.05. Values calculated and shown in figures 7 through 15 all show excellent agreement between the ATA, EMA, and CPA approximations below this threshold. It is only when the volume fraction is greater than 0.05 that the estimations from the various approximations begin to significantly differ. The agreement between these three approximation methods was consistent for all cases run using the model, as was their relationship with the output of the MOD\_ATA.

The magnitude of the effective permittivities calculated using the model were close to the expected values. According to De Loor, the effective complex dielectric constant of a heterogeneous media will be a value between that of the scatterers that constitute that medium. For the forest environment this would produce values between  $1.0+j0.0$  and  $40.0+j209$ . Because of the small volume fraction of the embedded scatterers, one would expect the effective dielectric constants of foliage media to have values slightly larger than that of air ( $1+j0$ ). The magnitude of the effective loss factor may be explained similarly. The calculated values of the effective values show good agreement other with values reported in the literature [Tamir 67] [Golden 78] for forest media.

Figures 7 through 15 demonstrate the dependence of the effective complex dielectric constant on the volume fraction of the embedded scatterers. In some cases the magnitude of the loss factor can increase two orders of magnitude for a sparse versus dense forest environment. The magnitude of the permittivity is also dependent on the volume fraction of the embedded scatterers but to a much lesser degree. The effect of varying the frequency of the incident radiation can be seen by comparing the curves on Figures 7 through 15, as each plot calculates the effective dielectric constants for a different frequency of incident radiation. The frequency dependence of the loss factor on frequency is readily observable and, although not as pronounced as the dependence on volume fraction, does appear to be significant. Alternately, the effect of frequency on the permittivity shows little or no change



over the 50MHz to 3.2GHz frequency range for which the calculations were done. This result is consistent with expectations, as the variation of the permittivity of the vegetation components shows little variation over frequency.

The format of the data presented in Figures 7 to 15 resulted in a great number of plots when an attempt was made to demonstrate the effects of varying conditions on the effective complex dielectric constants of a forest medium. A more compact presentation format was devised that has the effective dielectric constants plotted versus the frequency of the incident radiation, with each plot containing several curves that represent different forest densities. In order to produce such plots, the volume fractions of the components of the forest had to be estimated. To this end, two sets of plots were created; one for sparse vegetation where the total volume fraction falls between 0.01% and 1.0%, and the other for dense foliage where the total volume fraction of the vegetation falls between 1.0% and 5.0%. Each plot contains a maximum curve, a minimum curve, and a typical curve. For example, the dense foliage plot would contain a curve for extremely dense (total volume fraction 5.0%), dense (total volume fraction 2.0%), and normal (total volume fraction 1.0%) foliage and the sparse foliage plot would contain a curve for normal density (total volume fraction 1.0%), sparse (total volume fraction 0.1%), and extremely sparse (total volume fraction 0.01%) foliage. To create these plots using the model, the volume fraction of leaves must be held constant for the calculation. For the example plots in this report, this value was taken to be 10% of the total of the volume fraction of the vegetation, which is about what would be expected in a typical foliated forest [Brown 82] [Ulaby 83]. As an example, to produce a plot with the above format only a single point would be taken from each of the plots shown in Figures 7 through 15. The selected points in Figures 7 to 15 are shown on the respective figures (arrow from x-axis) and were used to produce the normal (1.0%) curves in figures 24, 25, 26 and 27. By using this condensed plotting format the eight plots in Figures 7 to 15 can be condensed to the single curve shown on the plots in Figures 25 through 27 making data interpretation more coherent. The plots shown in the effective dielectric constant versus frequency format use the complex effective dielectric constant values returned by the Self-Consistent version of the Coherent Potential Approximation. The results of only one of the estimation techniques are shown because the difference between the approximation methods only becomes significant above 0.05, which is outside the range of realistic volume fractions of forest environments.

The points chosen from the effective dielectric constant versus volume fraction curves are based on the value of the volume fraction of the leaves used in the creation of that curve. The leaf volume fraction in Figures 7 through 15 is 0.001, and since the leaf volume fraction is taken to be 10% of the total volume fraction, only the points corresponding to 0.009 on the x-axis are used here. The subsequent volume fraction versus frequency curves created from these points represent the complex effective dielectric constants of normal density hardwood vegetation in summer with a total volume fraction of 1.0, which is comprised of 0.9% wood and 0.1% leaves. Alternately, the extremely dense and dense curves in figures 26 and 27 are developed by taking points from two other sets of plots using the same conditions as those used in figures 7 through 15 but produced using different values for the volume fraction of the leaves; 0.005 and 0.002, respectively. Data presented in the condensed format allows the determination of the complex effective dielectric value for a particular incident radiation frequency by estimating the density of a vegetation environment and reading the corresponding value from the plot.

Curves were created that will demonstrate the effects of frequency, forest density, season, and wood grain orientation to the electric field polarization on the effective dielectric constants of forest media. Plots similar to those of Figures 7 to 15 were created varying these above mentioned conditions as well as the leaf volume fractions. A total of eight data sets were used as input to the model and consisted of the dielectric constants of the various components subdivided by the species (hard or softwood), season (winter or summer), and wood grain orientation relative to the electric field orientation (perpendicular or randomly oriented). For the case of hardwood species in the winter season the effective medium will be modeled as a background medium (air) and one embedded scatterer (wood), as the majority of leaves fall from hardwood tree types in the winter. Alternately, the softwood species in any season, and the hardwood species in summer, will be modeled as the background medium and two embedded scatterers; the wood and leaves or needles. Values for the dielectric constants of the components of the forest were obtained from the models discussed in section 3.0 and are shown in the tables in their respective section. Eight set of plots were created for total volume fractions of 0.0001, 0.001, 0.01, 0.02, and 0.05, with the leaf volume fractions being 10% of the total volume fraction for each data set. Each of

these plots were generated for 9 incident radiation frequencies; 50MHz, 100MHz, 200MHz, 400MHz, 600MHz, 800MHz, 1.3GHz, 2.4GHz, and 3.2GHz. Therefore, a total of 144 (permittivity and loss factor are plotted separately) plots were created showing the effective complex dielectric constants versus the wood volume fraction. By extracting the points of interest from these plots as discussed above, the effective dielectric constants versus the frequency of incident radiation can be plotted. A total of 16 plots showing the permittivity and loss factors versus frequency of dense foliage and 16 plots showing the permittivity and loss factors versus frequency of sparse foliage were created, these plots are shown in Figures 16 through 47.

#### 4.1 Effective Dielectric Constants of Hard Wood Vegetation

Section 4.1 contains the results of the calculation of the effective complex dielectric constants of foliage media comprised of hardwood type vegetation. Four sections are included that contain the results of calculations for different vegetation types and environmental conditions. The effects of temperature, wood grain orientation to the electric field, and volume fraction are demonstrated.

##### 4.1.1 Hard Wood With Perpendicular Electric Field at 25°C

Figures 16 and 17 depict the effective permittivity and loss factor of a sparse foliage medium composed of hardwood vegetation at an ambient air temperature of 25°C, with the wood grain perpendicular to the electric field, respectively. The perpendicular orientation of the wood grain with respect to the electric field polarization makes the values in these figures applicable to the propagation of electromagnetic waves through the trunks or stalks of trees, or through brush or young vegetation, where the majority of wood grain is perpendicular to the electric field. Sparse vegetation is an environment where the trees are sparsely to moderately populated. The volume fraction of 1.0% is representative of a "typical" forest density and values near this curve should be the most common referenced. The temperature (25°C) is representative of the summer season.

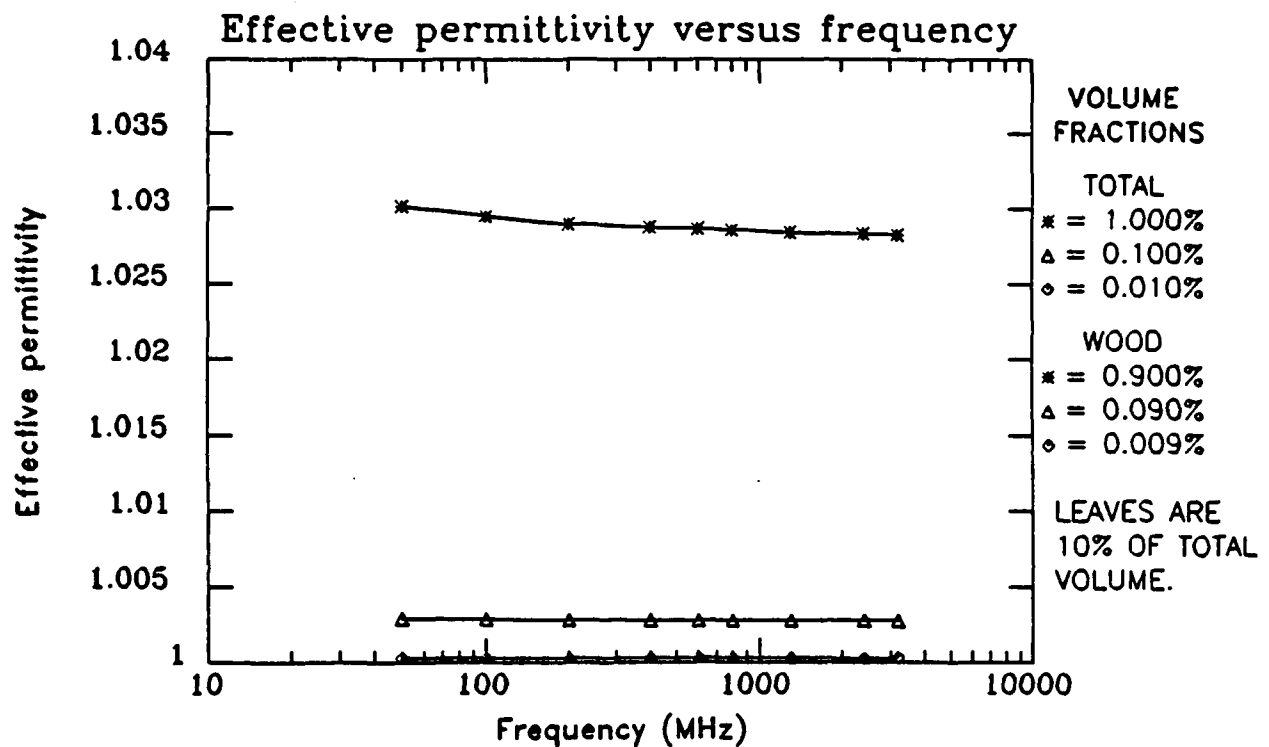


Figure 16. Effective permittivity of a sparse hardwood vegetation environment with the wood grain perpendicular to the electric field polarization. The three curves represent the highest, middle and lowest extremes of the volume fraction of the embedded scatterers. Leaf salinity is 6% and leaf moisture content 65% for all values. Wood moisture content is 80% and the temperature is 25°C representing the summer season.

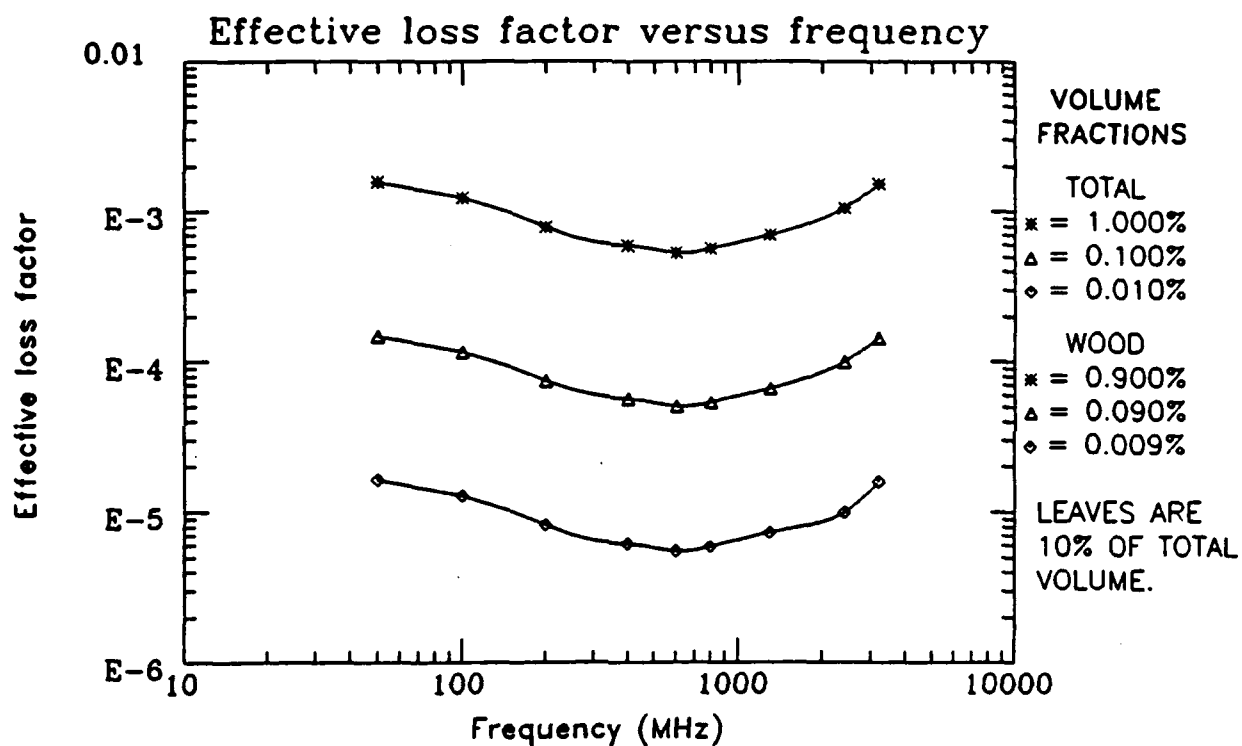


Figure 17. Effective loss factor of a sparse hardwood vegetation environment with the wood grain perpendicular to the electric field polarization. The three curves represent the highest, middle and lowest extremes of the volume fraction of the embedded scatterers. Leaf salinity is 6% and leaf moisture content 65% for all values. Wood moisture content is 80% and the temperature is 25°C representing the summer season.

As expected, the effective permittivity will vary little in the frequency range over which the calculations are done. Data found in the literature supports this conclusion [Golden 78] [Tamir 82] [Ulaby 82]. Variation of the effective permittivity with respect to the volume fraction of embedded scatterers, however, is quite prominent. The magnitude of this change can best be observed in the example plots of the effective permittivity versus the volume fraction shown in figures 7 through 15. All of the curves generated throughout this report displayed behavior similar to that observed in figures 7 through 15. It should be noted that the slope of the permittivity curve increases rapidly when the embedded scatterers volume fraction is greater than 2.0%. The effective permittivities for the extremely sparse to sparse volume fraction foliage (0.01% to 0.1%) are between 1.0003 and 1.0028; while the effective permittivities of sparse to normal foliage are between 1.003 and 1.028.

The variation in the effective loss factor versus frequency is shown in figure 17. The deviation in these values over frequency appears to somewhat mimic the behavior of the dielectric constants of the hardwood embedded scatterers (see figure 6) for the same frequency interval. The variation of the effective loss factor with respect to the volume fraction of embedded scatterers is pronounced and as expected increases as the volume fraction increases. The effective loss factors of the extremely sparse volume fraction foliage are between  $5.5\text{E-}6$  and  $1.5\text{E-}4$ ; while the effective loss factors of sparse to normal volume fraction foliage are between  $5.1\text{E-}5$  and  $1.6\text{E-}3$ , depending upon the frequency of the incident radiation.

Figures 18 and 19 depict the effective permittivity and loss factor of a dense foliage medium for the same conditions as those used to develop figures 16 and 17, respectively. A dense foliage medium is an environment where the trees are moderately to heavily populated. The values between the 1.0% and 2.0% curves are generally considered to be representative of "typical" dense forest environments with the 5.0% curve being an extremely dense medium. The permittivities shown in figure 18 shows little variation versus the frequency demonstrating that the effective permittivities do not change appreciably over the frequency range reported here regardless of the volume fraction of the embedded scatterers. The permittivities do, however, vary markedly as the volume fraction changes from values of 1.026 to 1.058 for normal to dense foliage (1.0% to 2.0%), to 1.053 to 1.156 for dense to extremely dense foliage (2.0% to 5.0%).

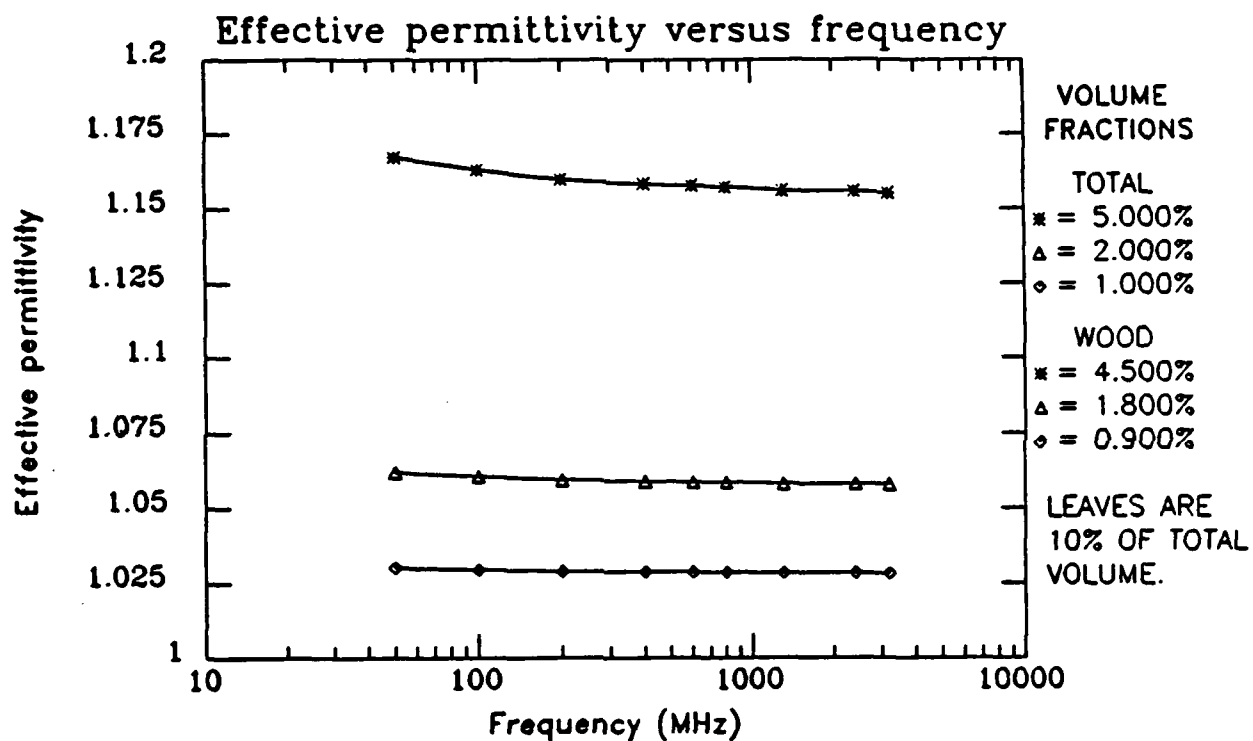


Figure 18. Effective permittivity of a dense hardwood vegetation environment with the wood grain perpendicular to the electric field polarization. The three curves represent the highest, middle and lowest extremes of the volume fraction of the embedded scatterers. Leaf salinity is 6% and leaf moisture content 65% for all values. Wood moisture content is 80% and the temperature is 25°C representing the summer season.

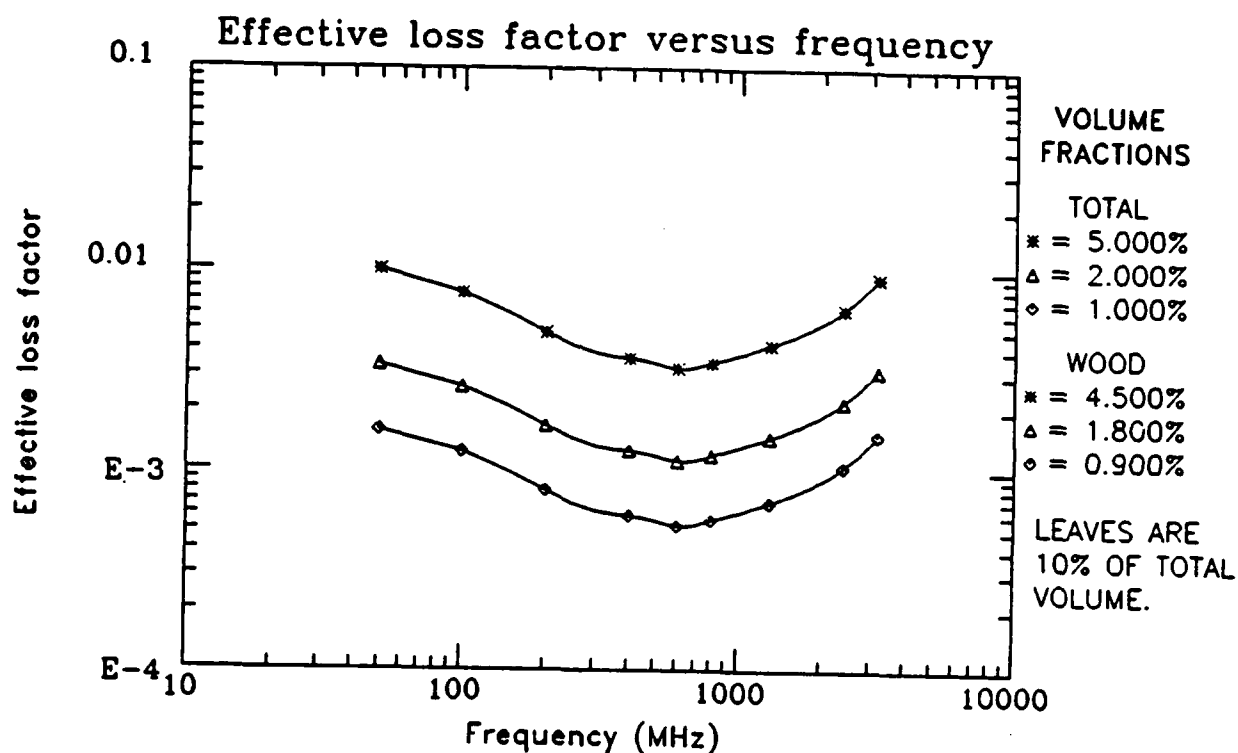


Figure 19. Effective loss factor of a dense hardwood vegetation environment with the wood grain perpendicular to the electric field polarization. The three curves represent the highest, middle and lowest extremes of the volume fraction of the embedded scatterers. Leaf salinity is 6% and leaf moisture content 65% for all values. Wood moisture content is 80% and the temperature is 25°C representing the summer season.



Figure 19 contains plots of the effective loss factors of a dense foliage medium for the same conditions as figure 18. From the curve it can be observed that the effective loss factor will have the same tendencies over frequency as the major embedded scatterer, similar to the trend exhibited by the curves in figure 17. The variation with respect to the volume fraction of embedded scatterers is again pronounced varying from  $5.3\text{E-}4$  to  $3.4\text{E-}3$  for normal to dense foliage, to  $1.1\text{E-}3$  to  $9.9\text{E-}3$  for dense to dense foliage, depending on the incident radiation frequency.

#### 4.1.2 Hard Wood With Perpendicular Electric Field at 4°C

Figures 20 through 23 present the results of the calculation of the effective complex dielectric constants of a foliage medium for the same conditions as those used in the determination of figures 16 through 19, respectively. The only difference being an ambient air temperature of 4°C for figures 20 to 23 rather than 25°C for figures 16 through 19. The 4°C value is intended to be representative of the winter season.

Observation of figures 20 through 23 reveals that there is no appreciable difference in the effective permittivity of forest environments for these conditions in winter and summer, while the effective loss factor exhibits only slight changes in magnitude versus the frequency. This leads to the conclusion that large variations in the dielectric constants of the embedded scatterers are necessary to produce even minimal effects on the effective parameters when the volume fractions are low.

The effective permittivities for the extremely sparse to sparse volume fraction foliage (0.01% to 0.1%) from figure 20 are between 1.0003 and 1.0029; while the effective permittivities of sparse to normal foliage are between 1.003 and 1.030. The effective permittivities for the normal to dense volume fraction foliage (1.0% to 2.0%) from figure 22 are between 1.027 to 1.058; while for dense to extremely dense foliage (2.0% to 5.0%) the values vary between 1.054 and 1.156.

The effective loss factors for the extremely sparse to sparse volume fraction foliage from figure 21 are between  $3.9\text{E-}6$  and  $9.2\text{E-}4$ ; while the effective permittivities of sparse to

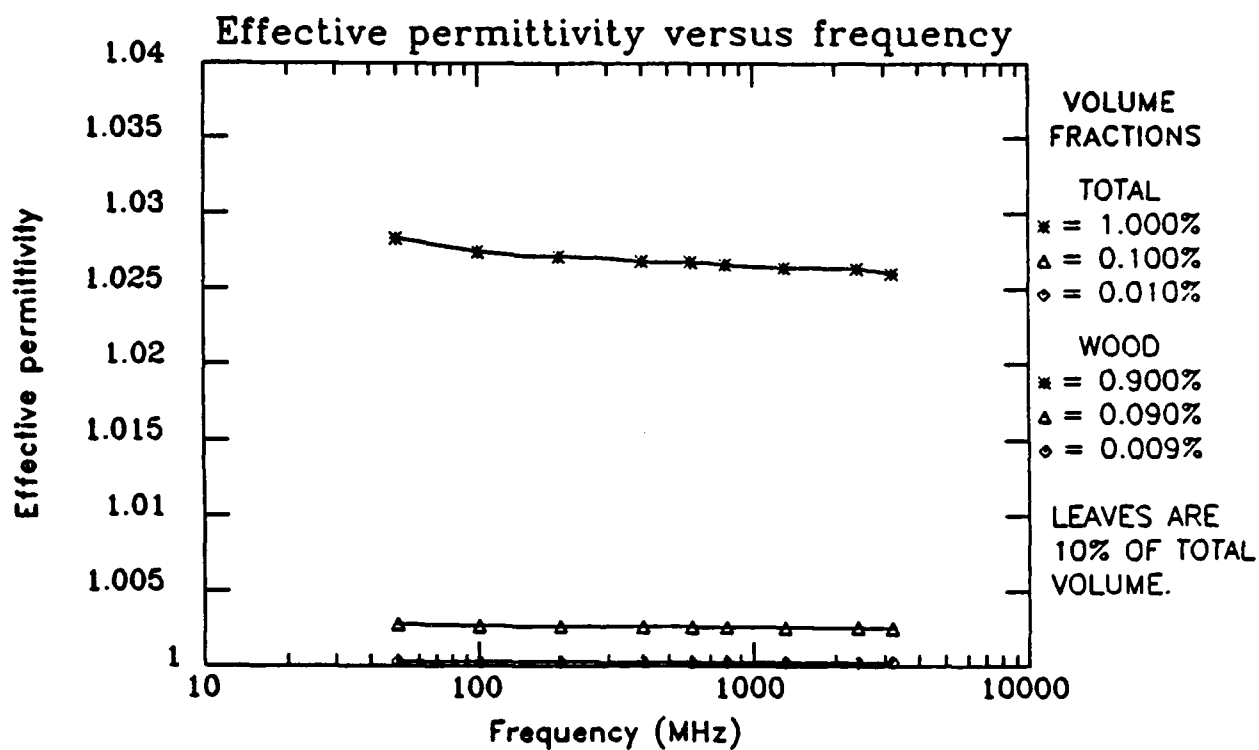


**Figure 20.** Effective permittivity of a sparse hardwood vegetation environment with the wood grain perpendicular to the electric field polarization. The three curves represent the highest, middle and lowest extremes of the volume fraction of the embedded scatterers. Leaf volume fraction is zero. Wood moisture content is 80% and the temperature is 4°C representing the winter season.

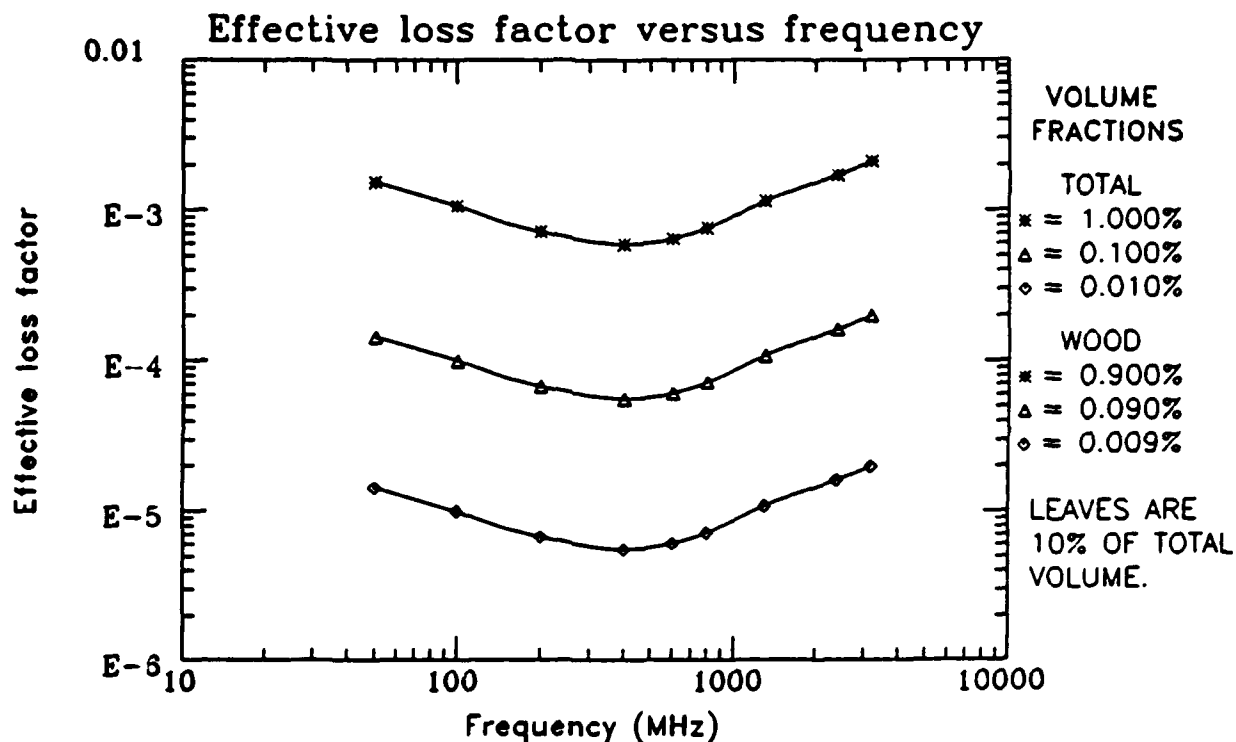


Figure 21. Effective loss factor of a sparse hardwood vegetation environment with the wood grain perpendicular to the electric field polarization. The three curves represent the highest, middle and lowest extremes of the volume fraction of the embedded scatterers. Leaf volume fraction is zero. Wood moisture content is 80% and the temperature is 4°C representing the winter season.

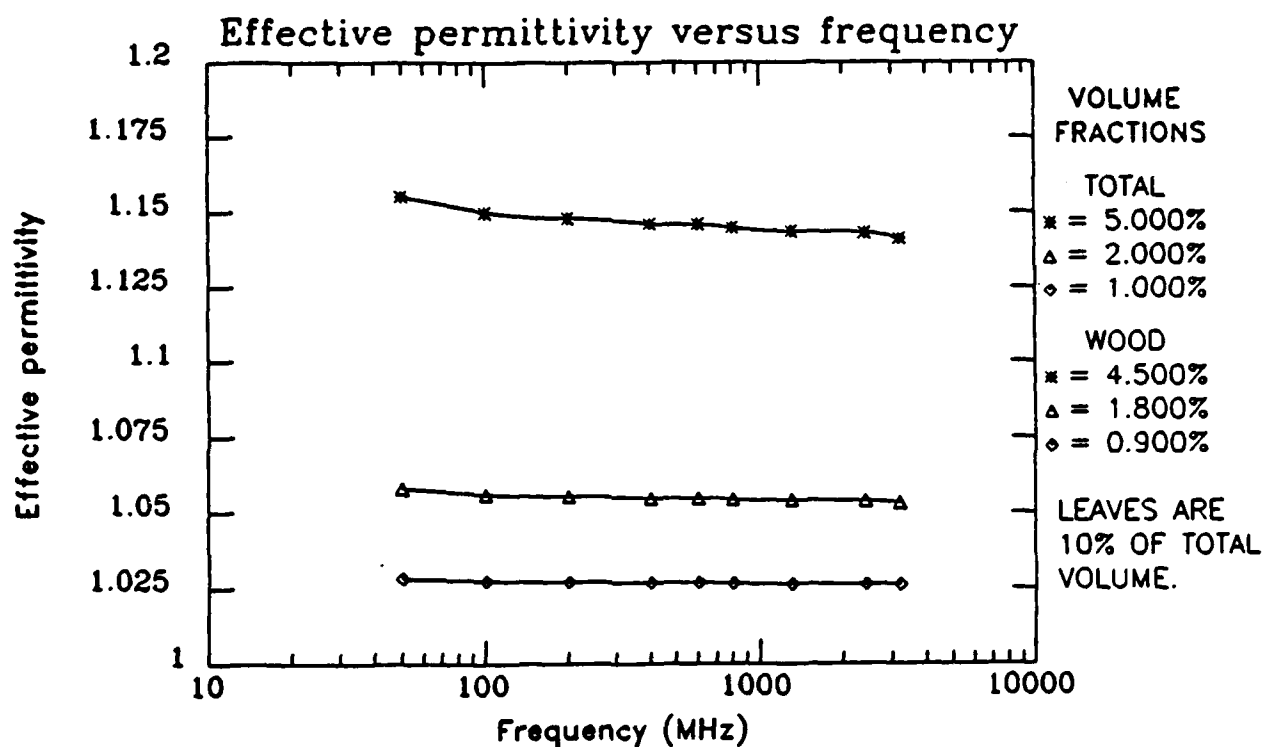


Figure 22. Effective permittivity of a dense hardwood vegetation environment with the wood grain perpendicular to the electric field polarization. The three curves represent the highest, middle and lowest extremes of the volume fraction of the embedded scatterers. Leaf volume fraction is zero. Wood moisture content is 80% and the temperature is 4°C representing the winter season.

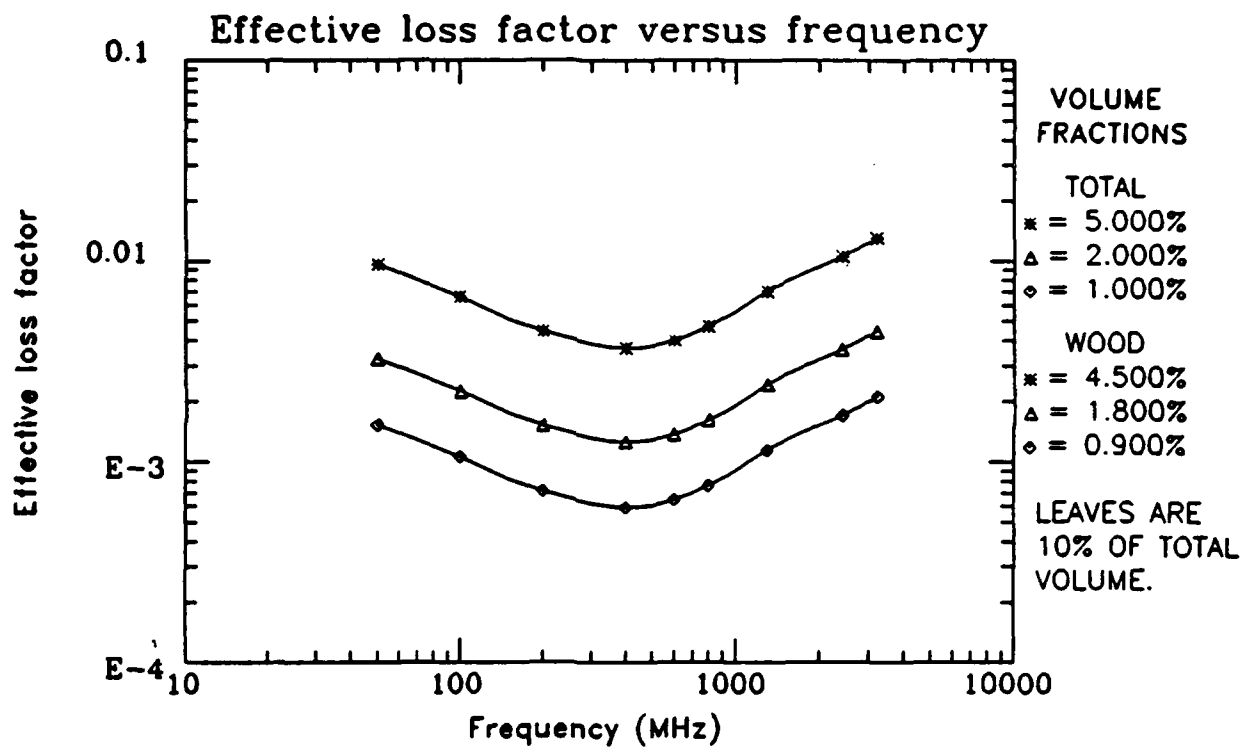


Figure 23. Effective loss factor of a dense hardwood vegetation environment with the wood grain perpendicular to the electric field polarization. The three curves represent the highest, middle and lowest extremes of the volume fraction of the embedded scatterers. Leaf volume fraction is zero. Wood moisture content is 80% and the temperature is 4°C representing the winter season.

normal foliage are between  $3.8\text{E-}5$  and  $9.8\text{E-}4$ . The effective permittivities for the normal to moderately dense volume fraction foliage from figure 23 are between  $5.9\text{E-}4$  to  $3.3\text{E-}3$ ; while for moderately dense to extremely dense foliage the values vary between  $1.3\text{E-}3$  and  $9.6\text{E-}3$ , depending on the frequency of the incident radiation.

Another notable occurrence that can be observed from figures 20 through 23 is the lack of a drastic change in the effective parameters attributable to the leafless state of hardwood vegetation in winter. Variation from the summer to winter data can be observed as a slight increase in the magnitude of the loss factor of the hardwood vegetation in the winter for incident radiation frequencies from 400MHz to 3.2GHz. For all other frequencies the values are essentially equivalent. The small volume fraction of leaves coupled with the behavior of the dielectric constants of wood and leaves combine to yield this result. The assumption of a leaf volume fraction that is 10% of the total volume fraction may not be consistent for all vegetation and could conceivably change this outcome. The lack of an effect by the presents of leaves on the propagation through foliage of electromagnetic waves having frequencies greater than 3.2GHz is documented in the literature [Brown 82]. It should be noted here that, for practical applications, the effective parameters calculated herein will only apply to the specific case described in the figure caption and are only as accurate as the values used for the dielectric constants of the embedded scatterers.

#### 4.1.3 Hard Wood With Randomly Oriented Electric Field at 25°C

Figures 24 and 25 depict the effective permittivity and loss factor of a sparse foliage medium composed of hardwood vegetation at 25°C, with the wood grain randomly oriented with respect to the electric field, respectively. The random orientation of the wood grain with respect to the electric field polarization makes the values in these figures applicable to the propagation of electromagnetic waves through the canopies of mature forests or through brush or young vegetation, where the majority of wood grain is randomly oriented with respect to the electric field. The temperature (25°C) is representative of the summer season.

The permittivity in figure 24 does not vary versus the frequency of the incident radiation. In fact, the magnitude of the permittivity does not differ appreciably from the values

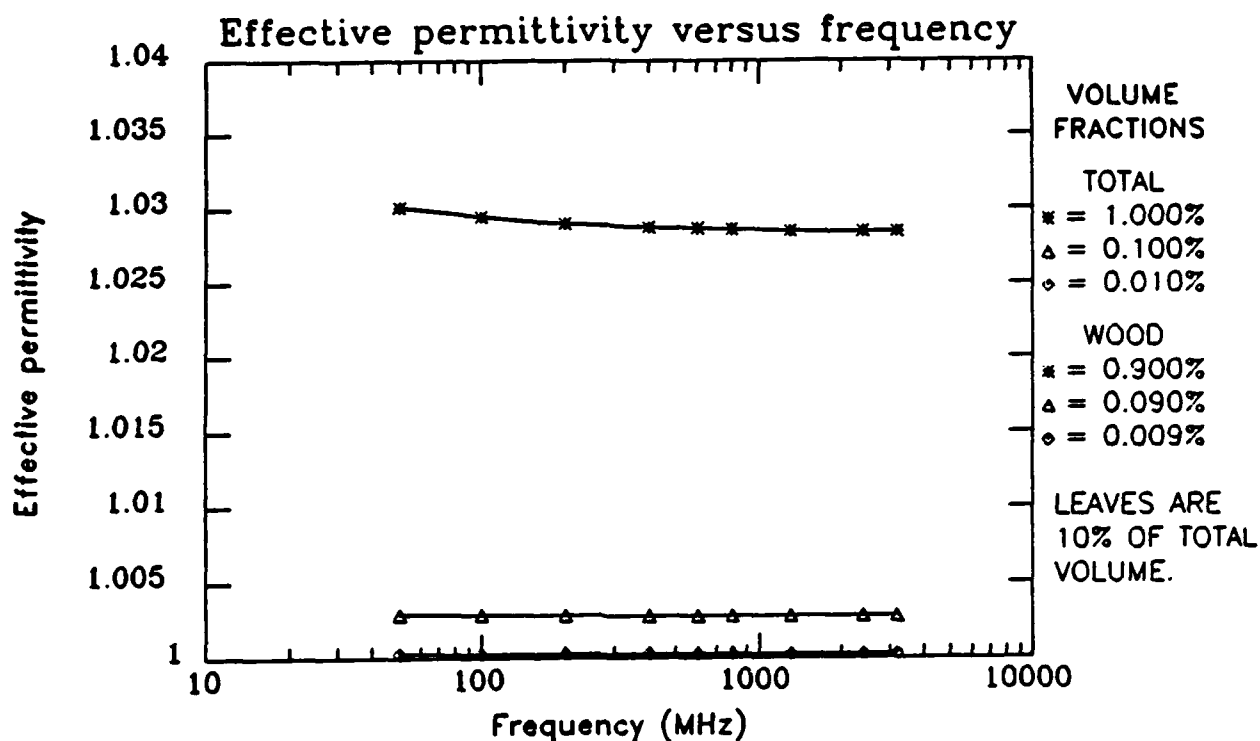


Figure 24. Effective permittivity of a sparse hardwood vegetation environment with the wood grain randomly oriented with respect to the electric field polarization. The three curves represent the highest, middle and lowest extremes of the volume fraction of the embedded scatterers. Leaf salinity is 6% and leaf moisture content 65% for all values. Wood moisture content is 80% and the temperature is 25°C representing the summer season.

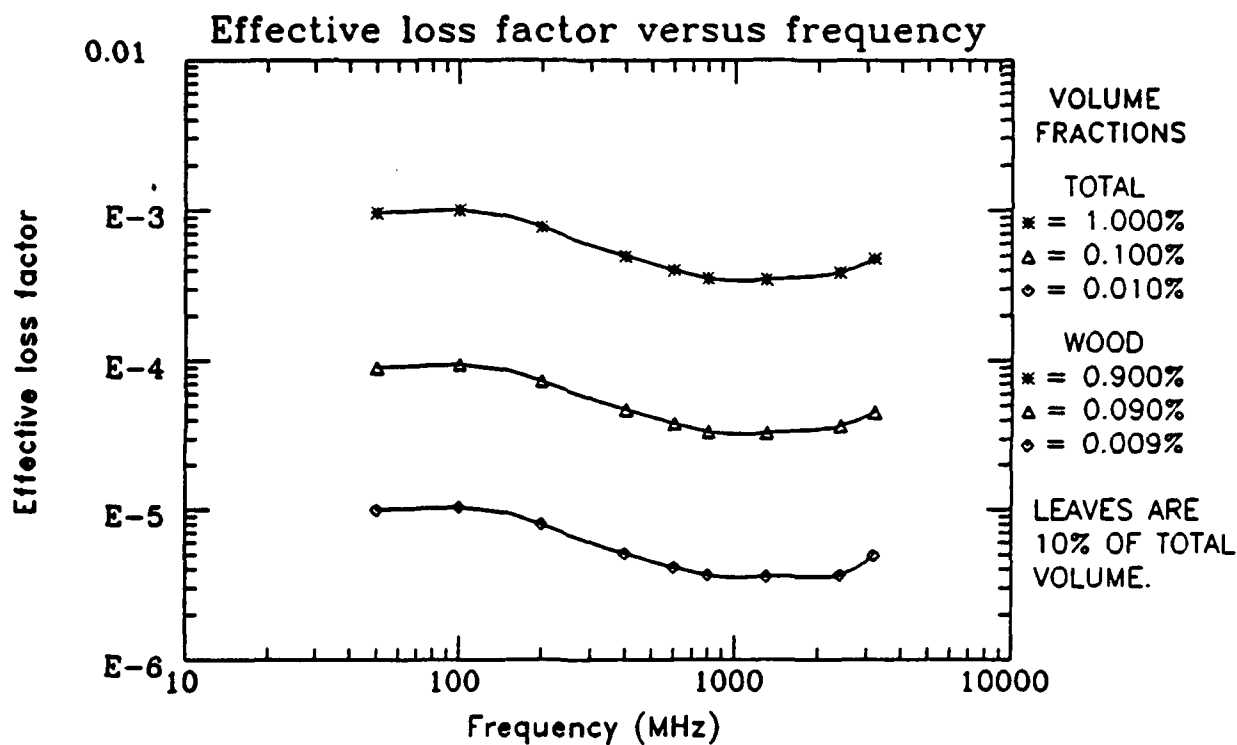


Figure 25. Effective loss factor of a sparse hardwood vegetation environment with the wood grain randomly oriented with respect to the electric field polarization. The three curves represent the highest, middle and lowest extremes of the volume fraction of the embedded scatterers. Leaf salinity is 6% and leaf moisture content 65% for all values. Wood moisture content is 80% and the temperature is 25°C representing the summer season.



reported for the wood grain perpendicular to the electric field with all other conditions constant. It could therefore be assumed that the volume fraction of the embedded scatterers is the primary determinant in the calculation of the effective permittivity and not the dielectric constants of the embedded scatterers. The values for the permittivity given in figure 24 give a permittivity between 1.0003 and 1.0029 for extremely sparse to sparse foliage, and 1.003 to 1.029 for sparse to normal vegetation, confirming the consistency of the permittivity regardless of wood type or electric field orientation.

The loss factors versus the frequency for the same conditions as those used in the development of figure 24 are shown in figure 25. Curve trends are different than those in the curves depicting the effective loss factors versus frequency when the wood grain orientation is perpendicular to the electric field. Showing that, although a great dependence still exists on the volume fraction, the effective loss factor is also influenced by the wood grain orientation with respect to the electric field polarization. The curve trend does reflect the same pattern as that of the major embedded scatterer (hardwood ) as can be seen be a comparison to figure 7. For the frequency range in this study, the effective loss factors describing the effects on an electric field propagating through a hardwood vegetation environment when the wood grain is randomly oriented with respect to the electric field polarization, appear to be less than the effective loss factors when the electric field polarization is perpendicular to the wood grain. The calculated effective loss factors for the extremely sparse to sparse foliage range between  $1.8\text{E-}6$  and  $4.6\text{E-}5$  and, between  $1.7\text{E-}5$  and  $4.9\text{E-}4$  for sparse to normal volume fraction foliage depending upon the incident radiation frequency.

Figures 26 and 27 depict the effective permittivity and loss factor of a dense foliage medium for the same conditions as those used to develop figures 24 and 25, respectively. The permittivities shown in figure 26 show little variation versus the frequency and little variation from the permittivities of dense vegetation for all conditions examined to this point. The permittivities do vary as the volume fraction changes from values of 1.028 to 1.062 for normal to dense foliage (1.0% to 2.0%), to 1.058 to 1.167 for dense to extremely dense foliage (2.0% to 5.0%).

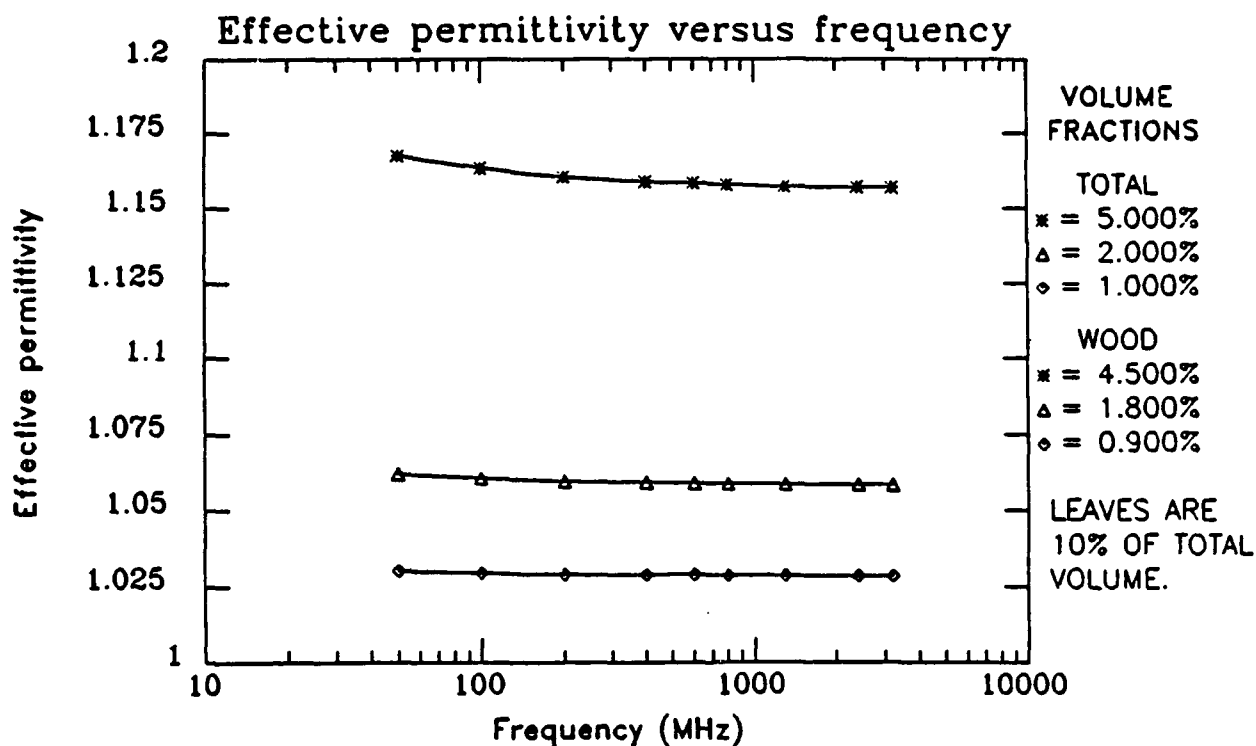


Figure 26. Effective permittivity of a dense hardwood vegetation environment with the wood grain randomly oriented with respect to the electric field polarization. The three curves represent the highest, middle and lowest extremes of the volume fraction of the embedded scatterers. Leaf salinity is 6% and leaf moisture content 65% for all values. Wood moisture content is 80% and the temperature is 25°C representing the summer season.

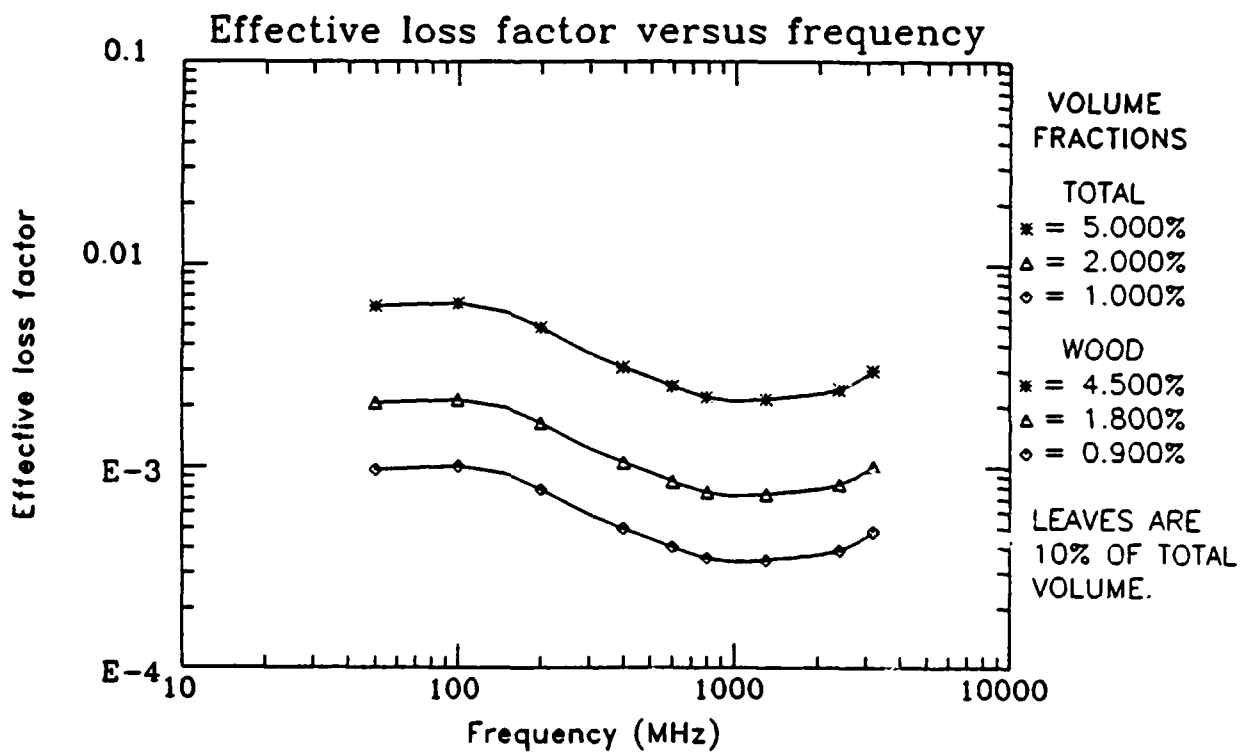


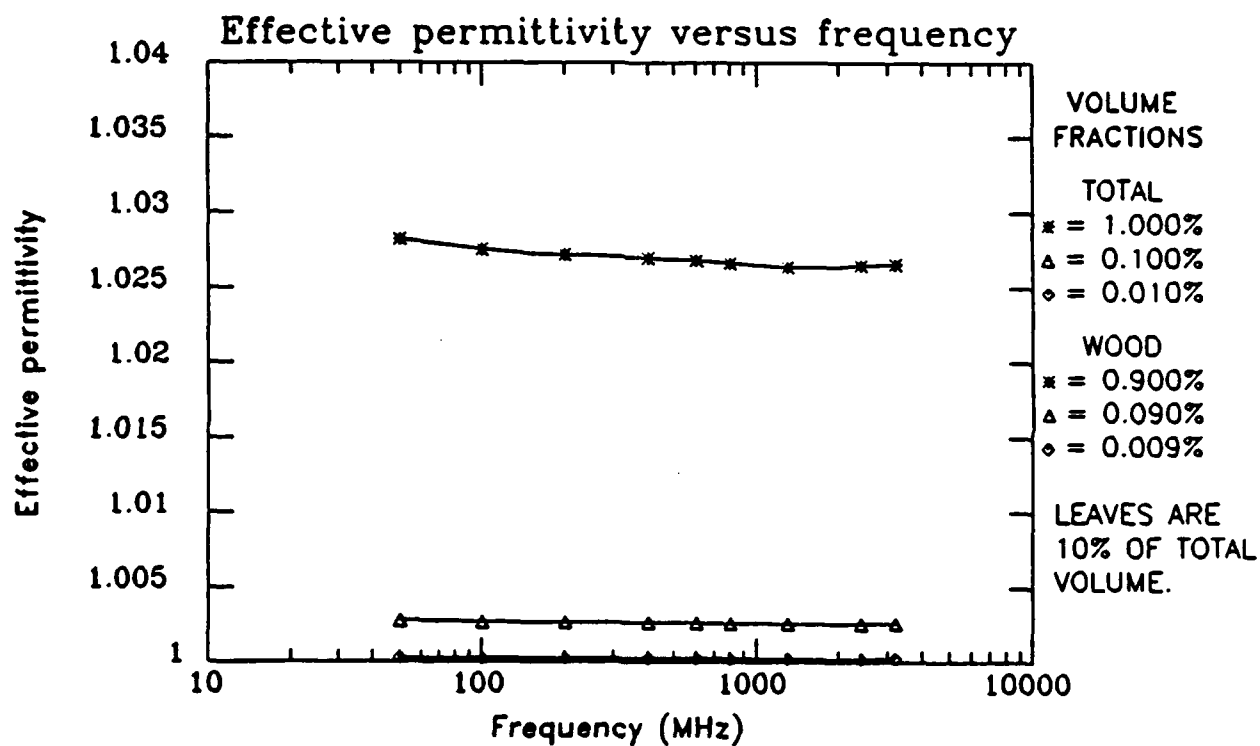
Figure 27. Effective loss factor of a dense hardwood vegetation environment with the wood grain randomly oriented with respect to the electric field polarization. The three curves represent the highest, middle and lowest extremes of the volume fraction of the embedded scatterers. Leaf salinity is 6% and leaf moisture content 65% for all values. Wood moisture content is 80% and the temperature is 25°C representing the summer season.

Figure 27 contains plots of the effective loss factors of a dense foliage medium for the same conditions as figure 26. Again it is apparent that the effective loss factor will have the same tendencies over frequency as the major embedded scatterer, similar to the trend exhibited by the previous effective loss factor curves. The variation with respect to the volume fraction of embedded scatterers is again pronounced varying from  $3.5\text{E-}4$  to  $2.1\text{E-}3$  for normal to dense foliage, to  $1.0\text{E-}3$  to  $6.4\text{E-}3$  for dense to dense foliage, depending on the incident radiation frequency.

#### 4.1.4 Hard Wood With Randomly Oriented Electric Field at 4°C

Figures 28 through 31 present the results of the calculation of the effective complex dielectric constants of a foliage medium for the same conditions as those used in the determination of figures 24 through 27, respectively. The only difference being an ambient air temperature of 4°C for figures 28 to 31 rather than 25°C for figures 24 through 27. The 4°C value is intended to be representative of the winter season. Observation of figures 28 through 31 reveals that there is no appreciable difference in the effective permittivity of hardwood vegetation in the summer and winter seasons with random wood grain orientation with respect to the electric field; while the effective loss factor exhibits minimal variations with respect to frequency from the summer to winter season for this case. Therefore, the conclusion that large variations in the dielectric constants of the embedded scatterers are necessary to produce even minimal effects on the effective parameters when the volume fractions are low is true regardless of the electric field orientation. Similar to the effective loss factors at 25°C the values of the loss factors, when the wood grain is randomly oriented with respect to the electric field polarization, are generally less than those when the electric field polarization is perpendicular to the wood grain. Therefore, the wood grain orientation relative to the electric field polarization will affect the values of the effective loss factors regardless of the air temperature.

The effective permittivities for the extremely sparse to sparse volume fraction foliage (0.01% to 0.1%) from figure 28 are between 1.0003 and 1.0029; while the effective



**Figure 28.** Effective permittivity of a sparse hardwood vegetation environment with the wood grain randomly oriented with respect to the electric field polarization. The three curves represent the highest, middle and lowest extremes of the volume fraction of the embedded scatterers. Leaf volume fraction is zero. Wood moisture content is 80% and the temperature is 4°C representing the winter season.

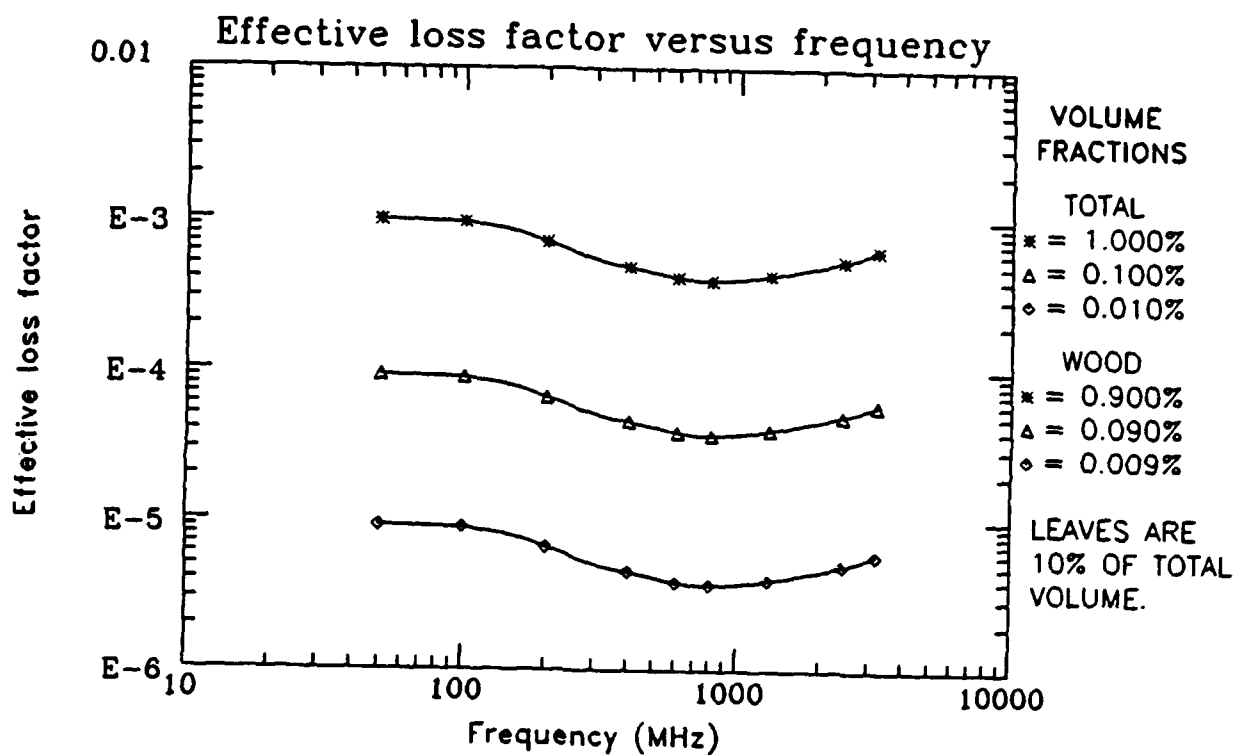


Figure 29. Effective loss factor of a sparse hardwood vegetation environment with the wood grain randomly oriented with respect to the electric field polarization. The three curves represent the highest, middle and lowest extremes of the volume fraction of the embedded scatterers. Leaf volume fraction is zero. Wood moisture content is 80% and the temperature is 4°C representing the winter season.

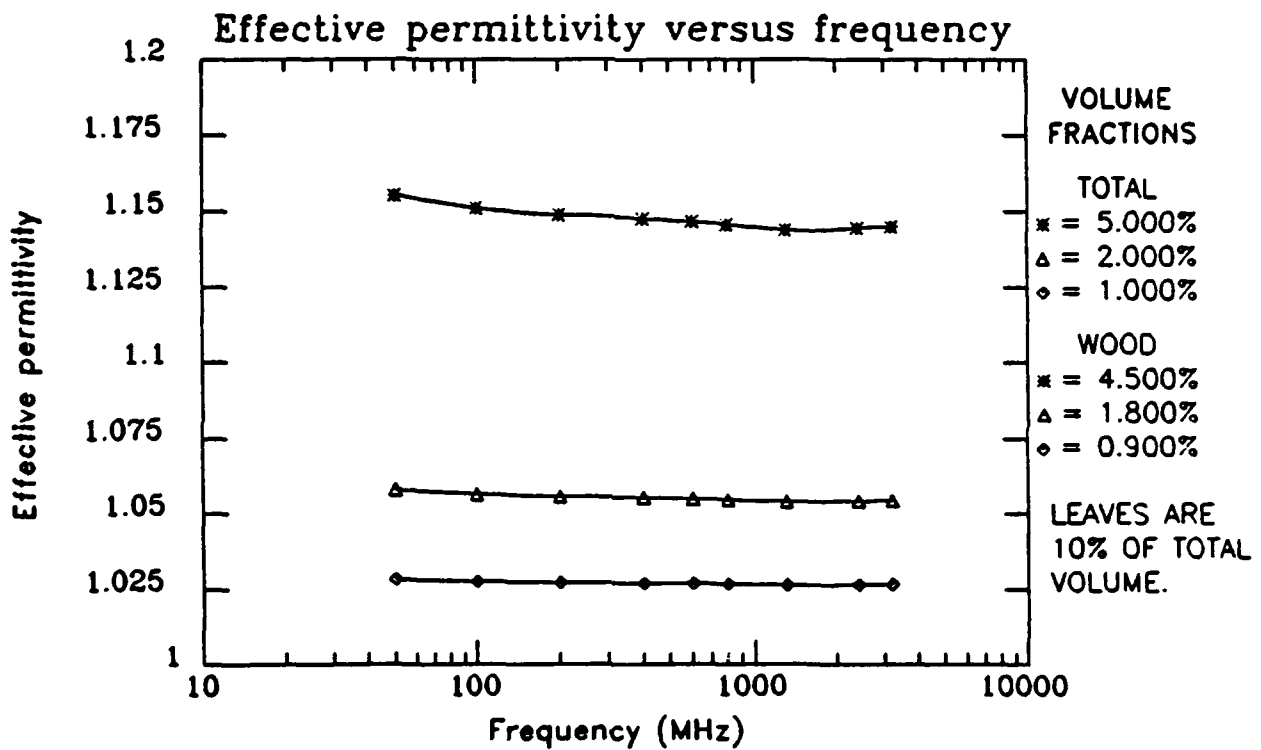


Figure 30. Effective permittivity of a dense hardwood vegetation environment with the wood grain randomly oriented with respect to the electric field polarization. The three curves represent the highest, middle and lowest extremes of the volume fraction of the embedded scatterers. Leaf volume fraction is zero. Wood moisture content is 80% and the temperature is 4°C representing the winter season.

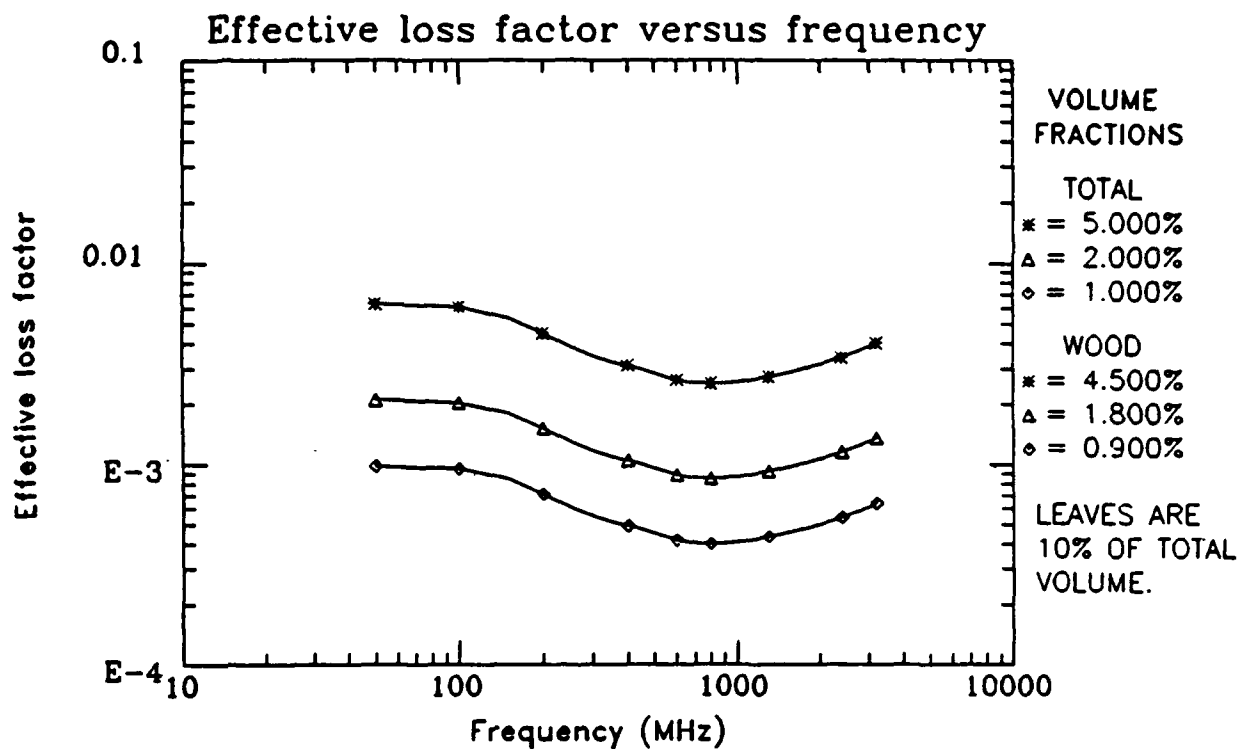


Figure 31. Effective loss factor of a dense hardwood vegetation environment with the wood grain randomly oriented with respect to the electric field polarization. The three curves represent the highest, middle and lowest extremes of the volume fraction of the embedded scatterers. Leaf volume fraction is zero. Wood moisture content is 80% and the temperature is 4°C representing the winter season.



permittivities of sparse to normal foliage are between 1.003 and 1.030. The effective permittivities for the normal to dense volume fraction foliage (1.0% to 2.0%) from figure 30 are between 1.028 to 1.062; while for dense to extremely dense foliage (2.0% to 5.0%) the values vary between 1.058 and 1.167.

The effective loss factors for the extremely sparse to sparse volume fraction foliage from figure 29 are between  $3.7\text{E-}6$  and  $9.2\text{E-}5$ ; while the effective permittivities of sparse to normal foliage are between  $3.8\text{E-}5$  and  $9.8\text{E-}4$ . The effective permittivities for the normal to moderately dense volume fraction foliage from figure 31 are between  $4.0\text{E-}4$  to  $2.1\text{E-}3$ ; while for moderately dense to extremely dense foliage the values vary between  $9.2\text{E-}4$  and  $4.0\text{E-}3$ , depending on the incident radiation frequency.

#### 4.2 Effective Dielectric Constants of Soft Wood Vegetation

Section 4.2 contains the results of the calculation of the effective complex dielectric constants of foliage media comprised of softwood type vegetation. The plots are created using the same conditions as those used in the development of figures 16 through 31, but use the dielectric constants of softwood foliage as embedded scatterers. The same four conditions used for the hardwood plots are repeated for the softwood s. The effects of temperature, wood grain orientation to the electric field, and volume fraction are again demonstrated.

##### 4.2.1 Soft Wood With Perpendicular Electric Field at 25°C

Figures 32 and 33 depict the effective permittivity and loss factor of a sparse foliage medium composed of softwood vegetation at an ambient air temperature of 25°C, with the wood grain perpendicular to the electric field, respectively. The perpendicular orientation of the wood grain with respect to the electric field polarization makes the values in these figures applicable to the propagation of electromagnetic waves through the trunks or stalks of trees, or through brush or young vegetation, where the majority of wood grain is

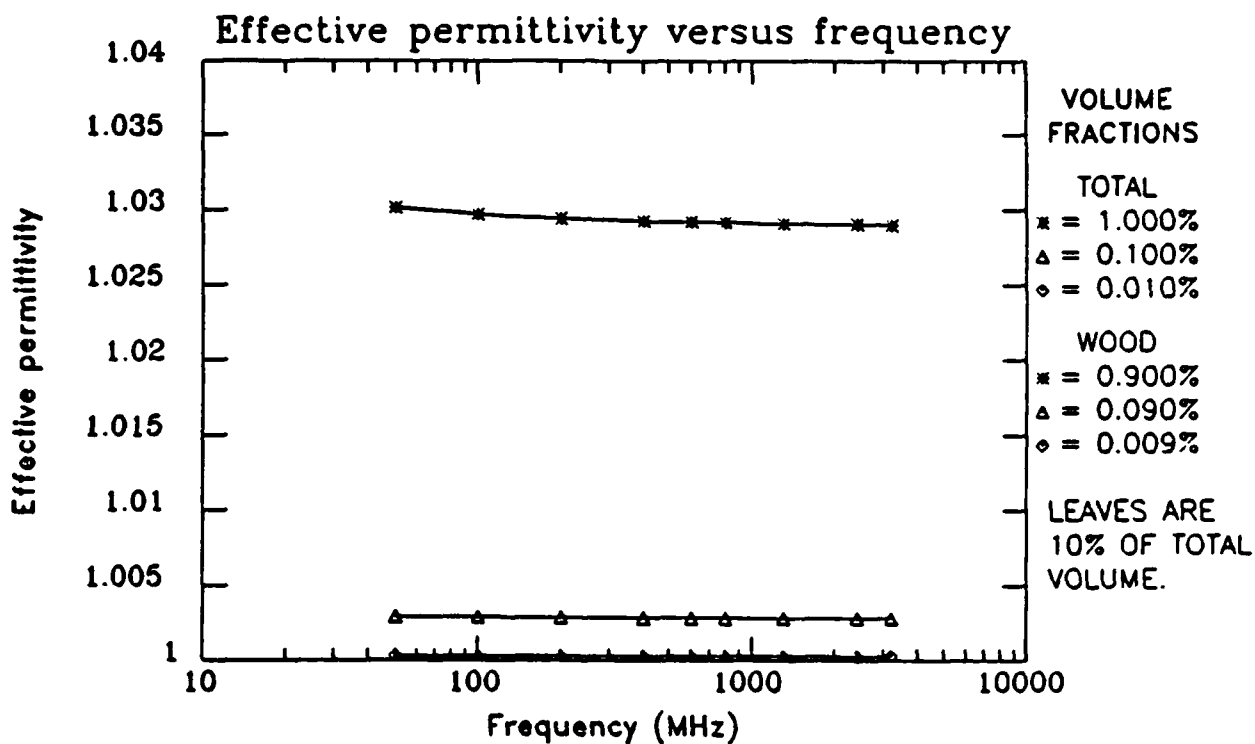


Figure 32. Effective permittivity of a sparse softwood vegetation environment with the wood grain perpendicular to the electric field polarization. The three curves represent the highest, middle and lowest extremes of the volume fraction of the embedded scatterers. Leaf salinity is 6% and leaf moisture content 65% for all values. Wood moisture content is 140% and the temperature is 25°C representing the summer season.

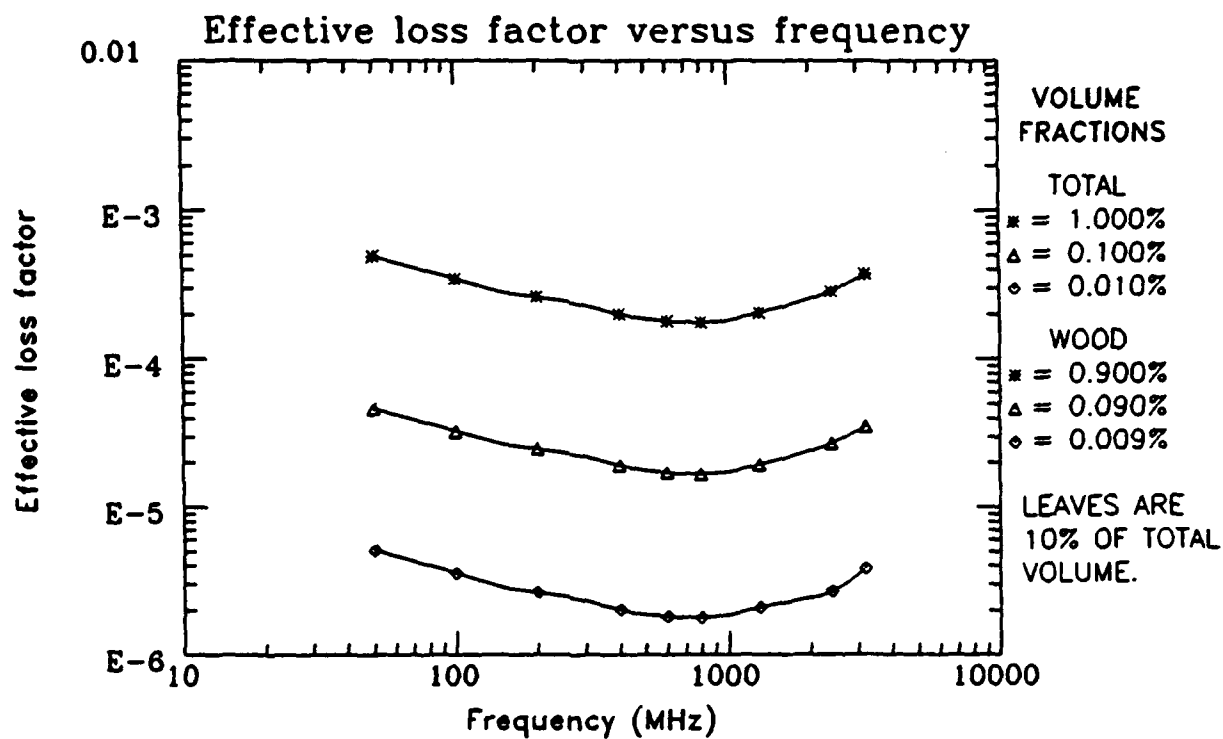


Figure 33. Effective loss factor of a sparse softwood vegetation environment with the wood grain perpendicular to the electric field polarization. The three curves represent the highest, middle and lowest extremes of the volume fraction of the embedded scatterers. Leaf salinity is 6% and leaf moisture content 65% for all values. Wood moisture content is 140% and the temperature is 25°C representing the summer season.

perpendicular to the electric field. The temperature (25°C) is representative of the summer season.

The effective permittivity shown in figure 32 varies little in the frequency range over which the calculations are done which is the expected result [Golden 78] [Tamir 82] [Ulaby 82]. Variation of the effective permittivity with respect to the volume fraction of embedded scatterers, however, is again quite prominent. Close observation reveals that the effective permittivity of the softwood is slightly smaller than that of the hardwood with all other conditions constant. The overall magnitude of the effective permittivity is surprisingly consistent with that shown in figure 16, depicting the permittivity of hardwood foliage for the same conditions. This further substantiates the claim that the volume fraction of the embedded scatterers will be the dominant factor in the determination of the effective permittivity. The effective permittivities for the extremely sparse to sparse volume fraction foliage (0.01% to 0.1%) from figure 32 are between 1.0003 and 1.0029; while the effective permittivities of sparse to normal foliage are between 1.003 and 1.029.

The variation in the effective loss factor versus frequency is shown in figure 33. The deviation in these values over frequency again appears to mimic the behavior of the dielectric constants of the softwood embedded scatterers (see figure 5) for the same frequency interval. The variation of the effective loss factor with respect to the volume fraction of embedded scatterers is pronounced and as expected increases as the volume fraction increases. Comparison of the effective loss factors of the hardwood, shown in figure 17, and the softwood vegetation demonstrates that they are markedly different in magnitude. The effective loss factors of the softwood vegetation are consistently lower than those of its hardwood counterpart, establishing that the effective loss factor is not only dependent upon the volume fraction of embedded scatterers but also on the complex dielectric constant of these scatterers. The effective loss factors of the extremely sparse volume fraction foliage are between  $1.8\text{E-}6$  and  $4.6\text{E-}5$ ; while the effective loss factors of sparse to normal volume fraction foliage are between  $1.7\text{E-}5$  and  $4.9\text{E-}4$ , depending upon the frequency of the incident radiation.



Figures 34 and 35 depict the effective permittivity and loss factor of a dense foliage medium for the same conditions as those used to develop figures 32 and 33, respectively. The permittivities shown in figure 34 shows little variation versus frequency demonstrating that the effective permittivities do not change appreciable over the frequency range reported here regardless of the volume fraction of the embedded scatterers and regardless of wood type. The permittivities do, however, vary markedly as the volume fraction changes from values of 1.029 to 1.060 for normal to dense foliage (1.0% to 2.0%), to 1.058 to 1.161 for dense to extremely dense foliage (2.0% to 5.0%). The effective permittivities here are consistent with those in figure 32.

Figure 35 contains plots of the effective loss factors of a dense foliage medium for the same conditions as figure 34. From the curve it can be observed that the effective loss factor will have the same tendencies over frequency as the major embedded scatterer, similar to the trend exhibited by all of the effective loss factor curves. The variation with respect to the volume fraction of embedded scatterers is again pronounced varying from  $1.8\text{E-}4$  to  $1.0\text{E-}3$  for normal to dense foliage, to  $3.7\text{E-}4$  to  $3.1\text{E-}3$  for dense to dense foliage, depending on the incident radiation frequency. These values are consistently lower than those of figure 19 containing the effective loss factors of hardwood vegetation for similar conditions.

#### 4.2.2 Soft Wood With Perpendicular Electric Field at 4°C

Figures 36 through 39 present the results of the calculation of the effective complex dielectric constants of a foliage medium for the same conditions as those used in the determination of figures 32 through 35, respectively. The only difference being an ambient air temperature of 4°C for figures 36 to 39 rather than 25°C for figures 32 through 35. The 4°C value is intended to be representative of the winter season. Comparison of figures 36 through 39 to the corresponding plots in figures 32 to 35 reveals that there is no appreciable difference in the effective permittivity of forest environments for these conditions in winter and summer. The effective loss factor exhibits only slight changes in magnitude versus the frequency for the winter versus summer season. This is similar to the findings for the

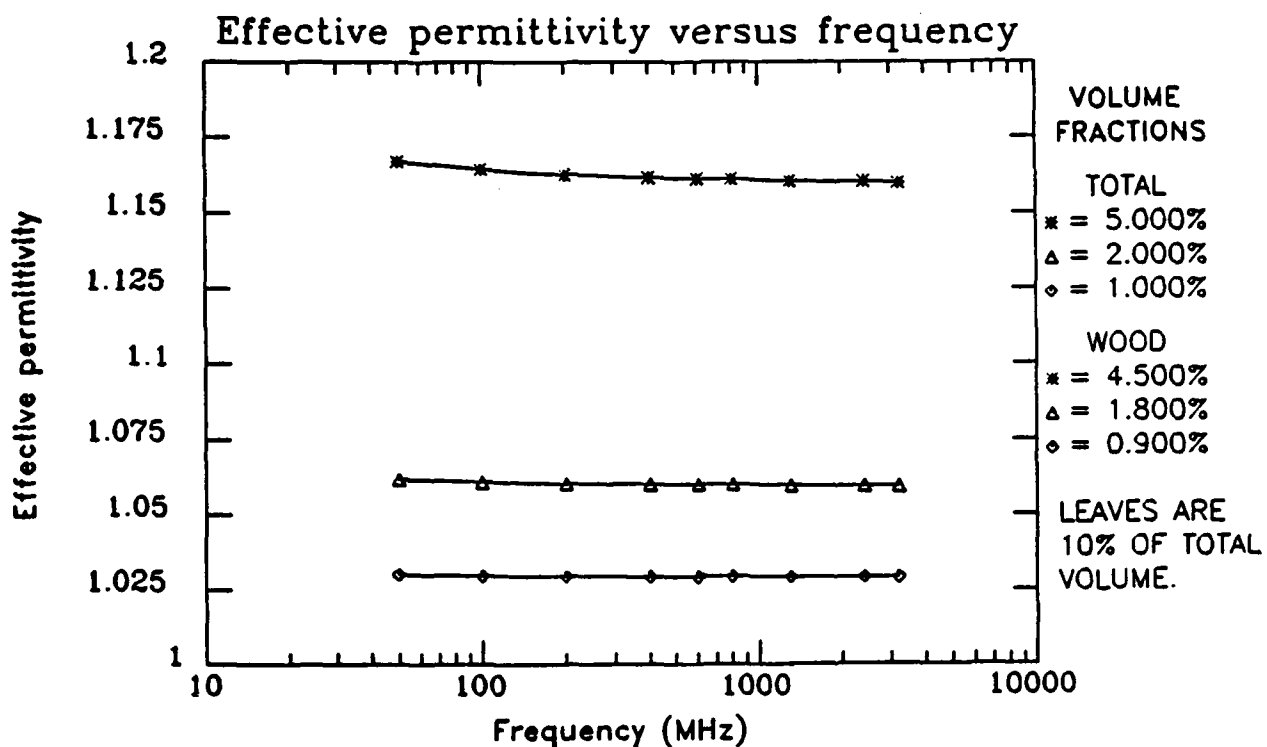


**Figure 34.** Effective permittivity of a dense softwood vegetation environment with the wood grain perpendicular to the electric field polarization. The three curves represent the highest, middle and lowest extremes of the volume fraction of the embedded scatterers. Leaf salinity is 6% and leaf moisture content 65% for all values. Wood moisture content is 140% and the temperature is 25°C representing the summer season.

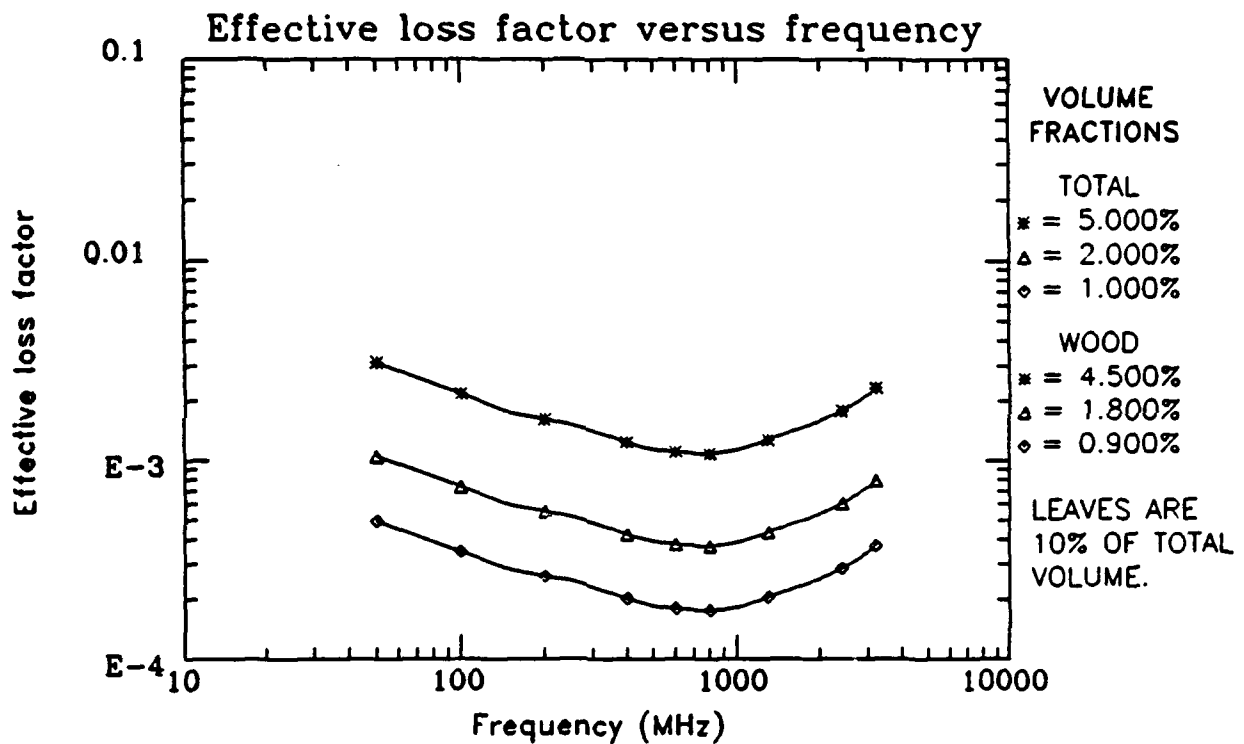


Figure 35. Effective loss factor of a dense softwood vegetation environment with the wood grain perpendicular to the electric field polarization. The three curves represent the highest, middle and lowest extremes of the volume fraction of the embedded scatterers. Leaf salinity is 6% and leaf moisture content 65% for all values. Wood moisture content is 140% and the temperature is 25°C representing the summer season.

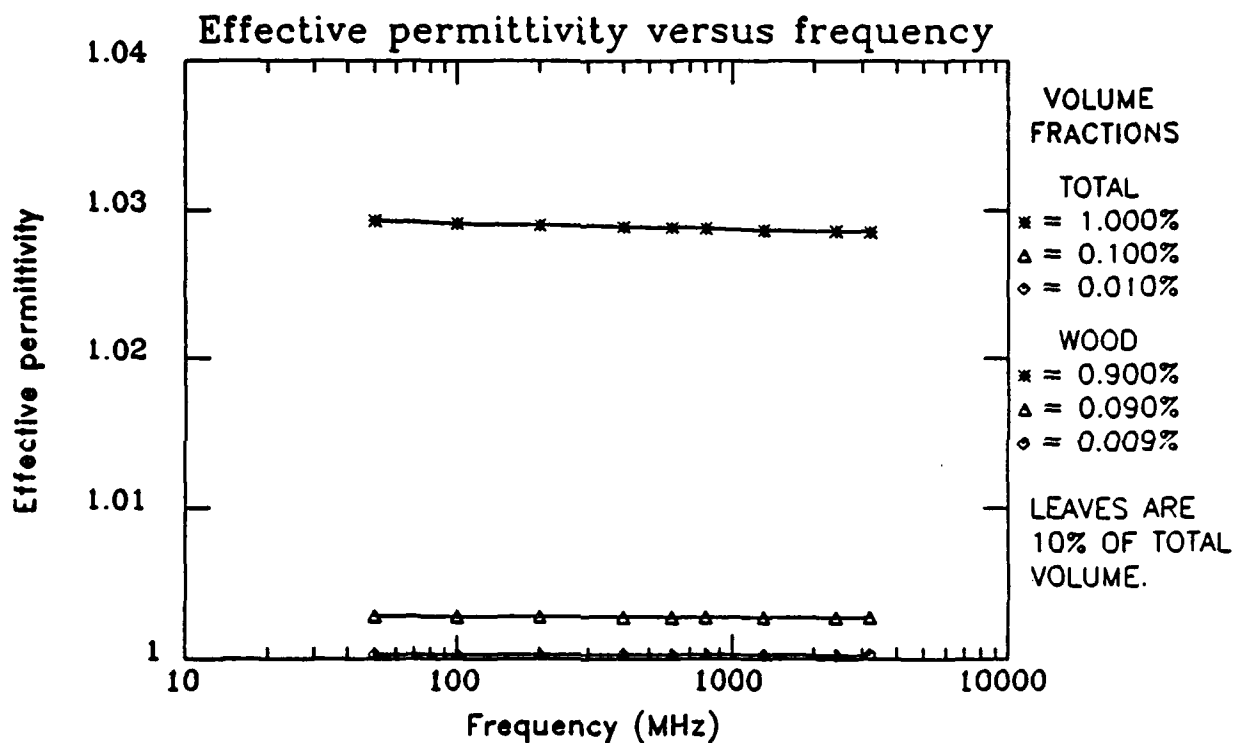


Figure 36. Effective permittivity of a sparse softwood vegetation environment with the wood grain perpendicular to the electric field polarization. The three curves represent the highest, middle and lowest extremes of the volume fraction of the embedded scatterers. Leaf salinity is 6% and leaf moisture content 65% for all values. Wood moisture content is 140% and the temperature is 4°C representing the winter season.



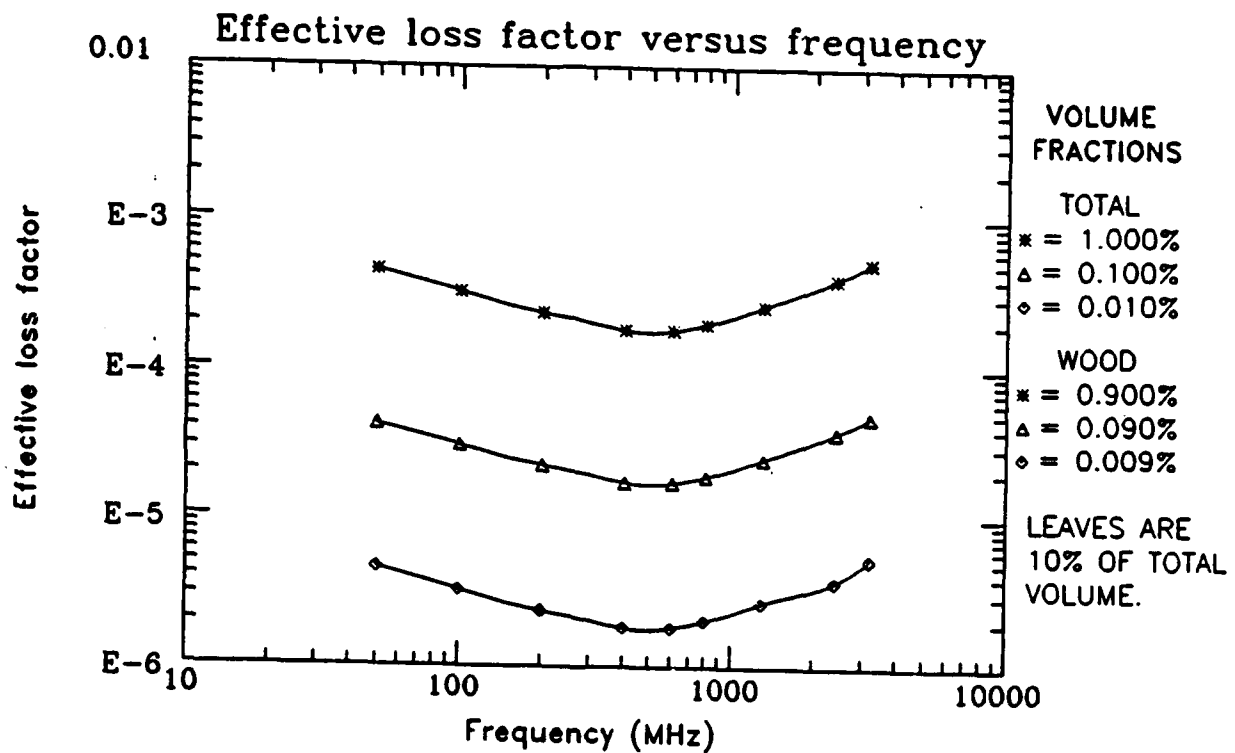


Figure 37. Effective loss factor of a sparse softwood vegetation environment with the wood grain perpendicular to the electric field polarization. The three curves represent the highest, middle and lowest extremes of the volume fraction of the embedded scatterers. Leaf salinity is 6% and leaf moisture content 65% for all values. Wood moisture content is 140% and the temperature is 4°C representing the winter season.

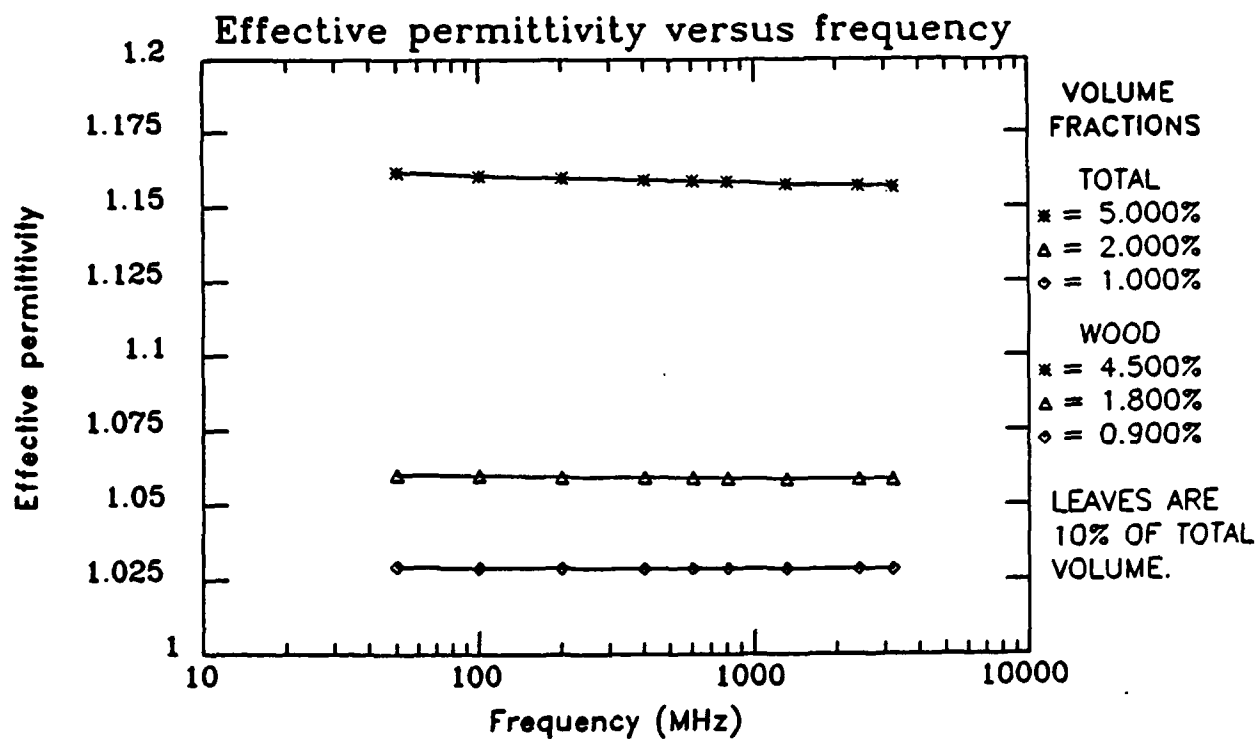


Figure 38. Effective permittivity of a dense softwood vegetation environment with the wood grain perpendicular to the electric field polarization. The three curves represent the highest, middle and lowest extremes of the volume fraction of the embedded scatterers. Leaf salinity is 6% and leaf moisture content 65% for all values. Wood moisture content is 140% and the temperature is 4°C representing the winter season.

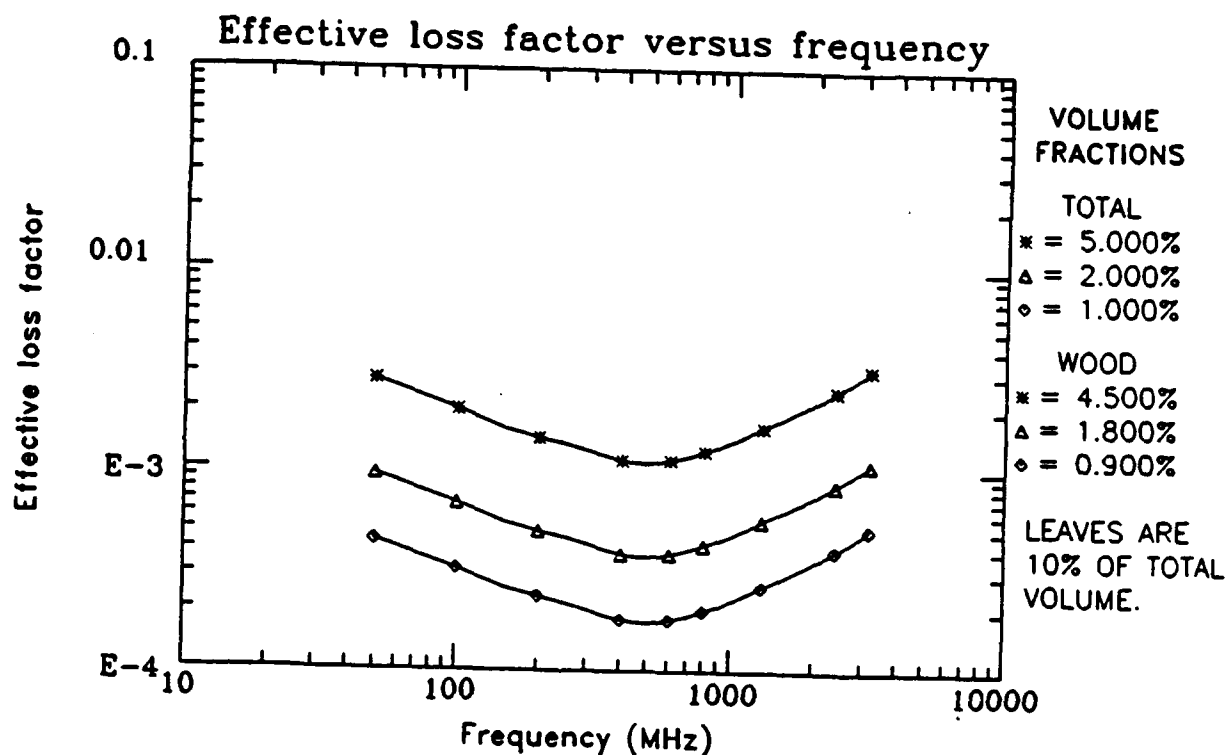


Figure 39. Effective loss factor of a dense softwood vegetation environment with the wood grain perpendicular to the electric field polarization. The three curves represent the highest, middle and lowest extremes of the volume fraction of the embedded scatterers. Leaf salinity is 6% and leaf moisture content 65% for all values. Wood moisture content is 140% and the temperature is 4°C representing the winter season.

hardwood vegetation. Overall the effective loss factors of the softwood vegetation with an air temperature of 4°C is less than the effective loss factors of hardwood vegetation at the same temperature, which is consistent with the findings at 25°C.

The effective permittivities for the extremely sparse to sparse volume fraction foliage (0.01% to 0.1%) from figure 36 are between 1.0003 and 1.0029; while the effective permittivities of sparse to normal foliage are between 1.003 and 1.029. The effective permittivities for the normal to dense volume fraction foliage (1.0% to 2.0%) from figure 38 are between 1.029 to 1.060; while for dense to extremely dense foliage (2.0% to 5.0%) the values vary between 1.059 and 1.162.

The effective loss factors for the extremely sparse to sparse volume fraction foliage from figure 37 are between  $1.8\text{E-}6$  and  $4.9\text{E-}5$ ; while the effective permittivities of sparse to normal foliage are between  $1.7\text{E-}5$  and  $5.1\text{E-}4$ . The effective permittivities for the normal to moderately dense volume fraction foliage from figure 39 are between  $1.8\text{E-}4$  to  $1.1\text{E-}3$ ; while for moderately dense to extremely dense foliage the values vary between  $3.8\text{E-}4$  and  $3.2\text{E-}3$ , depending upon the incident radiation frequency.

#### 4.2.3 Soft Wood With Randomly Oriented Electric Field at 25°C

Figures 40 and 41 depict the effective permittivity and loss factor of a sparse foliage medium composed of softwood vegetation at 25°C, with the wood grain randomly oriented with respect to the electric field, respectively. The random orientation of the wood grain with respect to the electric field polarization makes the values in these figures applicable to the propagation of electromagnetic waves through the canopies of mature forests or through brush or young vegetation, where the majority of wood grain is randomly oriented with respect to the electric field. The temperature (25°C) is representative of the summer season.

The permittivity in figure 40 does not vary much versus the frequency of the incident radiation. In fact, the magnitude of the permittivity does not differ appreciably from the values reported for the wood grain perpendicular to the electric field with all other variables

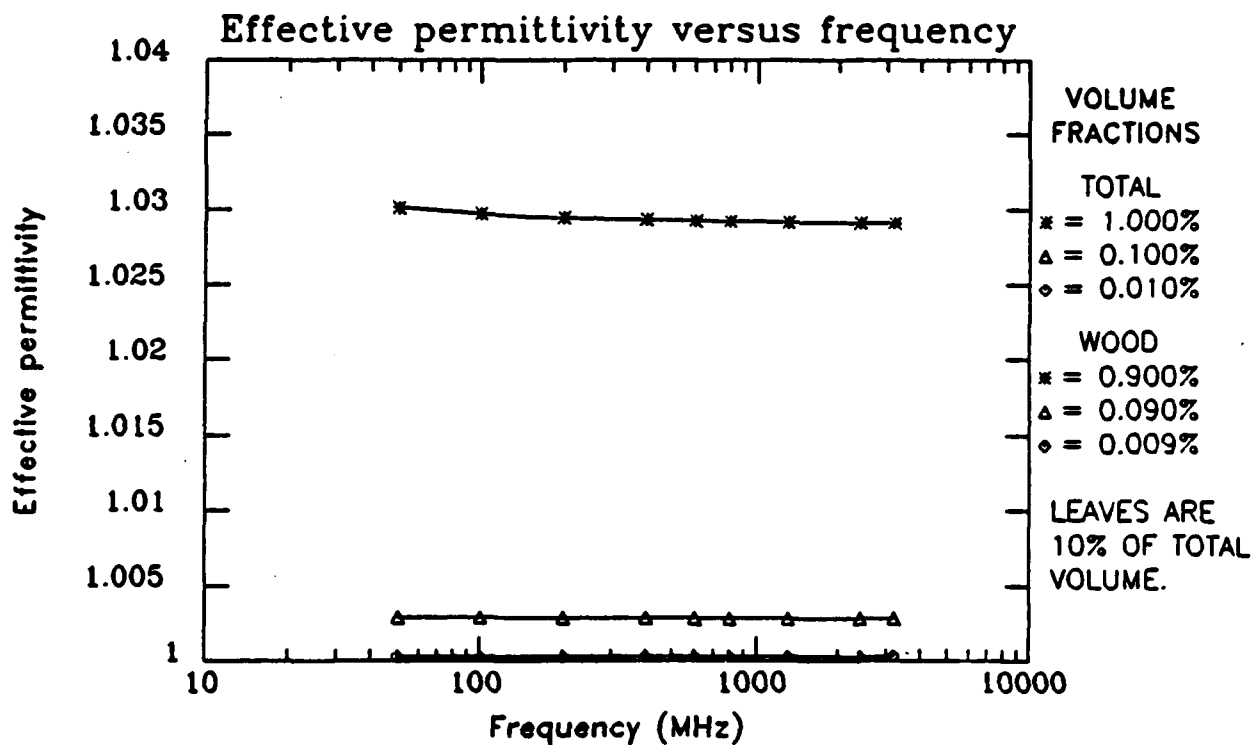


**Figure 40.** Effective permittivity of a sparse softwood vegetation environment with the wood grain randomly oriented with respect to the electric field polarization. The three curves represent the highest, middle and lowest extremes of the volume fraction of the embedded scatterers. Leaf salinity is 6% and leaf moisture content 65% for all values. Wood moisture content is 140% and the temperature is 25°C representing the summer season.

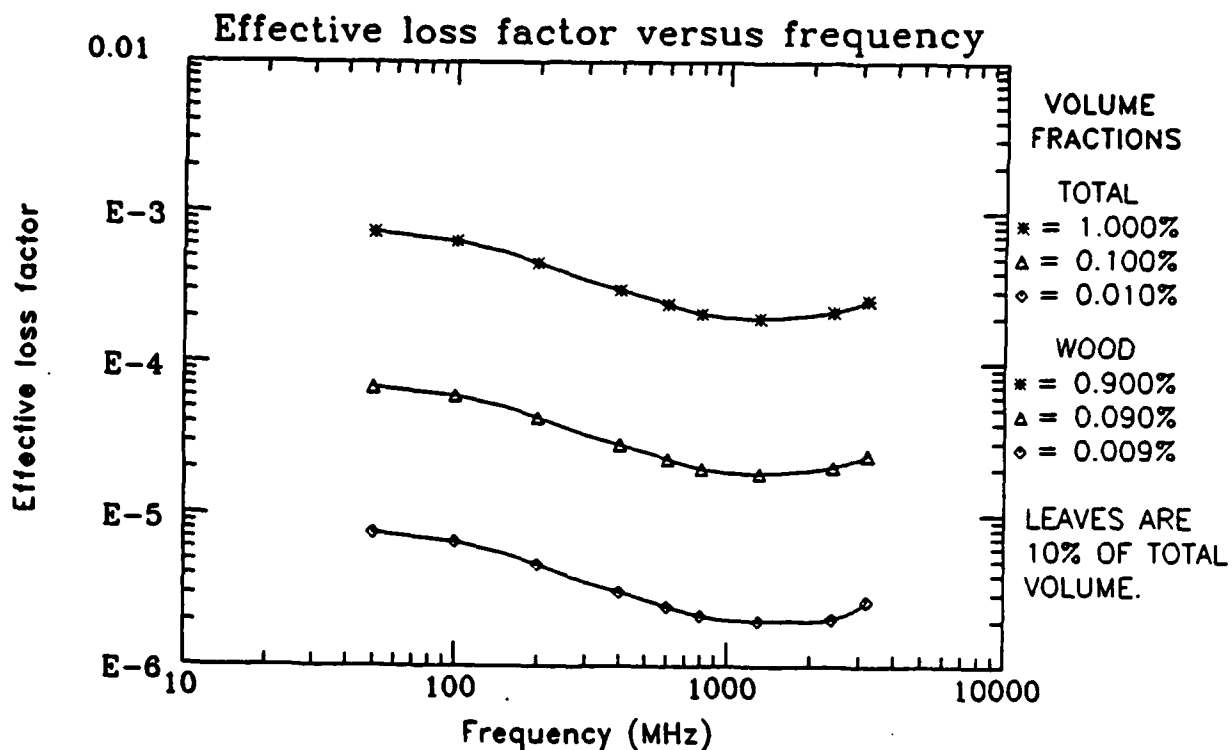


Figure 41. Effective loss factor of a sparse softwood vegetation environment with the wood grain randomly oriented with respect to the electric field polarization. The three curves represent the highest, middle and lowest extremes of the volume fraction of the embedded scatterers. Leaf salinity is 6% and leaf moisture content 65% for all values. Wood moisture content is 140% and the temperature is 25°C representing the summer season.

constant. It seems that the volume fraction of the embedded scatterers is the primary determinant in the calculation of the effective permittivity of a foliage environment regardless of the type of vegetation composing the medium. The values for the permittivity given in figure 40 give a permittivity between 1.0003 and 1.0029 for extremely sparse to sparse foliage, and 1.003 to 1.030 for sparse to normal vegetation, confirming the consistency of the permittivity regardless of wood type or electric field orientation.

The effective loss factors versus the frequency for the same conditions as those used in the development of figure 40 are shown in figure 41. Curve trends are different than those in the curves depicting the effective loss factors versus frequency when the wood grain orientation is perpendicular to the electric field, showing that, although a great dependence still exists on the volume fraction, the effective loss factor is also influenced by the wood grain orientation with respect to the electric field polarization. For the frequency range of interest in this study, the effective loss factors describing the effects on an electric field propagating through a softwood vegetation environment when the wood grain is randomly oriented with respect to the electric field polarization, appear to be greater than the corresponding effective loss factors when the electric field polarization is perpendicular to the wood grain. These curves are similar in magnitude and this conclusion could be effected by changes in the magnitude of the dielectric constants used for the embedded scatterers or changes in the leaf volume fraction ratio. The loss factor curves trends do reflect the same pattern as that of the major embedded scatterer (softwood ) as can be seen be a comparison to figure 5. The effective loss factor values for softwood vegetation and random electric field orientation are consistently lower than those of hardwood vegetation with the same electric field orientation. They are relatively closer in magnitude than those of hard and softwood vegetation when the electric field is perpendicular to the wood grain. The calculated effective loss factors for the extremely sparse to sparse foliage range between  $2.0\text{E-}6$  and  $6.9\text{E-}5$  and, between  $1.8\text{E-}5$  and  $7.3\text{E-}4$  for sparse to normal volume fraction foliage depending upon the incident radiation frequency.

Figures 42 and 43 depict the effective permittivity and loss factor of a dense foliage medium for the same conditions as those used to develop figures 40 and 41, respectively.

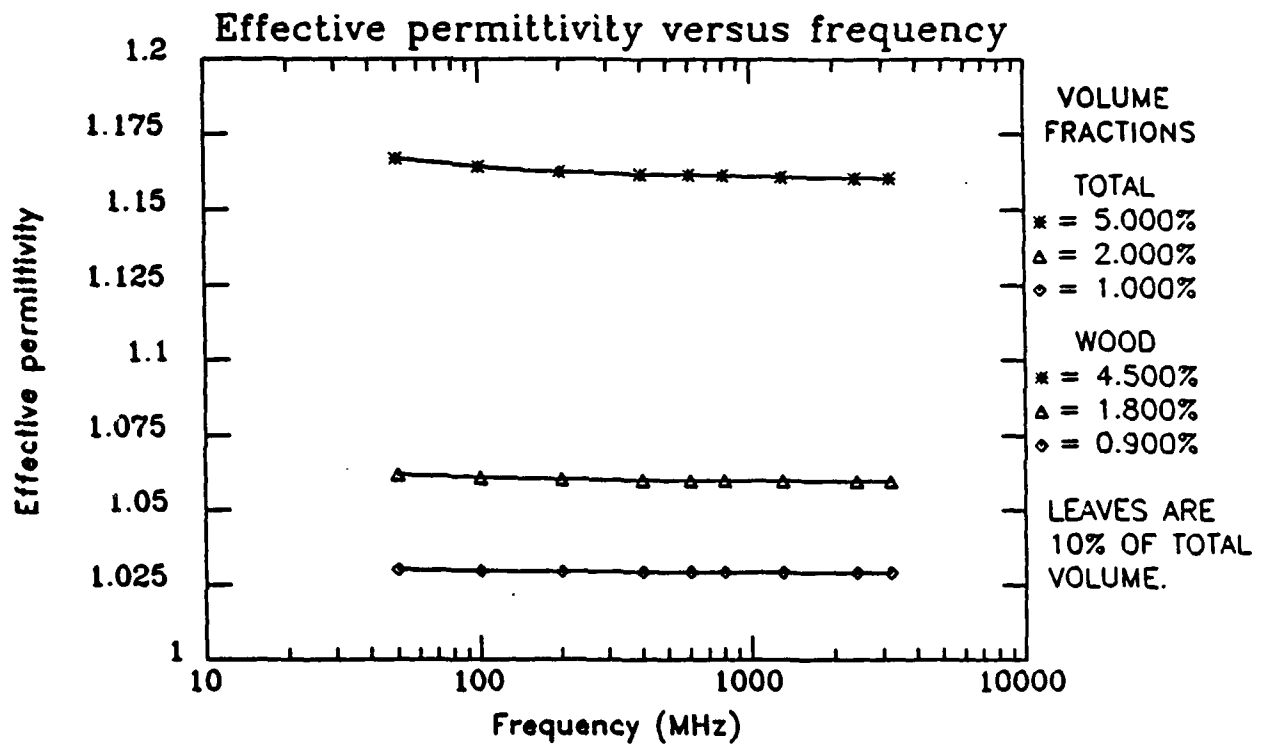


Figure 42. Effective permittivity of a dense softwood vegetation environment with the wood grain randomly oriented with respect to the electric field polarization. The three curves represent the highest, middle and lowest extremes of the volume fraction of the embedded scatterers. Leaf salinity is 6% and leaf moisture content 65% for all values. Wood moisture content is 140% and the temperature is 25°C representing the summer season.



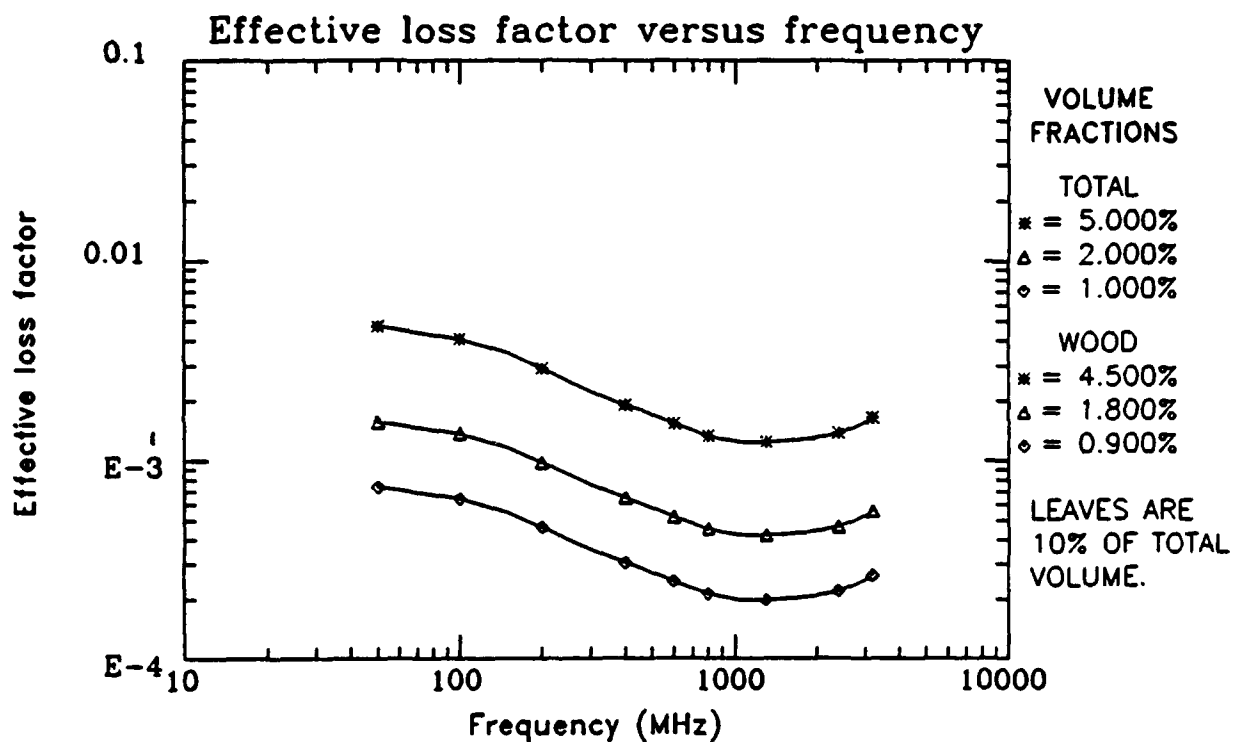


Figure 43. Effective loss factor of a dense softwood vegetation environment with the wood grain randomly oriented with respect to the electric field polarization. The three curves represent the highest, middle and lowest extremes of the volume fraction of the embedded scatterers. Leaf salinity is 6% and leaf moisture content 65% for all values. Wood moisture content is 140% and the temperature is 25°C representing the summer season.

The permittivities shown in figure 42 shows little variation versus the frequency and little variation from the permittivities of sparse vegetation of all conditions examined to this point. The permittivities do vary as the volume fraction changes from values of 1.029 to 1.062 for normal to dense foliage (1.0% to 2.0%), to 1.059 to 1.167 for dense to extremely dense foliage (2.0% to 5.0%).

Figure 43 contains plots of the effective loss factors of a dense foliage medium for the same conditions as figure 42. Again it is apparent that the effective loss factor will have the same tendencies over frequency as the major embedded scatterer, similar to the trend exhibited by the previous effective loss factor curves. The variation with respect to the volume fraction of embedded scatterers is again pronounced varying from  $2.0\text{E-}4$  to  $1.6\text{E-}3$  for normal to dense foliage, to  $4.2\text{E-}4$  to  $4.7\text{E-}3$  for dense to dense foliage, depending on the incident radiation frequency. These values are consistently lower than those of hardwood vegetation with similar parameters.

#### 4.2.4 Soft Wood With Randomly Oriented Electric Field at 4°C

Figures 44 through 47 present the results of the calculation of the effective complex dielectric constants of a foliage medium for the same conditions as those used in the determination of figures 40 through 43, respectively, the only difference being the ambient air temperature of 4°C for figures 44 to 47 rather than 25°C for figures 40 through 43. The 4°C value is intended to be representative of the winter season. Observation of figures 44 through 47 reveals that there is no appreciable difference in the effective permittivity of softwood vegetation in the summer and winter seasons, while the effective loss factor exhibits some variations with respect to frequency from the summer to winter season. This leads to the previously revealed assertion that large variations in the dielectric constants of the embedded scatterers are necessary to produce even minimal effects on the effective parameters when the volume fractions are low. Again, similar to the effective loss factors of softwood environments at 25°C, the effective loss factors when the wood grain is randomly oriented with respect to the electric field polarization are generally greater than the

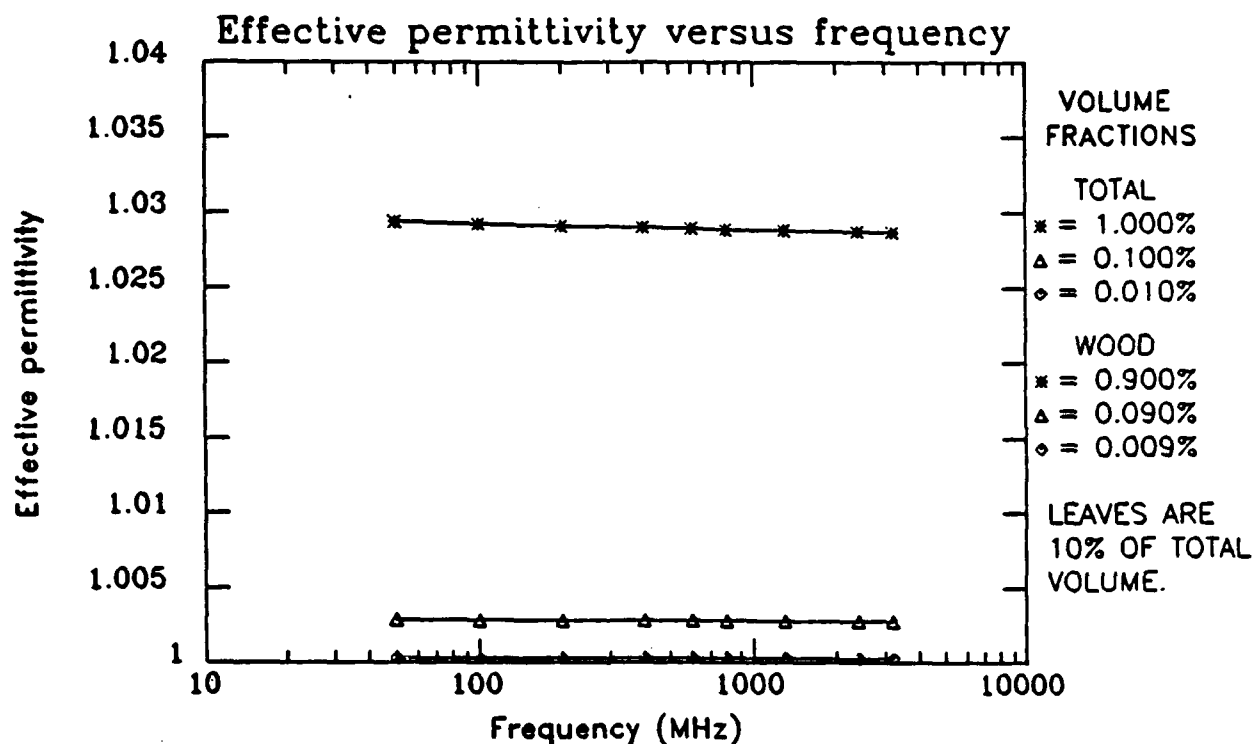


**Figure 44.** Effective permittivity of a sparse softwood vegetation environment with the wood grain randomly oriented with respect to the electric field polarization. The three curves represent the highest, middle and lowest extremes of the volume fraction of the embedded scatterers. Leaf salinity is 6% and leaf moisture content 65% for all values. Wood moisture content is 140% and the temperature is 4°C representing the winter season.

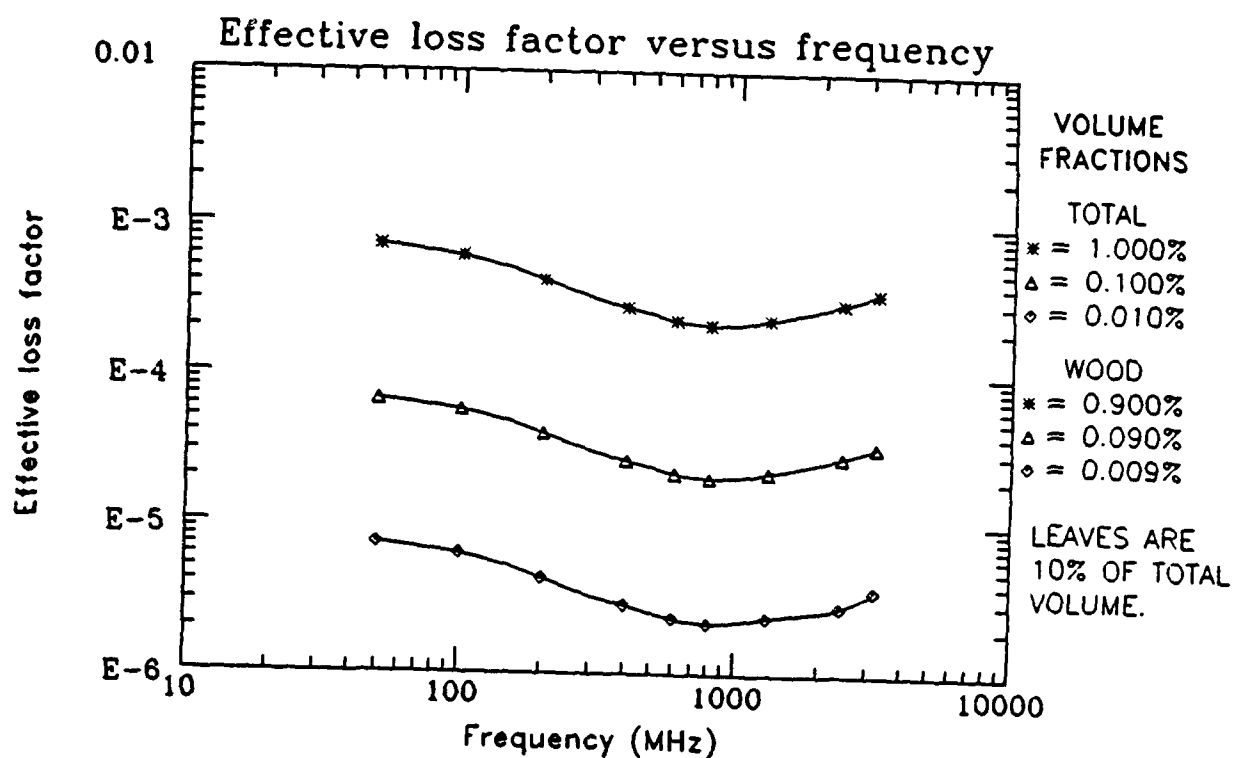


Figure 45. Effective loss factor of a sparse softwood vegetation environment with the wood grain randomly oriented with respect to the electric field polarization. The three curves represent the highest, middle and lowest extremes of the volume fraction of the embedded scatterers. Leaf salinity is 6% and leaf moisture content 65% for all values. Wood moisture content is 140% and the temperature is 4°C representing the winter season.

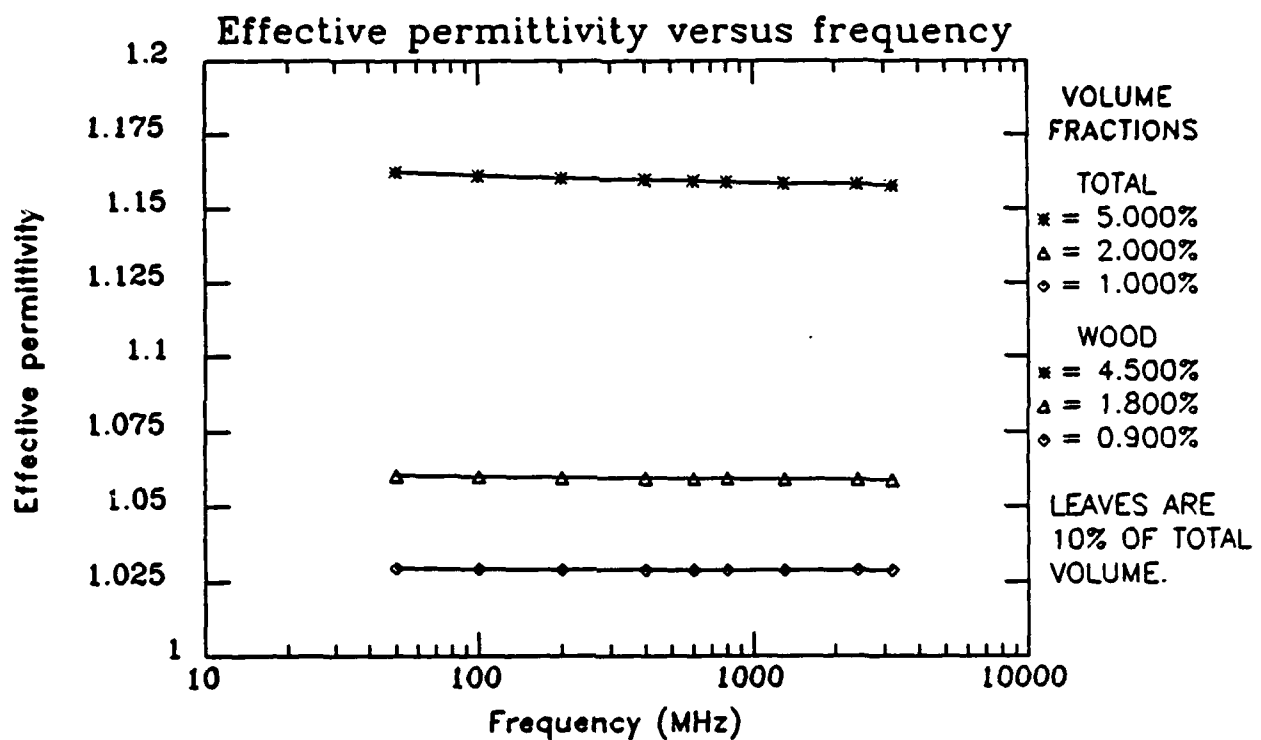


Figure 46. Effective permittivity of a dense softwood vegetation environment with the wood grain randomly oriented with respect to the electric field polarization. The three curves represent the highest, middle and lowest extremes of the volume fraction of the embedded scatterers. Leaf salinity is 6% and leaf moisture content 65% for all values. Wood moisture content is 140% and the temperature is 4°C representing the winter season.

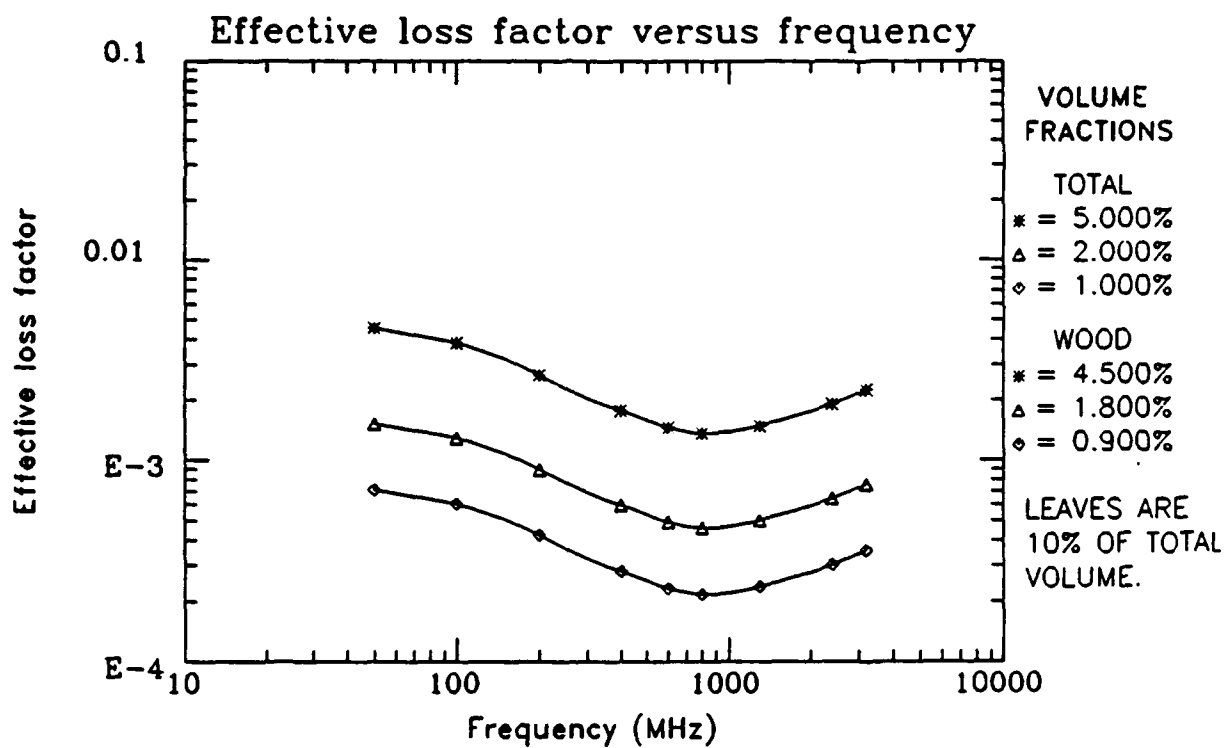


Figure 47. Effective loss factor of a dense softwood vegetation environment with the wood grain randomly oriented with respect to the electric field polarization. The three curves represent the highest, middle and lowest extremes of the volume fraction of the embedded scatterers. Leaf salinity is 6% and leaf moisture content 65% for all values. Wood moisture content is 140% and the temperature is 4°C representing the winter season.

corresponding effective loss factors when the electric field polarization is perpendicular to the wood grain. Therefore, the wood grain orientation with respect to the electric field polarization will affect the the values of the effective loss factors regardless of temperature or wood type. It should be noted that the effective loss factors for the perpendicular and random orientation of the wood grain with respect to the electric field polarization are very close in magnitude and could be affected by changes in the dielectric constants of the embedded scatterers or leaf volume fraction ratios.

The effective permittivities for the extremely sparse to sparse volume fraction foliage (0.01% to 0.1%) from figure 44 are between 1.0003 and 1.0029; while the effective permittivities of sparse to normal foliage are between 1.003 and 1.030. The effective permittivities for the normal to dense volume fraction foliage (1.0% to 2.0%) from figure 46 are between 1.029 to 1.062; while for dense to extremely dense foliage (2.0% to 5.0%) the values vary between 1.060 and 1.167.

The effective loss factors for the extremely sparse to sparse volume fraction foliage from figure 45 are between  $2.2\text{E-}6$  and  $6.7\text{E-}5$ ; while the effective permittivities of sparse to normal foliage are between  $2.0\text{E-}5$  and  $7.1\text{E-}4$ . The effective permittivities for the normal to moderately dense volume fraction foliage from figure 47 are between  $2.1\text{E-}4$  to  $1.5\text{E-}3$ ; while for moderately dense to extremely dense foliage the values vary between  $4.6\text{E-}4$  and  $4.6\text{E-}3$ , depending on the incident radiation frequency.

## 5.0 Conclusion

There was good agreement between the ATA, CPA, and EMA approximation methods used in this study to determine the effective parameters to describe the scattering and absorption of electromagnetic radiation by foliage environments. The relatively small volume fractions ( $< 5.0\%$ ) of vegetation matter in a forest environment is the major factor for the agreement between the approximation methods. As previously stated, the approximations concurred with the expected values found in the literature below the 5.0% volume fraction level, but began to significantly differ as the volume fraction increased above 5.0%. Fortunately, volume fractions of vegetation much above this 5.0% threshold

are considered unrealistic. The results obtained from the Modified ATA approximation were consistently higher than the other approximation methods. The large disparity between the dielectric constants of the host medium and the embedded scatterers could be the cause of the erroneous behavior. Therefore, the calculation of the effective parameters of a heterogeneous medium using the MOD\_ATA method is limited to media whose embedded scatterer dielectric constants are close in magnitude to the dielectric constant of the host medium. From this assumption, the MOD\_ATA method will not provide a good approximation of the effective parameters of a foliage medium because the dielectric constants of the embedded scatterers are much greater than the host medium of air.

Application of the ATA, CPA, and EMA approximations to determine the effective parameters of foliage has been questioned due to the variety of shapes of the component scatterers found in a vegetation medium. Whether this is accurate or not can only be established by experimental verification of the values presented herein, the values given in this report are consistent with the range of values that are presently reported in the literature for foliage media [Tamir 67] [Ulaby 82] [Broadhurst 71]. Precise verification of all of the effective parameters reported in this paper is difficult at the present time because of the lack of measurements describing the effective dielectric constants of forest environments or forest components.

Several findings have been established using the approximation methods to determine the effective parameters of a vegetation environment. The primary conclusion would be the establishment of values that can be used to determine the effect on the magnitude of an electric field propagating through a vegetation environment by representing the vegetation environment as a homogeneous dielectric slab. Although the values of the effective parameters did vary depending upon the dielectric constant of the foliage components, temperature, and wood grain orientation with respect to the electric field polarization, all values were within a certain range of values and varied primarily as a function of the volume fraction of embedded scatterers. It should be kept in mind that the dielectric constants of the embedded scatterers (wood, leaves, needles, etc.) were determined by the use of models and verified by comparison to experimental data. Therefore, the effective parameters presented here will only be as good as the models used to determine these values. Should a large discrepancy exist between the dielectric constants used for the



embedded scatterers in this report the the dielectric constants of the embedded scatterers of interest, recalculation of the effective parameters may be necessary. The changes in the dielectric constants of the component scatterers would probably have to be an order of magnitude or more to substantially affect the calculated effective dielectric constants since it is the volume fraction that will be the most decisive factor in the effective parameter determination. The effective permittivities of a vegetation medium were found to vary from 1.0003 to 1.2 for extremely sparse to extremely dense foliage, respectively. The effective loss factors of a vegetation medium were found to vary between  $1.8\text{E-}6$  and  $9.9\text{E-}3$  for extremely sparse to extremely dense foliage, respectively. The calculated effective permittivity of a normal volume fraction foliage environment (1.0% total volume fraction) was approximately 1.03 for all conditions. The effective loss factor, while more variant depending on the conditions, could be approximated by  $5.0\text{E-}4$  for the normal volume fraction foliage. The effective parameters calculated using the approximations methods in this report are all within the 1.01 to 1.5 and  $1\text{E-}3$  to  $1\text{E-}5$  reported in literature for the effective permittivity and conductivity of a vegetation environment [Tamir 67].

The effective permittivity was generally consistent for all cases considered in this study. There was a slight tendency for the permittivities of the softwood vegetation to be greater than that of hardwood vegetation under the same conditions. There was only a slight dependence of the permittivity on temperature with the winter values being slightly greater than the summer values. The values when the wood grain was randomly oriented with respect to the electric field polarization were somewhat greater the those of the perpendicular values. The differences attributable to temperature, vegetation composition and wood grain orientation were extremely small and should not be completely accepted without experimental verification.

In general, the values of the effective loss factors calculated in this study for vegetation composed of softwood were consistently smaller than those of foliage composed of hardwood with all conditions held constant. The values for the winter season were consistently smaller than those in the summer season. Values where the wood grain was perpendicular to the electric field polarization were greater than or equal to the randomly oriented wood grain

values. The differences in the effective loss factors versus the temperature and wood grain orientation were extremely small and may not be constant for all types of vegetation. The loss factors of the softwood vegetation, with random orientation of the wood grain with respect to the electric field polarization, are much smaller relative to the loss factors of hardwood vegetation with similar electric field orientation than the loss factors of the softwood vegetation with perpendicular orientation to the electric field are to the loss factors of the hardwood vegetation with perpendicular electric field orientation. The major contributor to the varying of the effective loss factors of the vegetation media is the volume fraction of the embedded scatterers or foliage density. Unlike the permittivity, however, there is some dependence on the dielectric constant of the embedded scatterers. This effect is not very pronounced at the small volume fractions necessary in the modeling of natural foliage.

It should be noted that the effective parameters calculated in this report were determined for specific volume fractions, temperatures, foliage compositions, and leaf to wood ratios. No attempt was made to determine the effects of varying moisture content, salinity, wood to leaf ratios, or below freezing temperatures; conditions that could be of concern. These variations could be the focus of further study. It is recommended that further theoretical studies be undertaken to verify the use of the effective parameters in describing the propagation of electromagnetic radiation through foliage environments. An experimental study that could determine, say, the skin depth penetration could also be done and used to verify the theoretical results.

## References

Bensoussan, A., Lions, J.L., Papanicolaou, G.C., *Asymptotic Analysis For Periodic Structures*, North-Holland, Amsterdam, 1978.

Blankenship, G.L., "Stochastic Modeling of EM Scattering From Foliage", Rep. RADC-TR-89-22, Rome Air Development Center, Hanscom, AFB, MA, March 1989, AD A213118.

Broadhurst, M.G., "Complex Dielectric Constants and Dissipation Factor of Foliage", NBS Report no. 9592, NBS project 3110107, US Naval Ordnance Laboratory, October 1970.

Brown, G.S., Curry, W.J., "An Analytical Study of Wave Propagation Through Foliage", Rep. RADC-TR-79-359, Rome Air Development Center, Hanscom, AFB, Mass., *Final Technical Report*, January 1980, AD A084548.

Brown, G.S., and Curry, W.J., "A Theory and Model for Wave Propagation Through Foliage", *Radio Science*, Vol. 17, pp. 1027-1036, 1982.

Brown, G.S., "A Theoretical Review of the Effects of Vegetation on Terrain Scattering", Rep. RADC Contract no. F19628-84-C-0012, Rome Air Development Center, Hanscom, AFB, Mass., *Final Technical Report*, August 1987.

Bush, T.F., and Ulaby, F.T., "Radar Return From a Continuous Vegetation Canopy", *IEEE Trans. Antennas and Propagation*, AP-24, pp. 269-276, 1976.

DeLoor, G.P., "Dielectric Properties of Heterogeneous Mixtures With Polar Constituents", *Jour. Appl. Sci. Res.*, Section B, Vol. 12, pp 311-321, 1963.

DeLoor, G.P., "Dielectric Properties of Heterogeneous Mixtures Containing Water", *Jour. Microwave Power.*, Vol. 3, no. 2, pp 67-73, 1968.

Elliott, R., et al, "The Theory and Properties of Randomly Disordered Crystals and Related Physical Systems", *Rev. Mod. Phys.*, Vol. 46, pp. 465-543, 1974.

Fung, A.K., Ulaby, F.T., "A scattering Model for Leafy Vegetation", *IEEE Trans. Antennas and Propagation*, Vol. AP-16, no. 4, pp 281-285, October 1978.

Fung, A.K., "Scattering From a Vegetation Layer", *Trans. Geo. Sci Elect.*, Vol. GE-17, no. 1, pp. 1-6, January 1979.

Fung, A.K., "A Review of Volume Scatter Theories for Modeling Applications", *Radio Science*, Vol. 17, no. 5, pp. 1007-1017, September-October 1982.

Golden, A., "A Foliage Penetration Study", Rep. RADC-TR-78-34, Rome Air Development Center, Hanscom AFB, Mass., 1978, AD A055391.

Grant, E., Buchanan, T., Cook, T., "Dielectric Behavior of Water at Microwave frequencies", *J. Chem. Phys.*, Vol. 26, pp. 156-161, 1957.

Ishimaru, A., "Wave Propagation and Scattering in Random Media", Vols. I and II, Academic Press, New York, 1978.

James, W.L., "Dielectric Properties of Wood and Hardboard: Variation With Temperature, Frequency, Moisture Content and Grain Orientation", *USDA Forest Service Res. Paper FPL 245*, USDA Forest Products Lab., Madison, MI, 1975.

Klein, L.A., Swift, C.T., "An Improved Model for the Dielectric Constant of Sea Water at Microwave Frequencies", *IEEE Trans. Antennas and Propagation*, AP-25, pp. 1041-111, 1977.

Kohler, W.E., and Papanicolaou, G.C., "Some Applications of The Coherent Potential Approximation", in *Multiple Scattering and Waves in Random Media*, Eds. Chow, P.L., Kohler, W.E., Papanicolaou, G.C., North-Holland, New York, pp. 199-223, 1981.

Kollmann, Côté, *Principals of Wood Science and Technology*, Springer Verlag, 1968.

Lane, J., Saxton, J., "Dielectric Dispersion in Pure Polar Liquids at Very High Radio Frequencies, III," in The Effect of Electrolytes in Solution, *Proc. Roy. Soc.*, 214A, pp. 531-545, 1952.

Lang, R.H., "Electromagnetic Backscattering From a Sparse Distribution of Dielectric Scatterers", *Radio Science*, Vol. 16, n0. 1, pp. 15-30, January 1981.

Lang, R.H., Sidhu, J.S., "Electromagnetic Backscattering From a Layer of Vegetation: A Discrete Approach", *Trans. Antennas and Propagation*, Vol. GE-21, no. 1, pp. 62-71, January 1983.

Lax, M., "Multiple Scattering of Waves", *Rev. Mod. Phys.*, Vol. 23 pp. 287-310, 1951, and *Phys. Rev.*, Vol. 85 pp. 621-629, 1952.

Lax, M., "Wave Propagation and Conductivity in Random Media", in *Stochastic Differential Equations*, SIAM-AMS Proc., Vol. VI, pp. 35-95, 1973.

McPetrie, J.S., and Ford, L.H., "Some Experiments on the Propagation of 9.2 cm Wavelength, Especially on the Effects of Obstacles, *Jour. IEE*, Vol. 93, Part III A, pp. 531, 1946.

Megaw, E.C.S., "Some Effects of Obstacles on the Propagation of Very Short Radio Waves", *Journal IEE*, pp.97-105, 1947.

Pounds, D.J., and LaGrone, A.H., "Considering Forest vegetation as an Imperfect Dielectric Slab", Rep. no. 6-53, *Electr. Eng. Res. Lab.*, Univ. of Texas, Austin, TX (Available as AD#410836, Natnl. Inf. Serv., Springfield, VA), 1963.

Sachs, D.L., and Wyatt, P.J., "A Conducting-Slab Model for Electromagnetic Propagation Within a Jungle Medium", Defense Research Corp., *Tech. Memo.* 376 and *Internal Memo.*, IMR-471, 1966.

Skaar, C., "The Dielectric Properties of Wood at Several Radio Frequencies", *Technical Publication*, no. 69, Vol. XXI, no. 1-d, New York State College of Forestry at Syracuse University, Syracuse, NY, 1948.

Stogryn, A., "Equations for Calculating the Dielectric Constant of Saline Water", *IEEE Trans. Microwave Theory Techn.*, MIT-19, pp. 733-736, 1971.

Stogryn, A., "Electromagnetic Scattering by Random Dielectric Constant Fluctuations in a Bounded Medium", *Radio Science*, Vol. 9, no. 5, pp. 509-518, May 1974.

Studzman, W.L., Colliver, F.W., Crawford, H.S., "Microwave Transmission Measurements for Estimation of the Weight of Standing Pine Trees", *IEEE Trans. Antennas and Propagation*, Vol. AP-27, pp. 22-26, January 1970.

Tamir, T., "On Radio-Wave Propagation in Forest Environments", *IEEE Trans. Antennas and Propagation*, Vol. AP-15, no. 6, pp. 806-817, November 1967.

Taylor, L.S., "Dielectric Properties of Mixtures", *IEEE Trans. Antennas and Propagation*, Vol. AP-13, no. 6, pp. 943-947, November 1965.

Tinga, W.R., Voss, W.A.G., and Blossey, D.F., "Generalized Approach to Multiphase Dielectric Mixture Theory", *Jour. Appl. Phy.*, Vol. 44, no. 9, pp. 3897-3902, September 1973.

Travor, B., "Ultra-High-Frequency Propagation Through Woods and Underbrush", *RCA Review*, Vol. 5, pp. 97-100, July 1940.

Ulaby, F.T., Razani, M., Dobson, M.C., "Effects of Vegetation Cover on the Microwave Radiometric Sensitivity to Soil Moisture", *IEEE Trans. Geoscience and Remote Sensing*, Vol. GE-21, no. 1, pp. 51-61, January 1983.

Ulaby, F.T., Moore, R.K., and Fung, A.K., *Microwave Remote Sensing Active and Passive*, Vol. I, II, III, Artech House, 1986.

VanBeek, L.K.H., "Dielectric Behaviour of Heterogeneous Systems", in *Progress in Dielectrics*, Vol. 7, Ed. Birks, J.B., Chemical Rubber Company, Cleveland, OH, 1967.

Varadan, V.K., Bringi, V.N., and Varadan, V.V., "Coherent Electromagnetic Wave Propagation Through Randomly Distributed Dielectric Scatterers", *Phys. Rev. D*, 19, pp. 2480-2486, 1979.

Weyl, P., "On the Change in Electrical Conductance of Seawater With Temperature", *Limnol. Oceanogr.*, vol. 9, pp. 75-78, 1964.

Yavorsky, J.M., "A Review of Electrical Properties of Wood", *Technical Publication*, no. 73, New York State College of Forestry at Syracuse University, Syracuse, NY, 1951.



## *MISSION of Rome Air Development Center*

*RADC plans and executes research, development, test and selected acquisition programs in support of Command, Control, Communications and Intelligence (C<sup>3</sup>I) activities. Technical and engineering support within areas of competence is provided to ESD Program Offices (POs) and other ESD elements to perform effective acquisition of C<sup>3</sup>I systems. The areas of technical competence include communications, command and control, battle management information processing, surveillance sensors, intelligence data collection and handling, solid state sciences, electromagnetics, and propagation, and electronic reliability/maintainability and compatibility.*